heat pump programme

IEA
OECD

Annex 18

Operating Agent:

USA

Comparisons of Equations of State with Experimental Data for R32 and R125

Comparisons of Equations of State with Experimental Data for R32 and R125

Annex 18

By:

John Kilner
and Robert JB Craven

IUPAC Thermodynamic Tables Project Centre
Department of Chemical Engineering and Chemical Technology
Imperial College of Science, Technology and Medicine
London SW7 2BY, England

March 1997

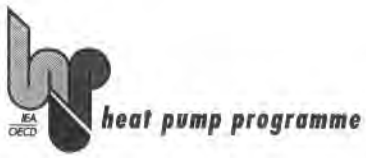

Report No. HPP-AN18-4

Published by

IEA Heat Pump Centre
Swentiboldstraat 21, 6137 AE Sittard
P.O. Box 17, 6130 AA Sittard
The Netherlands
Tel.: +31-46-420 2236
Fax: +31-46-451 0389

Production

IEA Heat Pump Centre, Sittard, the Netherlands

ISBN 90-73741-22-X

IEA Heat Pump Centre

The IEA Heat Pump Centre is the focal point for the heat pump related activities of the International Energy Agency (IEA).

International Energy Agency

The IEA was established in 1974 within the framework of the Organisation for Economic Cooperation and Development (OECD) to implement an International Energy Programme. A basic aim of the IEA is to foster cooperation among its 24 participating countries to increase energy security through energy conservation, utilization of alternative energy sources, and research and development on energy technologies.

IEA Heat Pump Programme

Set up by the IEA in 1978, the IEA Heat Pump Programme carries out a strategy to accelerate the development of heat pumps, and to stimulate their use in all applications where they can reduce energy consumption for the benefit of the environment. Under this programme, participants fro different countries collaborate in specific heat pump projects known as Annexes.

IEA Heat Pump Centre

A central role within the programme is played by the IEA Heat Pump Centre (HPC), itself an Annex. Using the network of its National Teams, along with links with other organizations, the HPC works towards the aims of the programme by providing a worldwide information exchange service. The functions of the HPC include:

- Collecting, analysing and disseminating heat pump related technical, market, regulatory, and environmental information.
- Fostering international cooperation in research and development.
- Facilitating contacts and information exchange among heat pump policy makers in governments and utilities, and those involved in research, development, design, manufacture, regulation, marketing, and application of heat pumps.

The HPC publishes the quarterly journal *'IEA Heat Pump Centre Newsletter'*, organizes *workshops*, provides an *enquiry service*, and conducts *analysis studies* on selected heat pump topics.

For further information about the HPC and its products, and for enquiries on heat pump issues in general, contact the HPC at the following address:

IEA Heat Pump Centre/TSSU
P.O.Box 17
6130 AA Sittard
THE NETHERLANDS
Phone: +31-46-420 2236
Fax: +31-46-451 0389

Contents

List of Figures R32

List of Figures R125

List of Figures – Appendix 1

List of Figures – Appendix 2

Tables in text

Symbols

Symbol	*Physical Quantity*
A	Molar Helmholtz function
B	Second virial coefficient
C	Molar heat capacity
M	Molar mass
P	Pressure
R	Molar gas constant
R_{R}	Specific gas constant
T	Thermodynamic temperature
V	Molar volume
$\mathcal{W}$	Speed of sound
Z	Compression factor
α	$A/(RT)$
θ	Reduced temperature
μ	Joule-Thomson coefficient
ρ	Reciprocal molar volume (Molar density)
τ	Reciprocal reduced temperature
ω	Reduced density

Subscripts	
b	at the boiling point
c	at the critical point
cal	property calculated by an equation of state
exp	experimental measurement
g	in the gas phase
l	in the liquid phase
$P, V, etc.$	at constant pressure, volume, etc.
t	at the triple point
σ	at constant saturation

Superscript	
ig	ideal gas value
r	residual part

Introduction

It was proposed at the meeting of Annex 18 of the International Energy Agency held in Heidelburg, Germany, in November 1990 and agreed at the meeting held in Boulder, Colorado, USA in June 1991, that comparison should be made of the existing equations of state (EOS) for the environmentally acceptable refrigerants. The two fluids, for which there were then the greatest amount of data and more than one equation of state for each, were R134a (1,1,1,2-tetrafluoroethane) and R123 (1,1-dichloro-2,2,2-trifluoroethane). These were selected for the first study which was completed in 1993 by the two independent groups; the Center for Applied Thermodynamic Studies (CATS) at the University of Idaho, Moscow, Idaho, USA (Richard Jacobsen and Steve Penoncello) and the International Union of Pure and Applied Chemisty (IUPAC) Thermodynamic Tables Project Centre, Imperial College, London, UK (Marjorie de Reuck).

At a further meeting at Boulder, Colorado, USA in June 1994, it was agreed that equations of state for the two alternative refrigerants, R32 (difluoromethane) and R125 (pentafluoroethane) should be developed. Groups wishing to participate, were invited to submit their equations to the Annex for evaluation by 30 June 1995. It was agreed that any data to be used in the evaluation should be deposited by 31 December 1994 at the University of Stuttgart electronic databank, where it would be available to all participants. The majority of the data, both published and unpublished, were supplied from a compilation prepared by Outcalt and McLinden from the National Institute of Science and Technology (NIST), Boulder, Colorado USA. An independent group, the International Union of Pure and Applied Chemisty (IUPAC) Thermodynamic Tables Project Centre, Imperial College, London, UK, agreed at the request of the Annex, to undertake the evaluations. A specification for the input and output routines for the equation of state programs was submitted by the Project Centre. Computer programs were sent to the Centre by the authors by e-mail and/or on diskette by the end of July 1995.

This report presents detailed comparisons between all the submitted equations of state and the data for R32 and R125 deposited at Stuttgart. Data for the liquid phase isobaric heat capacity and the gas phase speed of sound for R32 were taken from a later version of the database, as there were no data deposited by December 1994, and it was felt that inclusion of this data would help the evaluation process. All the comparisons have been made using the programs submitted by the individual authors. Minor modifications were made to some programs to avoid duplication of routine names and to improve convergence.

1 Refrigerant R32

Thirty-seven data sets containing about 2100 data points were lodged in the Stuttgart database for R32. The properties in these sets include: vapour pressures, saturated liquid and vapour densities, liquid phase saturated heat capacities (C_σ), PVT, isobaric (C_P) and isochoric (C_V) heat capacities, second virial coefficients, and speed of sound in the single phase. The extent of coverage of the data is shown on the data maps in Appendix 1. Comparisons of all the data have been made with the values predicted by the four equations of state, where possible, which resulted in 146 separate comparisons to be evaluated. Plots of the isobaric and isochoric heat capacities, the isenthalpic Joule-Thomson coefficient, and the speed of sound predicted by each EOS are shown in Appendix 2. A statistical analysis of each data set and of the combined data sets for each property, were made for each of the equations of state. The results are shown in Appendix 3.

1.1 Available equations of state for refrigerant R32

The four equations of state which are discussed in the following subsections, differ in their structure and range of validity. That developed by Outcalt and McLinden (1995) is a modified BWR equation with 32 coefficients, which was originally developed by Jacobsen and Stewart (1973) for nitrogen. The equation developed by Piao and Noguchi (1995) is also a modified BWR equation with 18 coefficients based on their earlier versions (Piao *et al.* (1992)). Ely (1995) and Tillner-Roth (1995) have developed new Helmholtz equations; the formulation of Ely has 28 terms and that of Tillner-Roth has 21 coefficients.

The temperature and pressure limits for their respective equations of state are shown when given by the authors. Caution should be taken when extrapolating any equation beyond the region of the fitted data.

Within each property table, the data sets used to fit the respective equations were not noted as full information was not available.

1.1.1 Ely equation of state

This equation has not yet been published and will be referred to in this report as the Ely EOS. It is written in terms of a dimensionless Helmholtz function as a function of reduced density and reciprocal reduced temperature in the form:

$$A^{\mathrm{r}}/RT = \sum_{i=1}^{28} n_i \omega^{r_i} \tau^{(s_i+0.25u_i)} (e^{-\omega^{t_i}} - \kappa_{r_i,0}) \tag{1.1}$$

where $\omega = \rho/\rho_c$ with $\rho_c = 8207.8$ mol m^{-3}, $\tau = T_c/T$ with $T_c = 351.35$ K and $R = 8.31451$ J K^{-1} mol^{-1}. $\kappa_{r_i,0}$ is a kronecker delta function defined as: $\kappa_{\alpha,\beta} = 1$ if $\alpha = \beta$ otherwise zero. The validity range of this equation is not given.

1.1.2 Outcalt and McLinden equation of state

This equation, which was presented at the Twelfth Symposium on Thermophysical Properties in June 1994 at Boulder, USA, will be referred to in this report as the OM EOS. This equation is written in terms of pressure as a function of temperature and density in the form:

$$\begin{aligned} P = {} & \rho RT + \rho^2(n_1T + n_2T^{1/2} + n_3 + n_4/T + n_5/T^2) \\ & + \rho^3(n_6T + n_7 + n_8/T + n_9/T^2) + \rho^4(n_{10}T + n_{11} + n_{12}/T) \\ & + \rho^5(n_{13}) + \rho^6(n_{14}/T + n_{15}/T^2) + \rho^7(n_{16}/T) \\ & + \rho^8(n_{17}/T + n_{18}/T^2) + \rho^9(n_{19}/T^2) \\ & + \rho^3 \exp(-[\rho/\rho_c]^2)\big[(n_{20}/T^2 + n_{21}/T^3) + \rho^2(n_{22}/T^2 + n_{23}/T^4) \\ & + \rho^4(n_{24}/T^2 + n_{25}/T^3) + \rho^6(n_{26}/T^2 + n_{27}/T^4) \\ & + \rho^8(n_{28}/T^2 + n_{29}/T^3) + \rho^{10}(n_{30}/T^2 + n_{31}/T^3 + n_{32}/T^4)\big]. \end{aligned} \tag{1.2}$$

where the value for $R = 8.314471$ J K^{-1} mol^{-1}. The critical density which was used as the reducing parameter in this EOS is $\rho_c = 8207.8$ mol m^{-3}(Higashi *et al.* (1992)). During the development of this equation of state, ancilliary equations were fitted to the saturation properties using their selected values for the critical temperature of $T_c = 351.35$ K (Schmidt and Moldover (1994)) and the critical density of $\rho_c = 8207.8$ mol m^{-3} (Higashi *et al.* (1992)); the value for the critical pressure of $P_c = 5.795$ MPa was determined from extrapolation of the experimental vapour pressures of Defibaugh *et al.* (1994).

The authors state that the equation accurately represents the thermodynamic properties in the temperature range 160 K to 393 K for pressures up to 35 MPa except for the critical region and should extrapolate reasonably to 500 K and 60 MPa.

1.1.3 Piao and Noguchi equation of state

This is a new equation of state which has not yet been published, and is based on earlier work : it will be referred to in this report as the PN EOS. It is a modified BWR equation with 18 coefficients, where the reduced pressure is given as a function of reduced temperature and reduced density in the form:

$$P/P_c = \omega\theta/Z_c + \sum_{i=1}^{14} n_i \omega^{r_i} \theta^{s_i} + \exp(-\omega^2) \sum_{i=15}^{18} n_i \omega^{r_i} \theta^{s_i} \tag{1.3}$$

with $\omega = \rho/\rho_c$, $\theta = T/T_c$, $Z_c = P_c/(R_R \rho_c T_c)$ and $R_R = R/M$.

The critical temperature and critical density were taken from Kuwabara *et al.* (1995). The values are $T_c = 351.255$ K and ρ_c=424 kg m^{-3}. The value of the critical pressure was P_c=5.7812 MPa and the value for $R = 8.314471$ J K^{-1} mol^{-1}. The equation is said to be valid for temperatures from 150 K to 500 K, for densities up to 1400 kg m^{-3} and pressures up to 80 MPa.

1.1.4 Tillner-Roth equation of state

This new equation of state, which has not yet been published, will be referred to in this report as the TR EOS. This equation is a reduced Helmholtz function, given in terms of reciprocal reduced temperature and reduced density where the residual part is of the form:

$$A^{\mathrm{r}}/R_{\mathrm{R}}T = \sum_{i=1}^{8} n_i \omega^{r_i} \tau^{s_i} + \sum_{i=9}^{21} n_i \omega^{r_i} \tau^{s_i} \exp(-\omega^{t_i}) \tag{1.4}$$

where A^{r} represents the residual part of the Helmholtz function, $\tau = T^*/T$ and $\omega = \rho/\rho^*$. The values taken for the reducing parameters are $T^* = 351.26$ K and $\rho^* = 427.0$ kg m^{-3}, and $R_{\mathrm{R}} = R/M$ where $R = 8.314471$ J K^{-1} mol^{-1}and $M = 0.052024$ kg mol^{-1}. The validity range for the equation is not given.

1.2 Ideal gas properties and fixed points

1.2.1 Ideal gas heat capacities

The OM EOS, the PN EOS and the TR EOS use simple polynomial equations in reduced temperature to represent the ideal gas heat capacity values whereas the Ely EOS uses an empirical fit to a truncated Einstein statistical mechanical equation.

The two data sets, Rodgers *et al.* (1974) and Chase *et al.* (1985), are based on spectroscopic data. The latter data set extends the former's range of 0 K to 1500 K to 6000 K. The deviations of the data from the Ely, OM, and TR EOSs for the restricted temperature range, $0 < \mathrm{T/K} < 700$ are given in figure 1.1. The deviations from the Ely EOS lie between -0.031% and 0.13% throughout the entire temperature range as might be expected from the functional form of the equation used. For $\mathrm{T} < 700$ K the upper bound is 0.067%. The deviations from the OM EOS within the temperature range $160 < \mathrm{T/K} < 500$ lie between -0.057% and 0.108%. Outside this range the deviations become very large, very rapidly, (the calculated heat capacity is negative at $\mathrm{T} > 1000$ K), so that above 500 K any extrapolation of the thermal properties will be in serious error. The data deviate from the TR EOS within the temperature range $160 < \mathrm{T/K} < 350$, where thermal data exist, by between -0.20% and 0.23%. The deviations outside this range are larger reaching -0.82% at 500 K then becoming rapidly positive with increasing temperature and the calculated heat capacity becomes negative at $\mathrm{T} > 1100$ K. Thus, extrapolation of the thermal properties above 350 K may well be in error. The PN EOS did not provide the functionality to calculate the ideal gas heat capacity. However, as it has the same functional form as the OM EOS, the deviations will be come large at some temperature so that extrapolation for the thermal properties will give erroneous values.

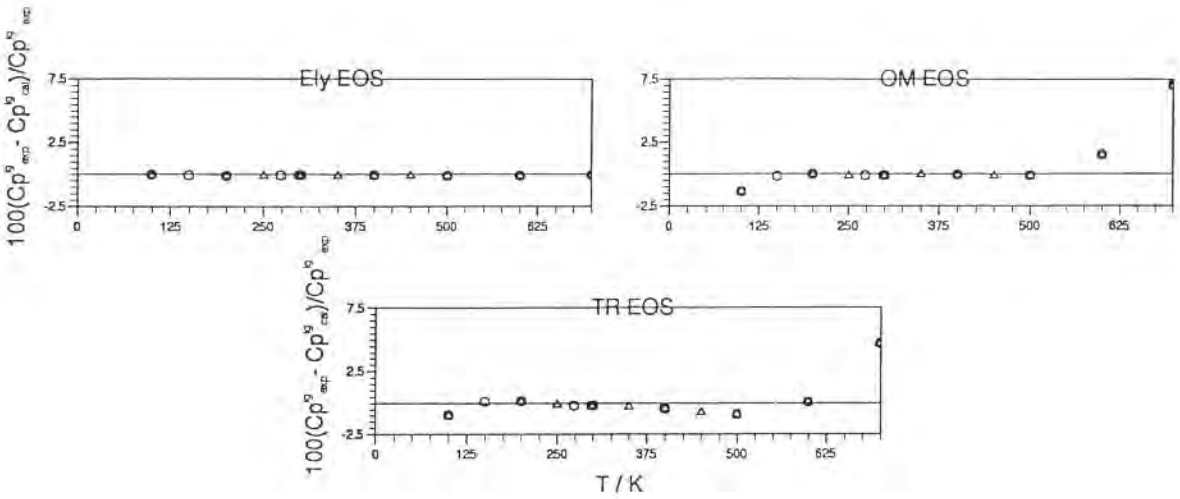

Figure 1.1 Comparison of ideal gas heat capacities with values calculated from the Ely, OM and TR EOSs. (△) Rodgers *et al.* (1974); (○) Chase *et al.* (1985).

1.2.2 Fixed points

Values for the measured triple point (Magee and Luddecke (1993)) and the critical points derived from the respective equations of state are listed in Table 1.A.

Table 1.A Fixed points for R32

EOS	T_t/K	T_b/K	T_c/K	P_c/MPa	ρ_c/(mol m^{-3})
OM	136.34	221.494	.	.	.
Ely		221.494	351.35	5.795	8207.8
PN		221.429	.	.	.
TR		221.493	351.351	5.7929	7956.2

1.3 Comparisons of the saturation properties

All the saturation properties were calculated from the equations of state by equating the Gibbs energies of the two phases, i.e. by setting $G_g(P,T) = G_l(P,T)$, so that along an isotherm

$$A_l + (P_\sigma/\rho_l) = A_g + (P_\sigma/\rho_g). \tag{1.5}$$

The saturated liquid heat capacities (C_σ) were calculated from each equation of state using the value for the saturated liquid density calculated using equation (1.5).

1.3.1 Vapour pressure

There are ten sets of measurements of the vapour pressure which are listed in Table 1.B. There is no single set which covers the whole temperature range from the triple point (136.34 K) to the critical point; the lowest temperature measurement is for the set by Kanungo *et al.* (1987).

Table 1.B Vapour pressure measurements for R32

Authors	Date	Temperature range/K	No. of points	Group
Bouchot & Richon	1994	253–334	8	2
Defibaugh *et al.*	1994	268–329	14	1
de Vries	1994	298–352	112	1
Holcomb *et al.*	1993	295–349	25	2
Kanungo *et al.*	1987	149–246	11	3
Magee & Howley	1993	270–330	7	1
Malbrunot *et al.*	1968	191–352	30	3
Nagel *et al.*	1993	204–352	27	2
Weber & Goodwin	1993	208–238	27	1
Weber & Silva	1994	235–267	17	1

We have classified the data into three groups. The first of these contains data, which are in close agreement with each other, are very precise, have small standard deviations (less than ±0.1%), and are mostly represented well within ± 0.15% for the Ely, OM and TR EOSs, as shown in figure 1.2. For the PN EOS, the data of Weber and Goodwin (1993) and Weber and Silva (1994) show systematic deviations. For the former at low temperatures this reaches -0.43% and all this data set's deviations are negative. As these deviations of group 1 data are larger than for the other EOSs so the limit of that graph in figure 1.2 has been extended to -0.5%.

Group 2 contains those data sets which deviate from the equations of state by more than those of group 1 but are still mostly within ±0.5%. The comparisons are shown in Figure 1.3.

Group 3 contains data which either deviate very systematically from all the equations, by amounts much greater than those of group 2 or display considerable scatter. Their comparisons are shown in figure 1.4. The TR EOS failed to find a solution for one datum point of the Malbrunot *et al.* (1968) data set as the experimental temperature of 351.54 K was above the critical temperature of the equation. Of some interest is the data of Kanungo *et al.* (1987) at the lowest temperatures since these are about 60 K below that of the Group 1 authors. At the lowest temperature of 149 K, these data deviate from the Ely, OM, PN, and TR EOSs by 0.005%, 1.517%, 0.328% and 1.107% respectively.

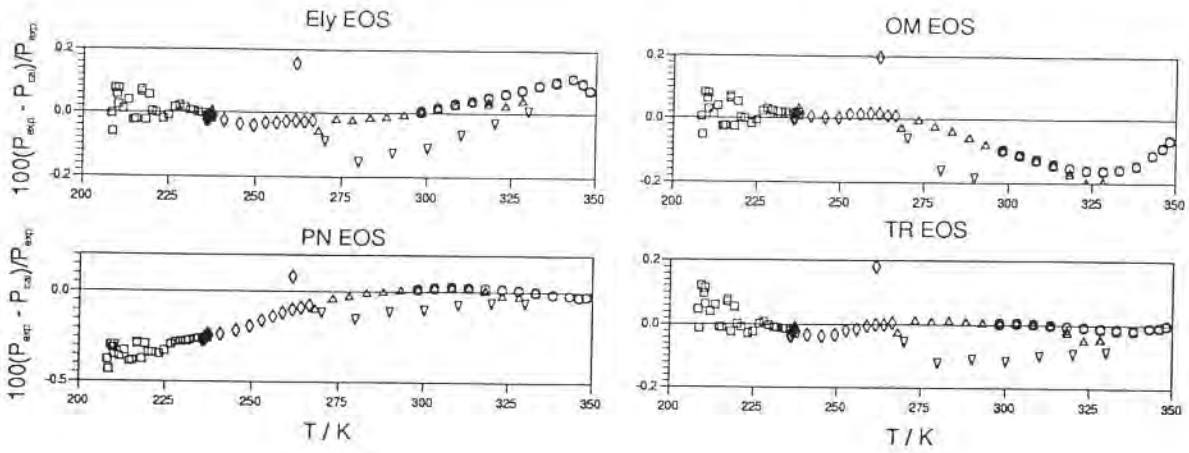

Figure 1.2 Comparison of group 1 experimental vapour pressures with values calculated from all four EOSs. (△) Defibaugh *et al.* (1994); (○) de Vries (1994); (▽) Magee & Howley (1993); (□) Weber & Goodwin (1993); (◇) Weber & Silva (1994).

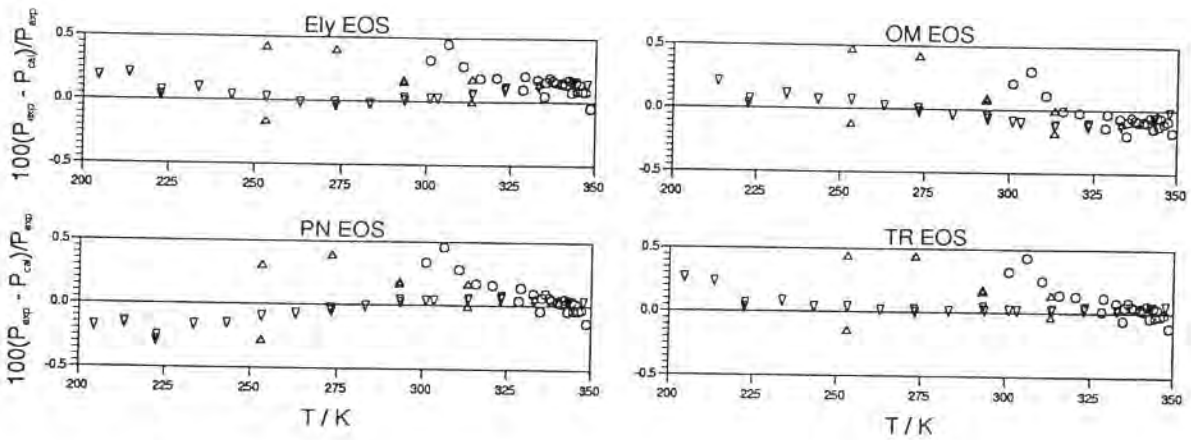

Figure 1.3 Comparison of group 2 experimental vapour pressures with values calculated from all four EOSs. (△) Bouchot and Richon (1994); (○) Holcomb *et al.* (1993); (▽) Nagel *et al.* (1993).

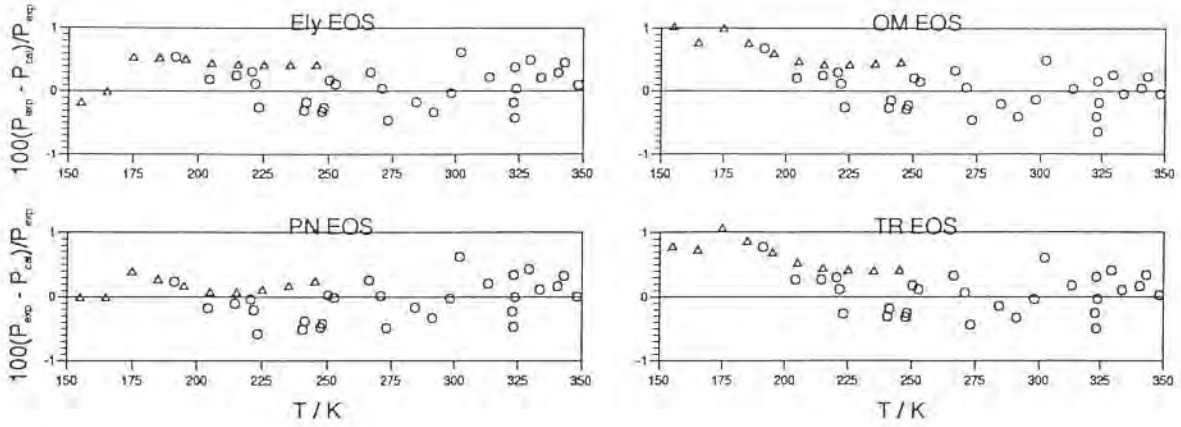

Figure 1.4 Comparison of group 3 experimental vapour pressures with values calculated from all four EOSs. (△) Kanungo *et al.* (1987); (○) Malbrunot *et al.* (1968).

1.3.2 Saturated liquid density

Seven sets of measurements of the saturated liquid density, which are listed in Table 1.C, have been compared with each of the equations of state and these comparisons are shown in figure 1.5.

Table 1.C Saturated liquid density measurements for R32

Authors	Date	Temperature range/K	No. of points
Bouchot and Richon	1994	253–334	5
Defibaugh *et al.*	1994	242–338	21
Higashi	1994	336–352	8
Holcomb *et al.*	1993	295–349	25
Magee and Howley	1993	138–305	13
Malbrunot *et al.*	1968	248–350	15
Shinsaka *et al.*	1985	150–222	20

All points in the data set of Shinsaka *et al.* (1985) systematically deviate from all four EOSs by between -0.6% and -1.0%. For the Malbrunot *et al.* (1968) data four points deviate by more than -0.2% from all the EOSs at temperatures well below the critical temperature. All of the remaining data sets up to 328 K are predicted by all of the EOSs to within ±0.15%. For the TR EOS, above 328 K, the data of Holcomb *et al.* (1993) and Defibaugh *et al.* (1994) deviate positively by up to 0.7% and 0.22% respectively, whereas the data of Higashi (1994) which is concentrated in the critical region show a strong negative bias with a maximum deviation of -9.4%. For the remaining three equations the Holcomb *et al.* (1993) data above 328 K show an increasingly negative bias as the

critical temperature is approached with maximum deviations ranging between -0.7% and -1.1%. The Defibaugh *et al.* (1994) data have small systematic positive deviations of up to 0.3% for the Ely EOS in this region. The Higashi (1994) data show increasingly negative deviations from the Ely and OM EOSs with maximum values of -13% and -12% respectively. For the PN EOS these data are randomly distributed with deviations ranging from -6.5% at 351 K to 9.0% at 351.3 K.

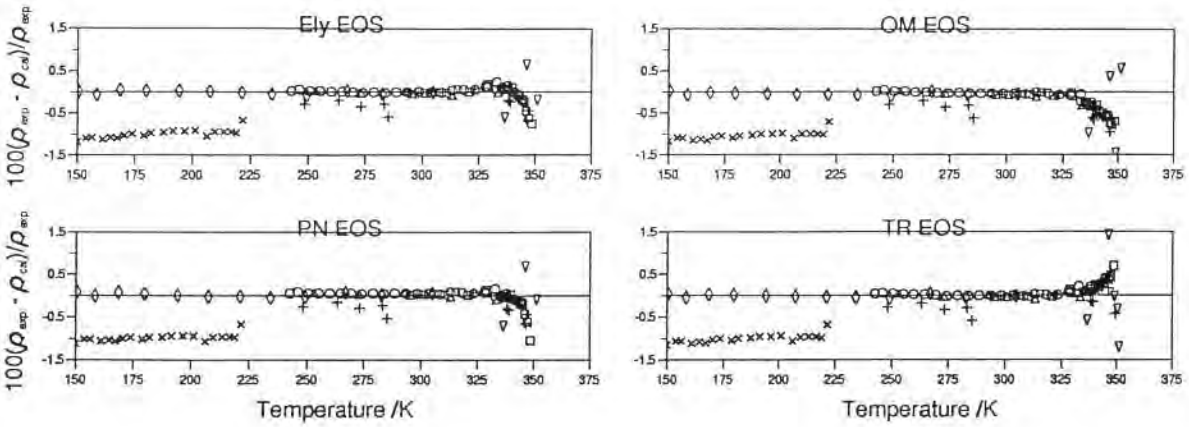

Figure 1.5 Comparison of experimental saturated liquid density measurements with values calculated from all four EOSs. (△) Bouchot and Richon (1994); (○) Defibaugh *et al.* (1994); (▽) Higashi (1994); (□) Holcomb *et al.* (1993); (◇) Magee and Howley (1993); (+) Malbrunot *et al.* (1968); (×) Shinsaka *et al.* (1985).

1.3.3 Saturated vapour density

There are four sets of data for the saturated vapour density which are listed in Table 1.D and comparisons of them with all the equations of state are shown in figure 1.6.

Table 1.D Saturated vapour density measurements for R32

Authors	Date	Temperature range/K	No. of points
Bouchot and Richon	1994	253–334	5
Defibaugh *et al.*	1994	219–343	28
Higashi	1994	340–352	9
Holcomb *et al.*	1993	295–349	25

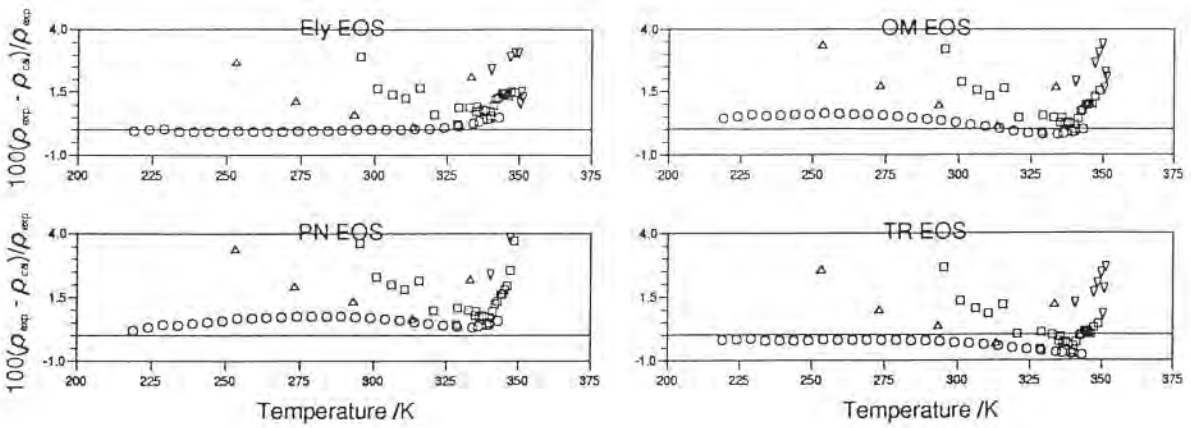

Figure 1.6 Comparison of experimental saturated vapour densities with values calculated from all four EOSs. (△) Bouchot and Richon (1994); (○) Defibaugh *et al.* (1994); (▽) Higashi (1994); (□) Holcomb *et al.* (1993).

The data of Defibaugh *et al.* (1994) span the widest range. For temperatures between 219 K and 319 K, the agreement with the Ely EOS is better than 0.1%. Above 319 K the deviations become increasingly positive, reaching 0.53% at 343 K. The remaining three EOSs show a different trend. The deviations of the Defibaugh *et al.* data from the OM and PN EOSs are predominantly positive reaching maxima of 0.67% at 254 K and 0.8% at 279 K repectively. The deviations from the TR EOS are all systematically negative. Between 219 K and 289 K they are within -0.2% or better, but above this temperature, the deviations increase reaching -0.75% at 343 K.

The data sets of Bouchot and Richon (1994), Higashi (1994) and Holcomb *et al.* are not represented as well by any of the EOSs. At 253 K the data of Bouchot and Richon (1994) deviate by more than 2.5% from all the EOSs, and from the Defibaugh *et al.* (1994) data. The data of Higashi (1994) are predominantly in the critical region and large deviations from all four EOSs are typical. The deviations from the Ely, OM, PN and TR EOSs are 5.8%, 5.3%, 5.8% and 4.7% respectively at 341.3 K. The data of Holcomb *et al.* (1993) agree with those of Defibaugh *et al.* (1994) to within 0.1% at 340 K, but at lower and higher temperatures, larger positive deviations are typical. Maximum values are 2.9%, 3.3% and 2.7% for the Ely, OM and TR EOSs respectively at 295.3 K and 3.7% at 348.6 K for the PN EOS.

1.3.4 Heat capacities of the saturated liquid

The range covered by the single set of data is listed in Table 1.E. Comparisons of the deviations from all four EOSs are shown in figure 1.7. The eight high temperature data points above 310 K all show increasingly negative deviations with all four EOSs with maximum deviations of -7.9% for the Ely EOS, -9.4% for the OM and PN EOSs and -11.0% for the TR EOS. At lower temperatures, the pattern of the deviations changes

with the EOS. Below 310 K the data are represented by the TR EOS to within ±0.7%. The data deviate positively from the Ely EOS at low temperature and between 175 K and 250 K by up to 1.4%. With the OM EOS the data deviate positively to a maximum of 4% at the lowest temperature. From 150 K to 310 K the data have smaller (up to -1.8%) negative deviations. With the PN EOS the data deviate strongly in a negative direction reaching -10.7% at 141 K which is just outside the stated range of the EOS. Between 170 K and 190 K the data show positive deviations (up to 0.8%) and from 190 K to 310 K the negative trend is resumed reaching -2% at 228 K.

Table 1.E Heat capacity measurements of the saturated liquid for R32

Authors	Date	Temperature range/K	No. of points
Magee & Luddecke	1993	141–343	95

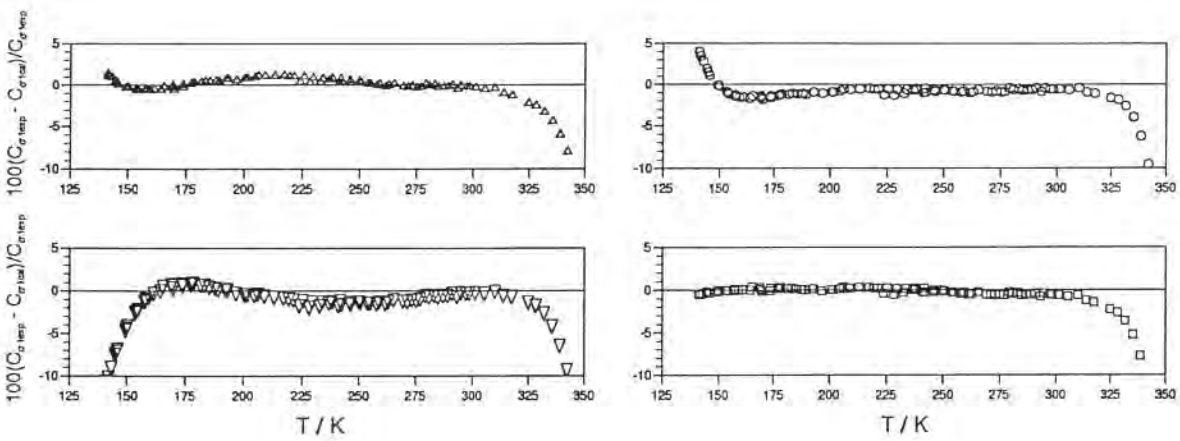

Figure 1.7 Comparison of the C_σ values of Magee and Luddecke (1993) with values calculated from all four EOSs. (△) Ely EOS; (○) OM EOS; (▽) PN EOS; (□) TR EOS.

1.4 Comparisons of the single-phase properties

The single-phase properties available for comparison include experimental values for PVT, second virial coefficient, isobaric (C_P) and isochoric (C_V) heat capacities, and the speed of sound ($\mathcal{W}$). These have been compared with all four equations of state.

1.4.1 PVT data

There are eight sets of density measurements by six authors, with a total of more than

1300 points, which are listed in Table 1.F together with the range covered by each author.

Table 1.F *PVT* data for R32

Authors	Date	No. of points	Temperature range/K	Pressure range/MPa	Density range/(mol m^{-3})
Bouchot and Richon	1994	36	253–334	0.1–9.5	51–21936
de Vries	1994	476	263–384	0.017–20.7	6–16756
Defibaugh *et al.*	1994	387	242–374	0.24–9.8	79-22427
Holste	1993	126	150–375	1.5–72	8673–27794
Malbrunot *et al.*	1968	143	248–474	0.5–20.2	381–22615
Magee and Howley	1993	137	139–396	3.6–35.1	13608–27350

Comparisons of the isothermal liquid phase data of Defibaugh *et al.* (1994) are shown in figures 1.8a, 1.8b and 1.8c.

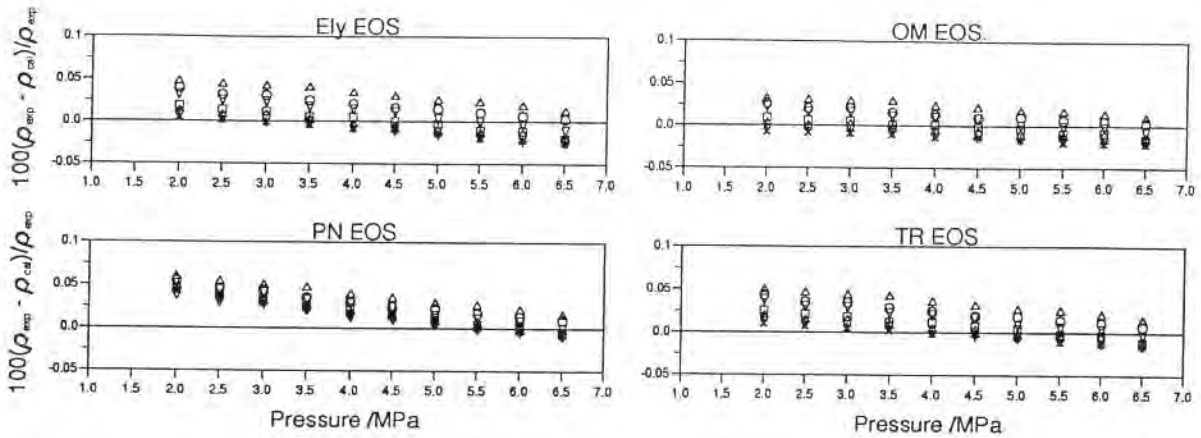

Figure 1.8a Comparison of experimental densities of Defibaugh *et al.* (1994) with values calculated from all four EOSs. Isotherms: (△) 243 K; (○) 246 K; (▽) 251 K; (□) 255 K; (◇) 260 K; (+) 265 K; (×) 269 K.

The densities on the near critical isotherm at 348.6 K deviate strongly from all four EOSs with all 25 points from the TR EOS and PN EOS, 11 points from OM EOS and 8 points from the Ely EOS in excess of 0.2%. The densities on the 347.7 K isotherm shows similar trends but on a reduced scale. The remaining six high temperature isotherms (313 K - 338 K) are fitted to within ±0.1% in density for the OM EOS except for one point, and to within 0.2% for the other three EOSs. The data from the eight intermediate (274 K - 308 K) and seven low temperature isotherms (242 K - 269 K) fit the OM EOS to within ±0.035%. For the low temperature isotherms, the deviations systematically become more positive with falling temperature and pressure, whereas the intermediate isotherms are systematically more positive with increasing temperature. The TR EOS shows a similar trend with the density deviations of the intermediate

isotherms being ±0.03%, whereas with the low temperature isotherms the deviations are up to 0.05%. The Ely EOS shows a similar trend, with the deviations of both sets of isotherms reaching 0.04% to 0.05%. The PN EOS has similar, but more marked trends. The density deviations of the data from the EOS become more positive with falling pressure for all isotherms with maxima of 0.06% for the low temperature isotherms and 0.09% for the intermediate ones.

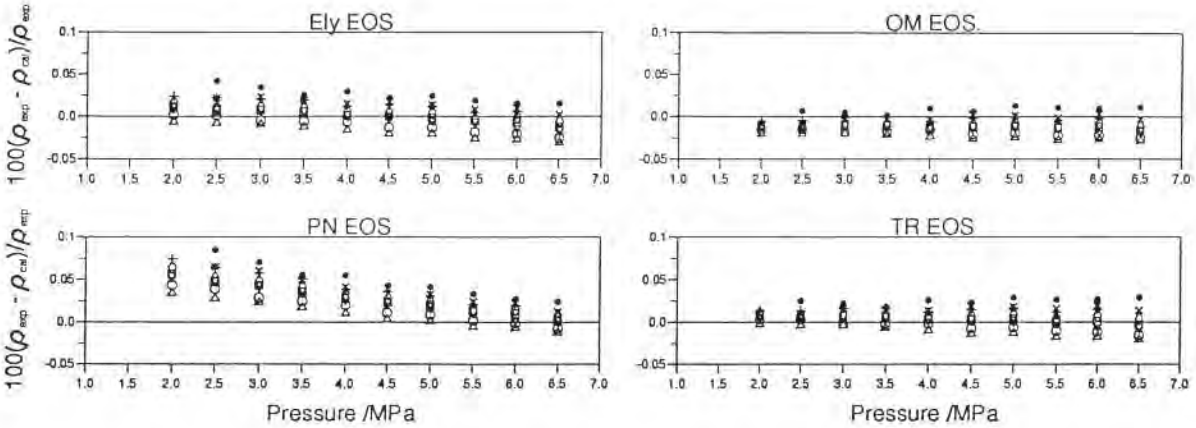

Figure 1.8b Comparison of experimental densities of Defibaugh *et al.* (1994) with values calculated from all four EOSs. Isotherms: (△) 274 K; (○) 279 K; (▽) 284 K; (□) 289 K; (◇) 293 K; (+) 298 K; (×) 303 K; (•) 308 K.

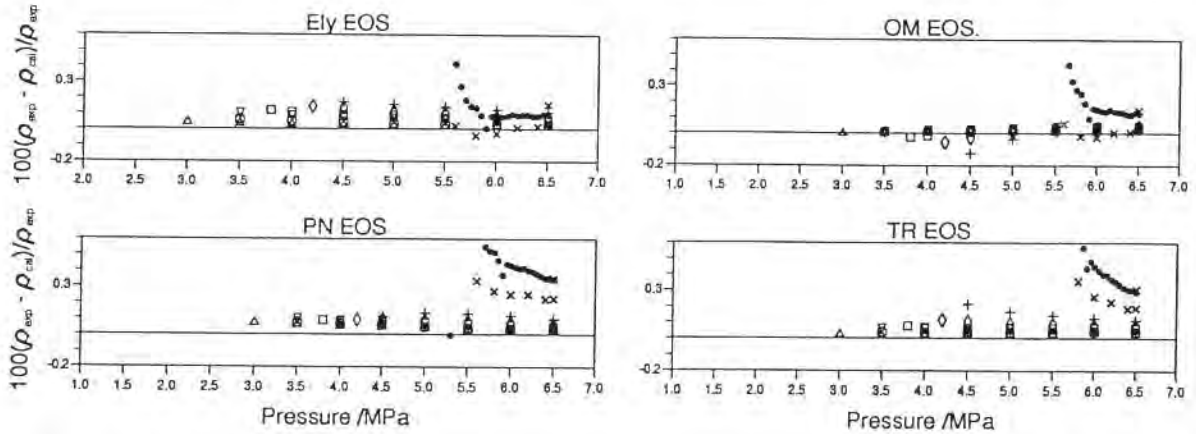

Figure 1.8c Comparison of experimental densities of Defibaugh *et al.* (1994) with values calculated from all four EOSs. Isotherms: (△) 313 K; (○) 318 K; (▽) 323 K; (□) 328 K; (◇) 333 K; (+) 338 K; (×) 347.7 K; (•) 348.6 K.

The isochoric liquid phase PVT data of Magee and Howley (1993), shown in figures 1.9a and 1.9b, are particularly well represented by the TR EOS, particularly be-

low temperatures of 340 K. The twelve high density isochores (19.6 mol dm^{-3} - 27.3 mol dm^{-3}) display deviations in density to within $\pm 0.026\%$. Of the two remaining isochores, only two out of thirteen points on the 17.9 mol dm^{-3} isochore and all the points on the 13.6 mol dm^{-3} isochore exceed this. Of the latter the deviations become more negative with increasing temperature reaching a maximum of -0.2% at 396 K.

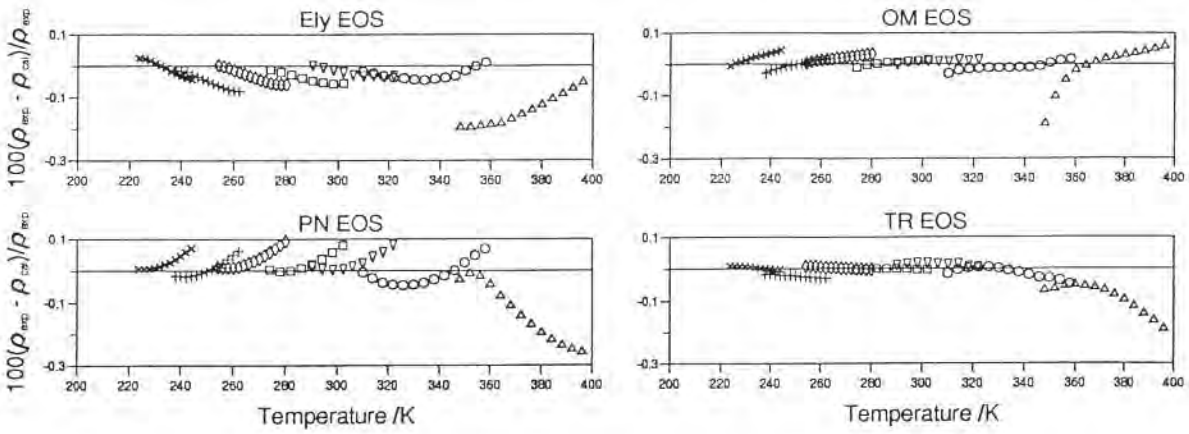

Figure 1.9a Comparison of experimental densities of Magee and Howley (1993) with values calculated from all four EOSs. Isochores in mol dm^{-3}: ($\triangle$) 13.6; ($\bigcirc$) 17.9; ($\triangledown$) 19.6; ($\square$) 20.6; ($\diamond$) 21.7; (+) 22.5;($\times$) 23.3.

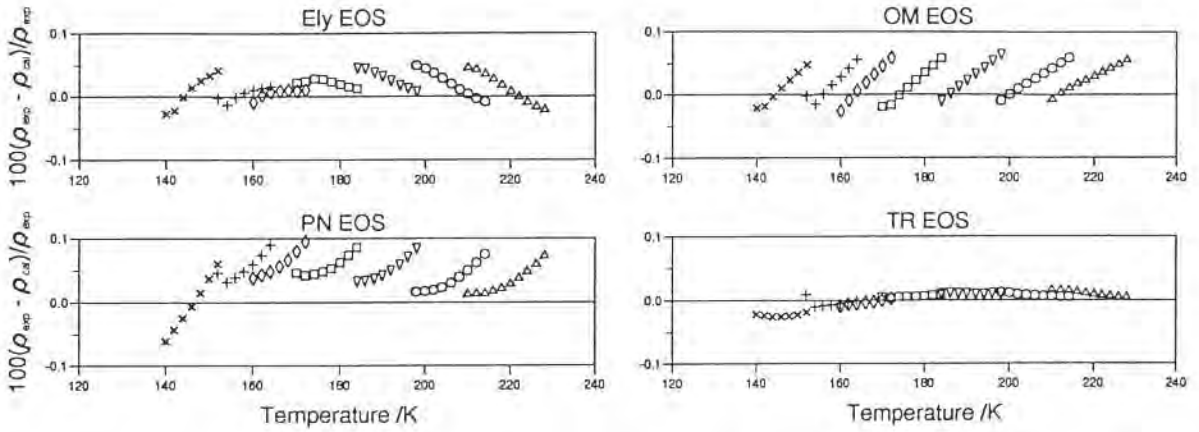

Figure 1.9b Comparison of experimental densities of Magee and Howley (1993) with values calculated from all four EOSs. Isochores in mol dm^{-3}: ($\triangle$) 24.0; ($\bigcirc$) 24.6; ($\triangledown$) 25.3; ($\square$) 25.9; ($\diamond$) 26.4;(+) 26.7;($\times$) 27.3.

For the Ely EOS the density deviations for the twelve high density isochores are within $\pm 0.06\%$ with the exception of five points on the 22.5 mol dm^{-3} isochore where the deviations reach a maximum of -0.08%. The lowest density isochore (13.6 mol dm^{-3})

has deviations in density from -0.05% to -0.2%. The deviation plots of the twelve isochores are systematic with significant slopes; the three highest density (26.4 mol dm^{-3} to 27.3 mol dm^{-3}) and the lowest density (13.6 mol dm^{-3}) isochores have positive slopes with respect to temperature, the central eight (19.6 mol dm^{-3} to 25.3 mol dm^{-3}) negative slopes and the two intermediate (17.9 mol dm^{-3},25.8 mol dm^{-3}) isochores pass through a turning point. The OM EOS shows deviations ranging from -0.026% to 0.064 % for the twelve high density isochores and -0.2% to 0.06% for the lowest density isochore (13.6 mol dm^{-3}). The deviations along all the isochores show positive slope with repect to temperature. The density deviations from the PN EOS are much greater. They range from -0.06% to 0.1% for the twelve high density isochores. Apart from the three high density isochores which show positive slopes the slopes of the deviations along each isochores are initially negative or zero but become significantly positive with increasing temperature. The lowest density isochore, as with all the other EOSs, shows anomalous behaviour. The deviations range from close to zero to -0.26% at 396 K.

The data of Holste (1993) range from the low temperature compressed liquid to the supercritical dense fluid region (figure 1.10) with a small overlap with the data of Defibaugh *et al.* (1994).

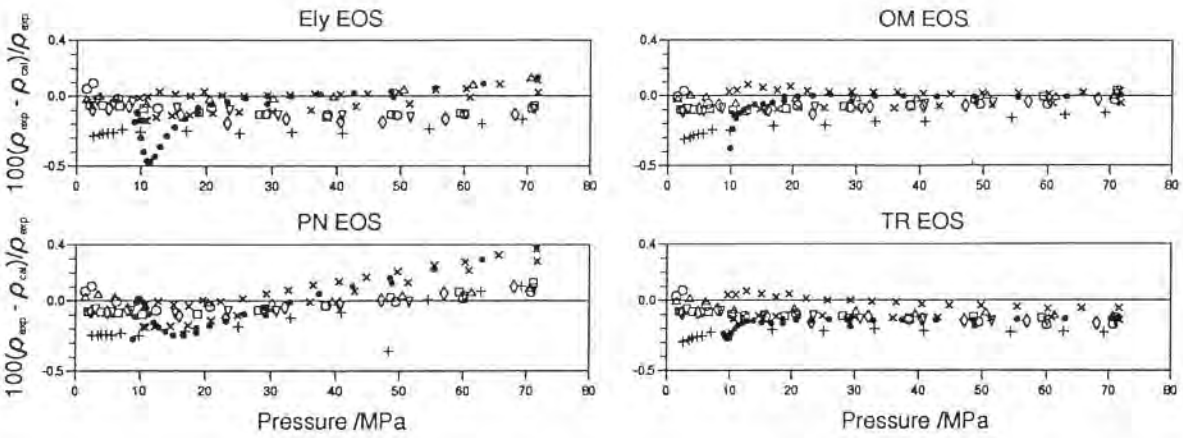

Figure 1.10 Comparison of experimental densities of Holste (1993) with values calculated from all four EOSs. Isotherms: (△) 150 K; (○) 175 K; (▽) 200 K; (□) 225 K; (◇) 250 K; (+) 300 K; (×) 350 K; (•) 375 K.

Two points on the 300 K isotherm at 1.9 MPa and 48.3 MPa deviate in density from all four EOSs by more than -0.31%. The remaining data deviate in density from the TR EOS by between -0.29% and 0.08%. In the region of overlap with the Defibaugh data, the deviations lie between -0.1% and -0.3%. In general the density deviations display a pronounced negative bias. For the OM EOS the density deviations are similar to the TR EOS but with a less negative bias and there are also five points on the 375 K isotherm between 9.0 MPa and 10.0 MPa which exceed -0.31% with a maximum of -1.54% at 9.0 MPa. With the Ely EOS, the density deviations are similar, lying generally between -0.3% and 0.15%. There are, however, five points on the 375 K

isotherm between 10.3 MPa and 12.9 MPa where the density deviations lie between -0.5% and -0.35%. Apart from the two outliers on the 300 K isotherm the PN EOS fits the data to within -0.3% and 0.4%. However, unlike the other EOSs, all of these isotherms show increasingly positive deviations as the pressure increases.

The liquid phase density measurements of Malbrunot *et al.* (1968) cover a more restricted range of PVT space than Holste (1993) and are overlapped by them completely. The deviations of the data (figure 1.11) from all four EOSs are similar, and similar to that of Holste (1993) lying between -0.35% and 0.06%. Two outliers, however, on the 343 K isotherm at 5.1 MPa and 6.1 MPa lie outside this range for all the EOSs. Their deviations are between -0.5% and -1.2% respectively.

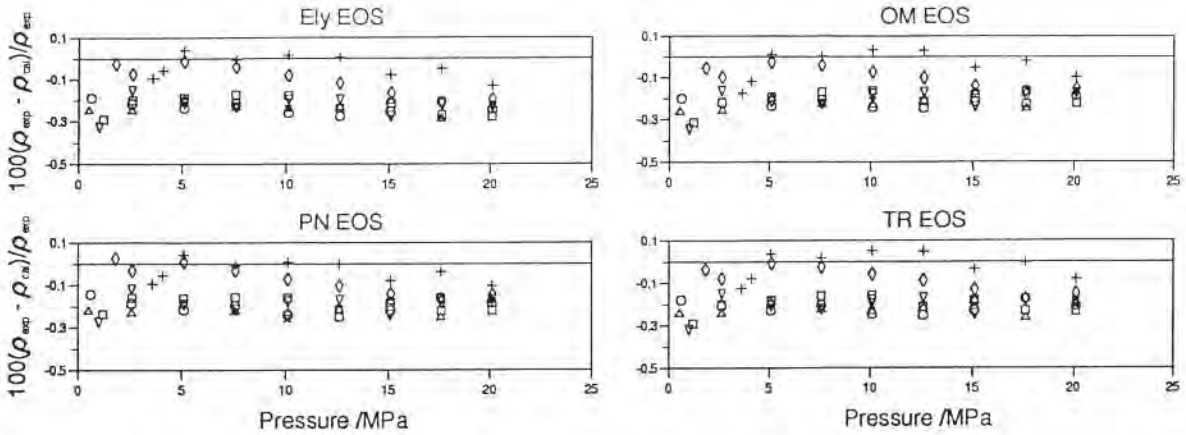

Figure 1.11 Comparison of experimental densities of Malbrunot *et al.* (1968) with values calculated from all four EOSs. Isotherms: (△) 248 K; (○) 263 K; (▽) 273 K; (□) 283 K; (◇) 298 K; (+) 323 K; (×) 343 K.

The isothermal gas phase data of de Vries (1994) cover an extensive range. The deviations are shown in figures 1.12a and 1.12b. With the exception of 18 data points the TR EOS represents all 476 densities to within ±0.1%. The majority of the exceptions (11) are clustered around the critical region in the range 352 K to 355.2 K and 5.8 MPa to 7.85 MPa. The remainder are scattered throughout the data set with five points on the low temperature isotherms (263 K - 343 K), one at high pressure on the near critical isotherms (347 K - 355 K) and one on the supercritical isotherms (373 K - 383 K). For the Ely EOS, 46 density deviations lie outside the 0.1% range with 17 clustered in the critical region from 352 K to 355.2 K and 5.6 MPa to 8.3 MPa. There are other clusters with 12 on the supercritical isotherms between 2 MPa and 12.7 MPa and with 6 on the 303.15 K isotherm between 0.7 MPa and 1.85 MPa. The remainder are scattered throughout the data set with eight points on the low temperature isotherms, and three further points on the near critical isotherms. The density deviations display a positive bias up to 5.4 MPa. With the OM EOS, the positive bias evident for the Ely EOS for pressures below 5.4 MPa is more pronounced and is most marked at the lowest

temperatures between 263 K and 313.2 K. In this region a total of 41 data points have deviations in density greater than 0.1%. In total 116 of the 476 data points have density deviations greater than 0.1% and 52 greater than 0.2%. Twenty five of the 116 are in the critical region (352 K - 355.2 K, and 2.9 MPa - 7.9 MPa), and 30 lie on the supercritical isotherms.

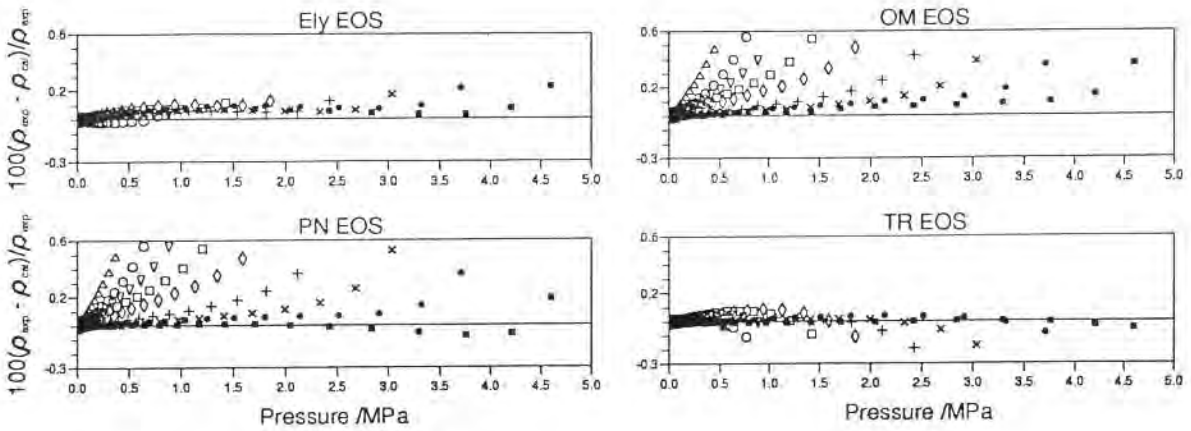

Figure 1.12a Comparison of experimental densities of de Vries (1994) with values calculated from all four EOSs. Isotherms: (△) 263 K; (○) 273 K: (▽) 283 K; (□) 293 K; (◇) 303 K; (+) 313 K; (×) 323 K; (•) 333 K; (▪) 343 K.

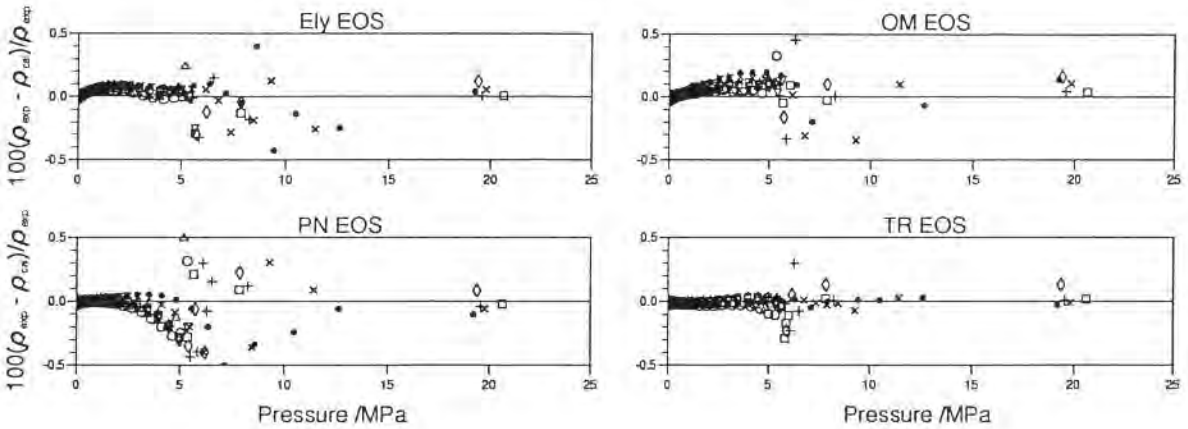

Figure 1.12b Comparison of experimental densities of de Vries (1994) with values calculated from all four EOSs. Isotherms: (△) 347 K; (○) 349 K; (▽) 351 K; (□) 352 K; (◇) 353 K; (+) 355 K; (×) 373 K; (•) 383 K.

Below 333.2 K, the PN EOS displays very similar trends in the density deviations as the OM EOS. In this region, 54 of the data points deviate by more than 0.1%. At higher temperatures, especially above 2.5 MPa, the positive bias is reversed. In the critical

region (352 K - 355.2 K, and 3.9 MPa - 8.3 MPa), 27 data points deviate in density by more than 0.1% from the EOS, while along the supercritical isotherms the number is 13. In total 110 data points deviate from the PN EOS by more than 0.1% and 71 by more than 0.2%.

The gas phase data of Defibaugh *et al.* (1994) consist of one isotherm at 373 K and eleven isochores. The differences in the density prediction along the 373 K isotherm of de Vries (1994) and Defibaugh *et al.* (1994) by all the EOSs are shown in figure 1.13 and indicate that there are some systematic differences which reach 0.18% in density at 3.5 MPa. The representation of the isotherm differs for each EOS. With the TR EOS, the deviations are all negative and reach a maximum value of -0.17% at 3.5 MPa. The density deviations of the Ely EOS shows in general a negative bias, which, with the exception of the value at 9.77 MPa, becomes more pronounced at pressures above 2 MPa. Even so, with the exception of a single point at 7.73 MPa the deviations remain within 0.1%. The density deviations from the OM EOS are less systematic and are with the exception of the single point at 7.73 MPa, within ±0.065%. The density deviations from the PN EOS display similar behaviour to the Ely EOS. Excluding the outlier at 7.73 MPa the maximum value is -0.47% at 6.1 MPa.

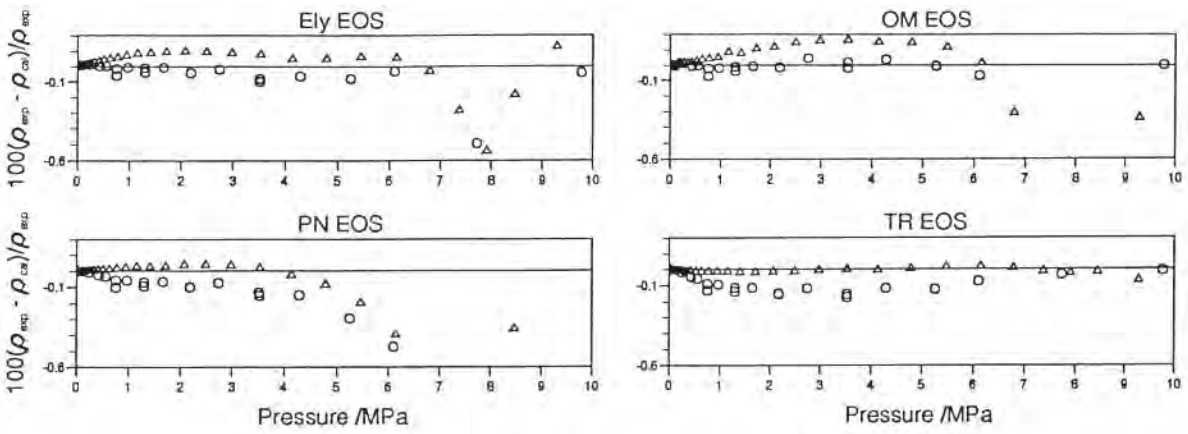

Figure 1.13 Comparison of experimental densities along the 373 K isotherm of de Vries (1994) and Defibaugh *et al.* (1994) with values calculated from all four EOSs. (△) de Vries (1994); (○) Defibaugh *et al.* (1994).

Comparisons of the isochoric data of Defibaugh *et al.* (1994) are shown in figures 1.14a and 1.14b. Along the low density isochores at 0.14 mol dm^{-3} and 0.25 mol dm^{-3} below 330 K the TR and Ely EOSs display similar behaviour. If the point at 322.13 K and 0.38 MPa, which appear to be in error, is discounted, the density deviations are positive and level out to values around 0.1% for the 0.25 mol dm^{-3} isochore and 0.25% for the 0.14 mol dm^{-3} isochore. Between 0.4 mol dm^{-3} and 3.4 mol dm^{-3} or above 330 K, the TR and Ely EOSs fit the data to within ±0.2% in general with 4 points for the TR EOS and one point for the Ely EOS outside this range.

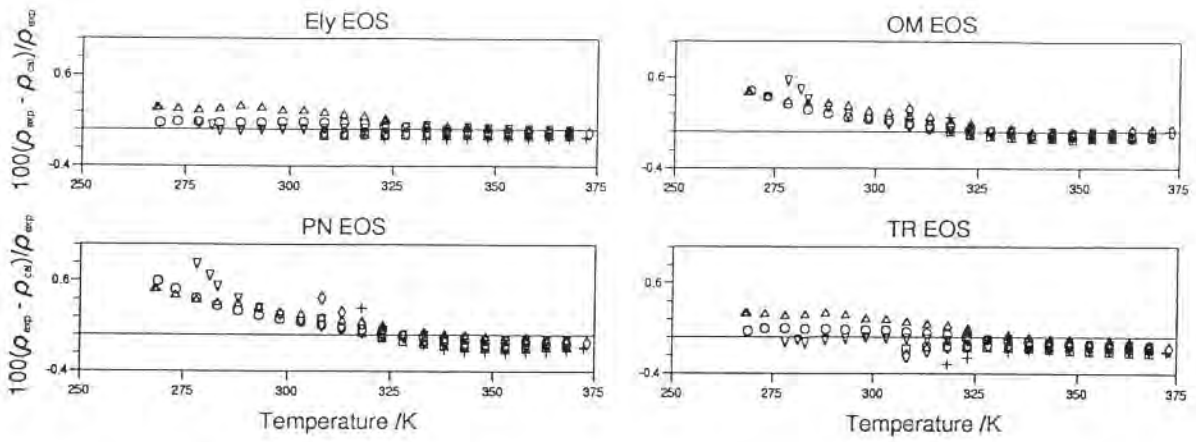

Figure 1.14a Comparison of experimental densities of Defibaugh *et al.* (1994) with values calculated from all four EOSs. Isochores in mol dm^{-3}: (△) 0.14; (○) 0.25; (▽) 0.45; (□) 0.81; (◇) 1.05; (+) 1.4.

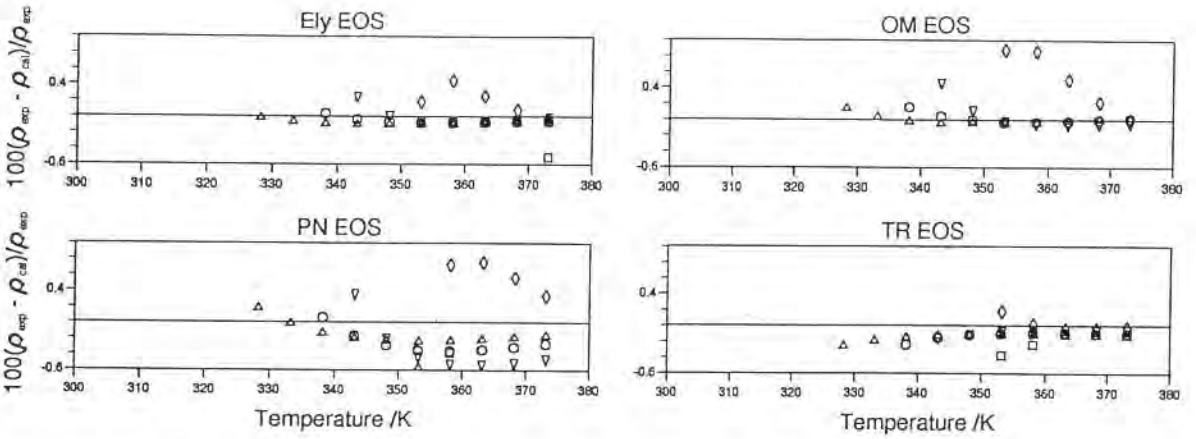

Figure 1.14b Comparison of experimental densities of Defibaugh *et al.* (1994) with values calculated from all four EOSs. Isochores in mol dm^{-3}: (△) 1.88; (○) 2.56; (▽) 3.34; (□) 5.95; (◇) 10.6.

The data point at 353.1 K on the 0.14 mol dm^{-3} isochore appears to be in error and deviates positively by about 1.5% from both EOSs. The TR EOS in this region displays a bias of around -0.1% which is not so pronounced for the Ely EOS. For the near critical isochores at 5.95 mol dm^{-3} and 10.6 mol dm^{-3}, the deviations in density for the TR and Ely EOSs are larger. For the Ely EOS the deviations along the 5.95 mol dm^{-3} isochore are systematically negative reaching a maximum value of -1.44% at 353.1 K and 5.93 MPa. The TR EOS displays smaller deviations, with a maximum value of -0.37% at 353.11 K and 5.93 MPa.

For the OM and PN EOSs, the positive trend in density deviation on the 0.14 mol dm^{-3} and 0.25 mol dm^{-3} isochores below 330 K noted for the TR EOS and

Ely EOS is also apparent, except that the deviations become increasingly positive with falling temperature. Also this trend is apparent for the 0.45 mol dm^{-3} and to a lesser extent the 0.81 mol dm^{-3} and 1.05 mol dm^{-3} isochores. Maximum values for the density deviations in this region are 0.56% and 0.78% for the OM EOS and PN EOS respectively on the 0.45 mol dm^{-3} isochore at 278.15 K and 0.88 MPa. Above 330 K for isochores between 0.14 mol dm^{-3} and 2.56 mol dm^{-3}, the OM EOS represents the data within 0.1% in density except for one point on the 2.56 mol dm^{-3} isochore at 338.1 K and 4.0 MPa. The representation of the data in this range by the PN EOS is less precise and there is a distinct negative bias. In general the representation is within ±0.2% with 12 points outside this range, and 33 points exceed 0.1%. Of the 12 points which exceed ±0.2%, eight are along the 2.56 mol dm^{-3} isochore. For the isochores between 3.3 mol dm^{-3} and 10.7 mol dm^{-3}, which span the critical density, the density deviations are in general greater than elsewhere. For the OM EOS, four of the five densities along the 5.95 mol dm^{-3} isochore have deviations greater than 2%. For the PN EOS, the maximum density deviation along this isochore is 2.26% at 353.11 K and 5.93 MPa.

The gas phase data of Malbrunot *et al.* (1968) extend into the supercritical region up to 473 K and 20.0 MPa. The deviations from all four EOSs are shown in figure 1.15a and 1.15b. Large deviations in density from all four EOSs are typical over the entire temperature and pressure range and these frequently exceed ±1% with several points lying in the ±4% range.

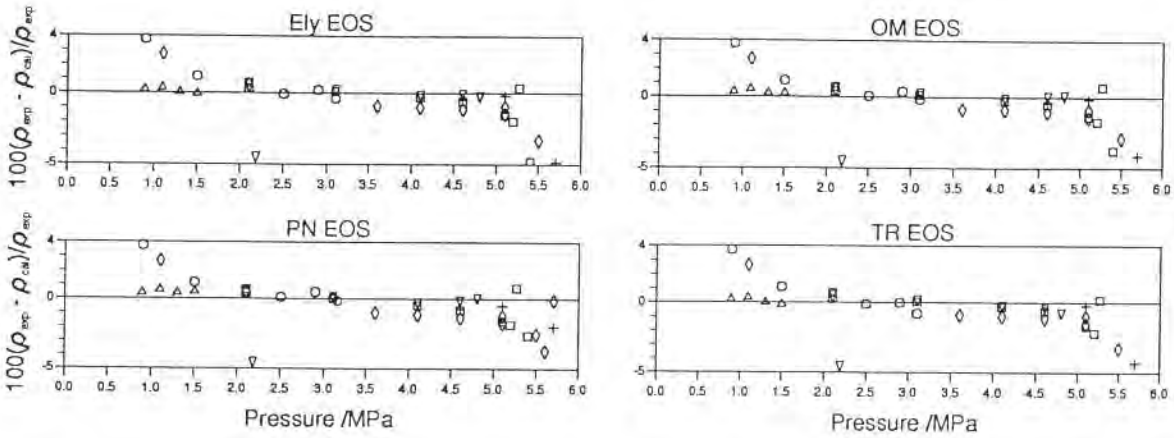

Figure 1.15a Comparison of experimental densities of Malbrunot *et al.* (1968) with values calculated from all four EOSs. Isotherms: (△) 298 K; (○) 323 K; (▽) 343 K; (□) 348 K; (◇) 350 K; (+) 351 K.

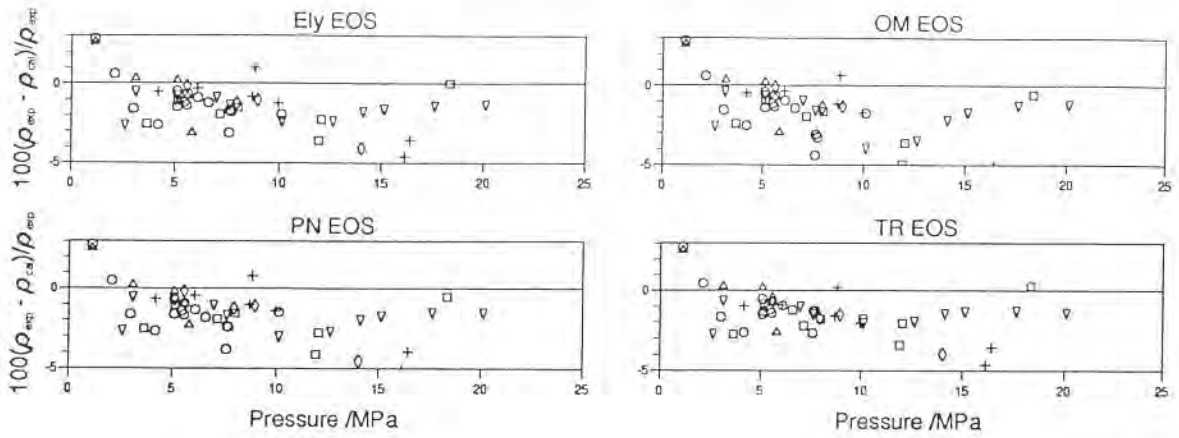

Figure 1.15b Comparison of experimental densities of Malbrunot *et al.* (1968) with values calculated from all four EOSs. Isotherms: (△) 353 K; (○) 373 K; (▽) 398 K; (□) 423 K; (◇) 448 K; (+) 473 K.

The data of Bouchot and Richon (1994) cover both the liquid and gas phases along each isotherm. The density deviations from all four EOSs are shown in figure 1.16.

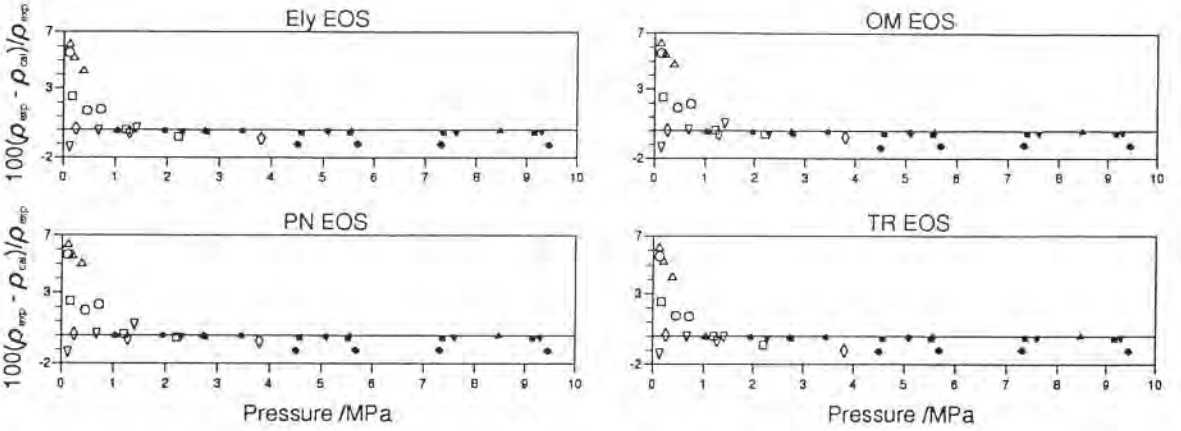

Figure 1.16 Comparison of experimental densities of Bouchot and Richon (1994) with values calculated from all four EOSs. Isotherms: (△) 253 K; (○) 273 K; (▽) 293 K; (□) 313 K; (◇) 333 K. - open symbols represent the gas phase, filled symbols the liquid phase

The liquid phase data overlaps that of Holste (1993). The liquid phase density deviations from all four EOSs are very similar and show a slight negative bias. With the exception of the OM EOS at 333.4 K and 4.5 MPa all the EOSs represent the data to within ± 0.2%. The gas phase data show large deviations from all four EOSs, especially below 1.0 MPa. On the 253.2 K isotherm at 0.118 MPa the deviations in density for all four EOSs exceed 6%.

1.4.2 Second virial coefficient

The temperature range for the single set of second virial coefficient values is given in Table 1.G. The TR, OM and Ely EOSs all gave similar results, within the restricted temperature range with systematic negative deviations to within -3.0%. The PN EOS did not provide a virial coefficient calculation.

Table 1.G Second virial coefficient data for R32

Authors	Date	No. of points	Temperature range/K
Bignell and Dunlop	1993	3	290–310

1.4.3 Isochoric heat capacity

There is one set of 74 measurements of the isochoric heat capacity, C_V, in the liquid phase by Magee and Luddecke (1993) which covers the temperature range 152–342 K for densities from 17.4 to 26.8 mol dm^{-3}. The deviations in C_V from the four EOSs are given in figure 1.17. This shows good agreement with the Ely, OM and TR EOSs where the C_V deviations are in general ±1.0%, with six values for the Ely EOS, two for the TR EOS and 13 for the OM EOS outside this range. Along the 17.5 mol dm^{-3} isochore all the data points deviate positively from the OM EOS. On the other hand, the deviations from the PN EOS are greater, and generally to ±2%. Thirty eight points lie outside the ±1.0% range. The deviations along individual isochores are more systematic than for the other three EOSs and increase with increasing temperature.

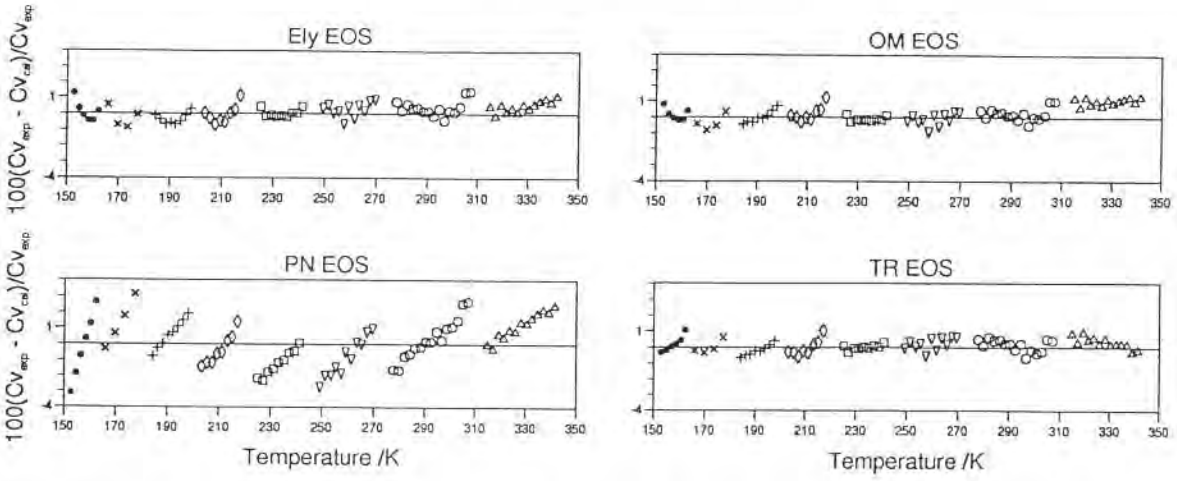

Figure 1.17 Comparison of experimental isochoric heat capacities of Magee and Luddecke (1993) with values calculated from all four EOSs. (△) 17.5 mol dm^{-3}; (○) 20.3 mol dm^{-3}; (▽)22.0 mol dm^{-3}; (□) 23.3 mol dm^{-3}; (◇) 24.4 mol dm^{-3}; (+) 25.3 mol dm^{-3}; (×) 26.1 mol dm^{-3}; (•) 26.8 mol dm^{-3}.

1.4.4 Isobaric heat capacity

There is one set of measurements of the liquid phase isobaric heat capacity, C_P, and its temperature and pressure range is given in Table 1.H. The deviations of the isobaric heat capacity data, shown in figure 1.18, indicate a negative bias with all four EOSs. There are small differences between the equations but all four EOSs display similar trends. The deviations range from -0.12% to -1.03%, -0.36% to -1.42%, -0.15% to -1.64% and 0.04% to -2.06% for the Ely, TR, OM and PN EOSs respectively.

Table 1.H Isobaric heat capacity measurements for R32

Authors	Date	No. of points	Temperature range/K	Pressure range/MPa
Yomo *et al.*	1994	26	275–315	2.1–3.0

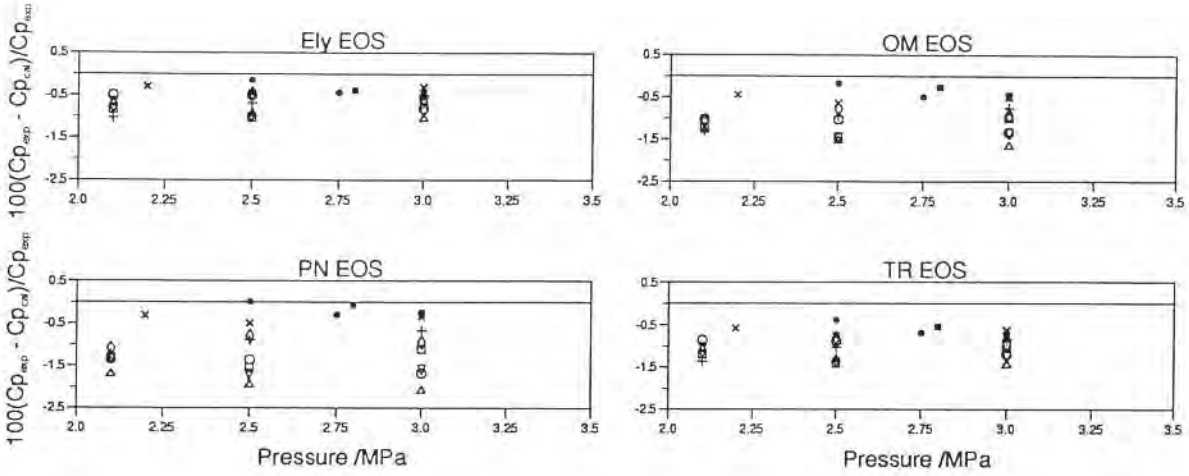

Figure 1.18 Comparison of experimental isobaric heat capacities of Yomo *et al.* (1994) with values calculated from all four EOSs. Isotherms: (△) 276 K; (○) 280 K; (▽) 285 K; (□) 290 K; (◇) 295 K; (+) 300 K; (×) 305 K; (•) 310 K; (▪) 315 K.

1.4.5 Speed of sound

There are speed of sound measurements in both the liquid and vapour phases and the ranges covered by the two sets are listed in Table 1.I. Speed of sound measurements are related to the second density derivative of the Helmholtz function and thus are a severe test of any EOS.

Table 1.I Speed of sound measurements for R32

Authors	Date	Temperature range/K	Pressure range/MPa	No. of points
Grebenkov *et al.*	1994	286–341	1.4–10.4	30
Hozumi *et al.*	1994	273–343	0.019–0.26	66

The comparisons of the liquid phase data of Grebenkov *et al.* (1994) are shown in figure 1.19. These data are well represented by the Ely EOS with deviations generally in the range ±0.35%, with only one point outside the range at 325.9 K and 4.29 MPa. The comparisons show a slight positive bias. The deviations from the TR EOS are all negative and range from -0.70% and -0.05%. The data deviate more widely from both the OM EOS and the PN EOS. The deviations of the speed of sound data from the OM EOS are all negative with a maximum value of -2.59% at 325.9 K and 3.36 MPa. With the exception of the 287 K and 302.4 K isotherms for which positive deviations up to 2.4% and 1.8% respectively are typical, the data scatter more uniformly about the PN EOS to within ±0.5%.

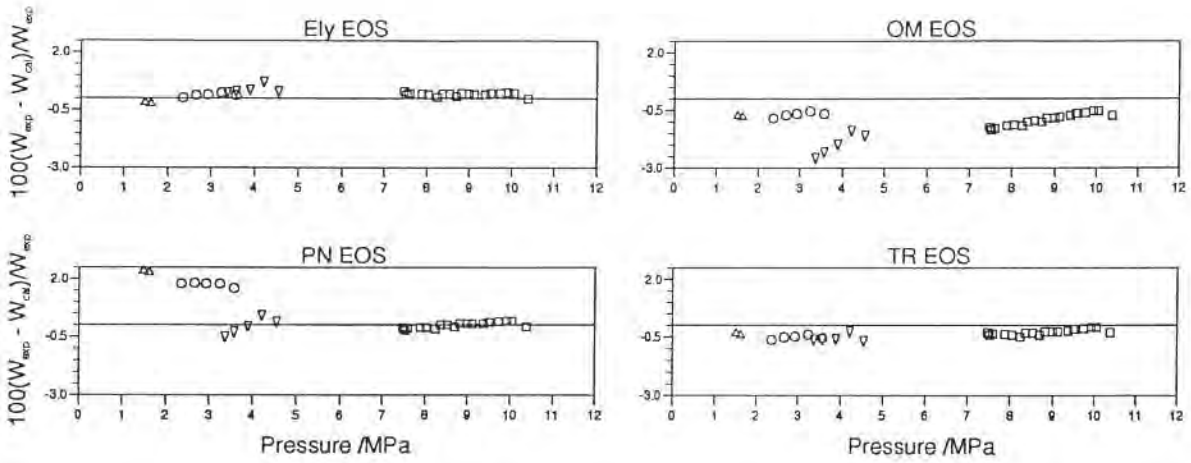

Figure 1.19 Comparison of experimental speed of sound measurements of Grebenkov *et al.* (1994) with values calculated from all four EOSs. Isotherms: (△) 287 K; (○) 302 K; (▽) 326 K; (□) 341 K.

The comparisons of the gas phase data of Hozumi *et al.* (1994) with the four EOSs are shown in figure 1.20. The TR EOS represents these data within ±0.023%. The experimental values deviate systematically from the Ely EOS between -0.025% at 323.15 K, 0.04 MPa and -0.05% at 343.15 K, 0.26 MPa. The small negative offset (-0.032%) for the deviations near zero pressure and the nearly constant offset as the pressure increases suggest that the Hozumi *et al.* (1994) data and the ideal gas heat capacity equation used by the Ely EOS are inconsistent. The differences are thus attributable to the ideal part of the Helmholtz equation of state and not the residual part. The deviations from the PN EOS lie between 0.014% at 0.02MPa and -0.067% at 0.12 MPa for the 273 K

isotherm and -0.05% to -0.001% for the rest. With a zero pressure deviation in the speed of sound of about zero, the differences between the data and the PN EOS can be attributed to the residual part of the equation of state. The deviations from the OM EOS are larger, lying between -0.027% at 323.15 K and 0.2 MPa and -0.081% at 273.16 K and 0.12 MPa. The zero pressure deviation of about -0.03% and the increasingly negative deviations with increasing pressure, imply that the differences can be attributed partly to an inconsistency between this data set and the OM EOS ideal gas heat capacity equation and partly to the representation of the residual part of the equation of state.

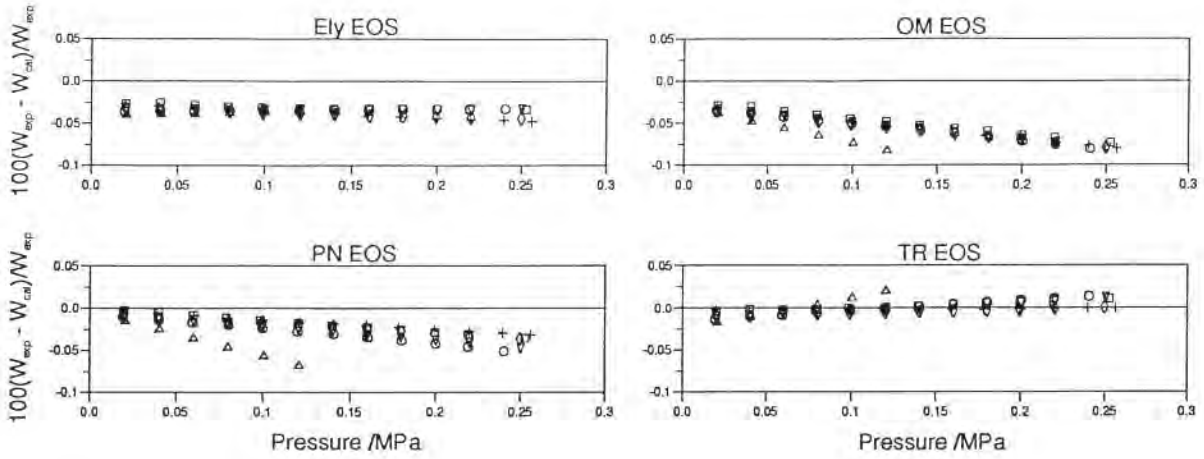

Figure 1.20 Comparison of experimental speed of sound measurements of Hozumi *et al.* (1994) with values calculated from all four EOSs. Isotherms: (△) 273 K; (○) 308 K; (▽) 313 K; (□) 323 K; (◇) 333 K; (+) 343 K.

1.5 Summary for R32

The five group 1 vapour pressure data sets are represented by the Ely, OM and TR EOSs to within ±0.15%. The data sets of Weber and Goodwin (1993) and Weber and Silva (1994) show systematic deviations from the PN EOS.

Below 328 K, with the exception of the Malbrunot (1968) and Shinsaka *et al.* (1995) data sets, the saturated liquid density data sets are represented by all four EOSs to within ±0.15%. Above 328 K the data have small positive deviations from the TR EOS, and small negative deviations from the Ely EOS. Those from the TR EOS are closer to zero. The deviations from the OM and PN EOSs are larger in this region.

The Defibaugh *et al.* (1994) saturated vapour density data are best represented by Ely EOS (to within ±0.1%), although the TR EOS does nearly as well it has a negative bias. Other authors' data sets are not well represented by any of the EOSs.

The saturated liquid heat capacity data of Magee and Luddecke (1993) are best represented by the TR EOS (to within ±0.7% below 310 K).

The low temperature (242 K to 269 K) isotherms and high temperature (313 K to 338 K) isotherms of the Defibaugh *et al.* (1994) liquid phase PVT data set are

best represented by the OM EOS. The intermediate (274 K to 308 K) isotherms are best represented by the TR EOS, although the representation by OM EOS is very similar. The liquid phase isochoric data of Magee and Howley (1993) are particularly well represented by the TR EOS. The Holste data set shows a greater variation amongst the four EOSs. The TR EOS has fewest outliers and generally represents the data well but above 20 MPa the OM EOS best represents the data.

The gas phase data of de Vries (1994) is best represented by the TR EOS with the density deviations of only 18 out the 476 points lying outside the $\pm 0.1\%$ range. The Ely EOS represents the data quite well, but with a larger number of points (46) outside this range. Above 0.75 MPa the gas phase data of de Vries (1994) and Defibaugh *et al.* (1994) show systematic differences in density along their common 373 K isotherm of up 0.18%. The low density isochores ($\rho \leq 1.4$ mol dm^{-3}) are well represented by the Ely and TR EOSs with the former doing slightly better. Above 330K, the representation of the data by these EOSs is very similar in general, but the TR EOS represents the data better along the near critical isochores (5.95 mol dm^{-3} and 10.6 mol dm^{-3}).

The isochoric heat capacity data of Magee and Luddecke (1993) are well represented by the Ely, OM and TR EOSs with the last having the fewest deviations outside the $\pm 1.0\%$ range. The deviations from the isobaric heat capacity data of Yomo *et al.* (1994) are similar for all four EOSs, with the Ely EOS showing the least scatter.

The liquid speed of sound data of Grebenkov *et al.* (1994) are best represented by the Ely EOS. The deviations from the TR EOS are similar but have a pronounced negative bias. The gas phase speed of sound data is best represented by the TR EOS. The representations of the gas phase speed of sound data by all four EOSs suggest that there are inconsistencies between this data set and the values of the ideal gas heat capacity calculated from spectroscopic data (Rodgers *et al.* (1974), Chase *et al.* (1985)).

2 Refrigerant R125

The number of measurements for R125 is smaller than that for R32 with about 1800 experimental points in 30 data sets. The properties in these sets include: vapour pressures, saturated liquid and vapour densities, liquid phase saturated heat capacities (C_σ); PVT, isobaric (C_P) and isochoric (C_V) heat capacities, second virial coefficients, and speed of sound in the single phase. The extent of coverage of the data is shown on the data maps in Appendix 1. Comparisons have been made of all the data with the values predicted by the three equations of state, which resulted in 90 separate comparisons to be evaluated. Plots of the isobaric and isochoric heat capacities, the isenthalpic Joule-Thomson coefficient, and the speed of sound predicted by each EOS are shown in Appendix 2. A statistical analysis of each data set and of the combined data sets for each property, were made for each of the equations of state. The results are shown in Appendix 3.

2.1 Available equations of state for refrigerant R125

The three equations of state which are discussed in the following subsections, differ in their structure and range of validity. That developed by Outcalt and McLinden (1995) is a modified BWR equation with 32 coefficients, which was originally developed by Jacobsen and Stewart (1973) for nitrogen. The equation by Piao and Noguchi (1995) is also a modified BWR equation with 18 coefficients based on their earlier versions (Piao *et al.* (1992)). Ely (1995) has developed a new Helmholtz equation with 27 coefficients.

The temperature and pressure limits for their respective equations of state where quoted are those given by the authors. Caution should be taken when extrapolating any equation beyond the region of the fitted data.

Within each property table, the sets of data used to fit the respective equations have not been noted as full information was not available.

2.1.1 Ely equation of state

This equation has not yet been published and will be referred to in this report as the Ely EOS. It is written as a dimensionless Helmholtz function in terms of reduced density and reciprocal reduced temperature in the form:

$$A^{\mathrm{r}}/RT = \sum_{i=1}^{27} n_i \omega^{r_i} \tau^{(s_i+0.25u_i)} (e^{-\omega^{t_i}} - \kappa_{r_i,0}) \tag{2.1}$$

where $\omega = \rho/\rho_c$ with $\rho_c = 4759.96$ mol m^{-3}, $\tau = T_c/T$ with $T_c = 339.33$ K and $R = 8.31451$ J K^{-1} mol^{-1}. $\kappa_{r_i,0}$ is a kronecker delta function defined as: $\kappa_{\alpha,\beta} = 1$ if $\alpha = \beta$ otherwise zero. The validity range of this equation is not given .

2.1.2 Outcalt and McLinden equation of state

This equation, which was presented at the Twelfth Symposium on Thermophysical Properties in June 1994 at Boulder, USA, will be referred to in this report as the OM EOS.

This equation is written in terms of pressure as a function of temperature and density in the form:

$$\begin{aligned} P = {} & \rho RT + \rho^2(n_1T + n_2T^{1/2} + n_3 + n_4/T + n_5/T^2) \\ & + \rho^3(n_6T + n_7 + n_8/T + n_9/T^2) + \rho^4(n_{10}T + n_{11} + n_{12}/T) \\ & + \rho^5(n_{13}) + \rho^6(n_{14}/T + n_{15}/T^2) + \rho^7(n_{16}/T) \\ & + \rho^8(n_{17}/T + n_{18}/T^2) + \rho^9(n_{19}/T^2) \\ & + \rho^3 \exp(-[\rho/\rho_c]^2)\left[(n_{20}/T^2 + n_{21}/T^3) + \rho^2(n_{22}/T^2 + n_{23}/T^4)\right. \\ & + \rho^4(n_{24}/T^2 + n_{25}/T^3) + \rho^6(n_{26}/T^2 + n_{27}/T^4) \\ & \left. + \rho^8(n_{28}/T^2 + n_{29}/T^3) + \rho^{10}(n_{30}/T^2 + n_{31}/T^3 + n_{32}/T^4)\right]. \end{aligned} \tag{2.2}$$

where the value for $R = 8.314471$ J K^{-1} mol^{-1}. The critical density which was used as the reducing parameter in this EOS is $\rho_c = 4759.96$ mol m^{-3}(Wilson *et al.* (1992)). During the development of this equation of state, ancilliary equations were fitted to the saturation properties using their selected values for the critical temperature of $T_c = 339.33$ K (Schmidt *et al.* (1994)) and the critical density of $\rho_c = 4759.96$ mol m^{-3} (Wilson *et al.* (1992)); the value for the critical pressure of $P_c = 3.629$ MPa was determined from extrapolation of the experimental vapour pressure data of Weber and Silva (1994).

The authors state that the equation accurately represents the thermodynamic properties in the temperature range 174 K to 448 K for pressures up to 68 MPa except for the critical region and should extrapolate with reasonable accuracy to 500 K and 60 MPa.

2.1.3 Piao and Noguchi equation of state

This is a new equation of state which has not yet been published, and is based on earlier work: it will be referred to in this report as the PN EOS. It is a modified BWR equation with 18 coefficients, where the reduced pressure is given as a function of reduced temperature and reduced density in the form:

$$P/P_c = \omega\theta/Z_c + \sum_{i=1}^{14} n_i \omega^{r_i} \theta^{s_i} + \exp\left(-\omega^2\right) \sum_{i=15}^{18} n_i \omega^{r_i} \theta^{s_i} \tag{2.3}$$

with $\omega = \rho/\rho_c$, $\theta = T/T_c$, $Z_c = P_c/(R_R \rho_c T_c)$ and $R_R = R/M$.

The critical temperature and critical density were taken from Kuwabara *et al.* (1995). The values are $T_c = 339.165$ K and ρ_c=568 kg m^{-3}. The value of the critical pressure was P_c=3.6175 MPa and the value for $R = 8.314471$ J K^{-1} mol^{-1}. The range of this equation is given as 150 to 500 K for pressures up to 80 MPa and densities up to 1600 kg m^{-3}.

2.2 Ideal gas properties and fixed points

2.2.1 Ideal gas heat capacities

The OM EOS, and the PN EOS use simple polynomial equations in reduced temperature to represent the ideal gas heat capacity values whereas the Ely EOS uses an empirical fit to a truncated Einstein statistical mechanical equation. The two sets of ideal gas heat capacity data and temperature ranges are given in Table 2.A and the deviations from the Ely and OM EOSs are shown in figure 2.1. The PN EOS did not provide the functionality to calculate the ideal gas heat capacity explicitly.

Table 2.A Ideal gas heat capacity data for R125

Authors	Date	Temperature range/K	No. of points
Chen *et al.*	1975	0–1500	19
Gillis & Moldover	1993	240–380	8

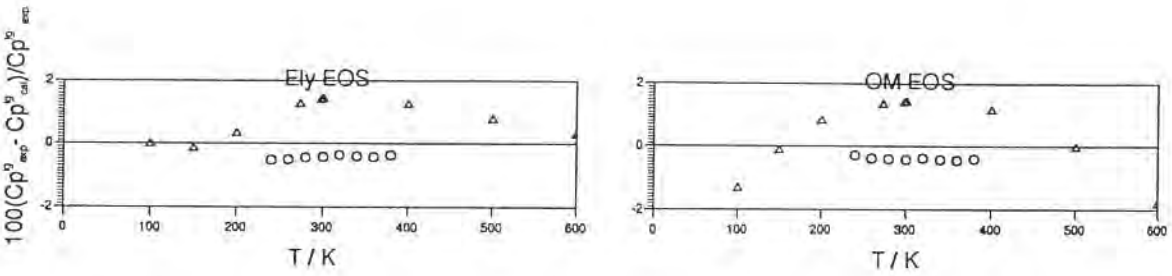

Figure 2.1 Comparison of ideal gas heat capacities with values calculated from the Ely and OM EOSs. (△) Chen *et al.* (1975); (○) Gillis and Moldover (1993).

The data of Chen *et al.* (1975) are based on spectroscopic data and completely overlap those of Gillis and Moldover (1993) which are based on speed of sound measurements. The two sets of data show systematic differences of about 2% in the region of overlap. At T < 500 K the data of Chen *et al.* (1975) deviate from the Ely EOS by up to 1.4%, although above this temperature the deviations lie between ±0.32%. The Gillis and Moldover (1993) data, however, are well represented throughout its range with a maximum deviation of -0.50%. The deviations of the data of Chen *et al.* (1975) from the OM EOS show a similar pattern below 500 K although the scatter is greater lying between ±1.4%. Above 500 K the deviations first become more negative and then become increasingly positive. The calculated heat capacity decreases above 1100 K. The Gillis and Moldover (1993) data is also well represented by the OM EOS with a slightly less negative bias than the Ely EOS and a maximum deviation of -0.42%. Because of the incorrect behaviour of the ideal gas heat capacity above 500 K, extrapolation of

the thermal properties outside the stated limits of the OM EOS will lead to erroneous values.

2.2.2 Fixed points

Values for the measured triple point (Luddecke and Magee (1993)) and the critical point derived from the equation of state are listed in Table 2.B.

Table 2.B Fixed points for R125

EOS	T_t/K	T_b/K	T_c/K	Pc/MPa	ρ_c/(mol m^{-3})
Ely	172.52	225.037	339.33	3.629	4759.9
OM		225.007	.	.	
PN		225.183	.	.	

2.3 Comparisons of the saturation properties

All the saturation properties were calculated from the equations of state by equating the Gibbs energies of the two phases, i.e. setting $G_g(P,T) = G_l(P,T)$, so that along an isotherm

$$A_l + (P_\sigma/\rho_l) = A_g + (P_\sigma/\rho_g). \tag{2.3}$$

The heat capacities of the saturated liquid were calculated from each equation of state using the value for the saturated liquid density calculated from equation (2.3).

2.3.1 Vapour pressure

The nine sets of vapour pressure measurements are listed in Table 2.C. No set extends to the triple point.

Table 2.C Vapour pressure measurements for R125

Authors	Date	Temperature range/K	No. of points	Group
Boyes and Weber	1995	273–336	29	1
de Vries	1994	303–340	81	2
Holste	1993	220–340	18	2
Magee and Howley	1993	215–335	33	2
Monluc *et al.*	1991	303–340	23	1
Nagel *et al.*	1993	205–340	18	3
Weber and Silva	1994	218–247	40	2
Wilson *et al.*	1992	195–340	39	3
Ye *et al.*	1995	290–339	12	1

The accuracy of the vapour pressure measurements for R125 is not as high as that for R32, often due to impurities, and the representation by the different equations is less consistent. We have classified as Group 1 three sets which generally agree amongst

themselves to within ±0.1% in general, have small standard deviations (less than 0.1%), and show deviations from all three EOSs of better than ±0.25%. The deviations of the group 1 data from all the equations are shown in figure 2.2.

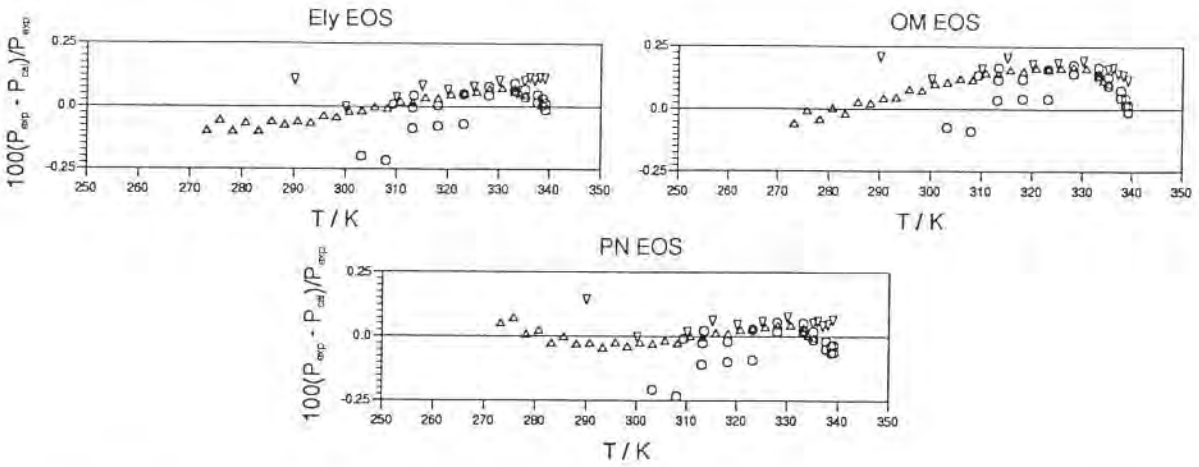

Figure 2.2 Comparison of group 1 experimental vapour pressures with values calculated from all three EOSs. (△) Boyes and Weber (1995); (○) Monluc *et al.* (1991); (▽) Ye *et al.* (1995).

The four sets classified as group 2 are in general predicted by the equations to better than ±0.5% but the patterns of the deviations are different. The deviations are shown in figure 2.3.

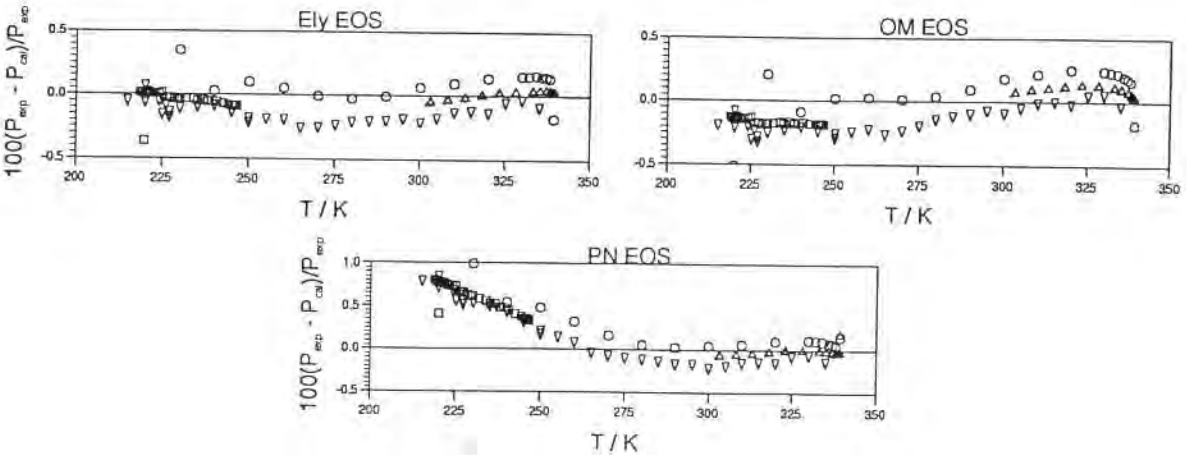

Figure 2.3 Comparison of group 2 experimental vapour pressures with values calculated from all three EOSs. (△) de Vries (1994); (○) Holste (1993); ▽) Magee and Howley (1993); (□) Weber and Silva (1994).

The de Vries (1994) data have in general deviations of less than ±0.15% from all three EOSs. The Weber and Silva (1994) data deviate systematically from the OM EOS by -0.18%. Below 250 K all the group 2 data deviate positively from the PN EOS

approaching 1% at 225 K. The upper bound of figure 2.3 has been extended for the PN EOS to show this.

The data of Wilson *et al.* (1992) and of Nagel *et al.* (1993) show a systematic scatter of different pattern for all three EOSs, with maximum deviations often greater than 1%. We have classified these as group 3 and comparisons are shown in figure 2.4.

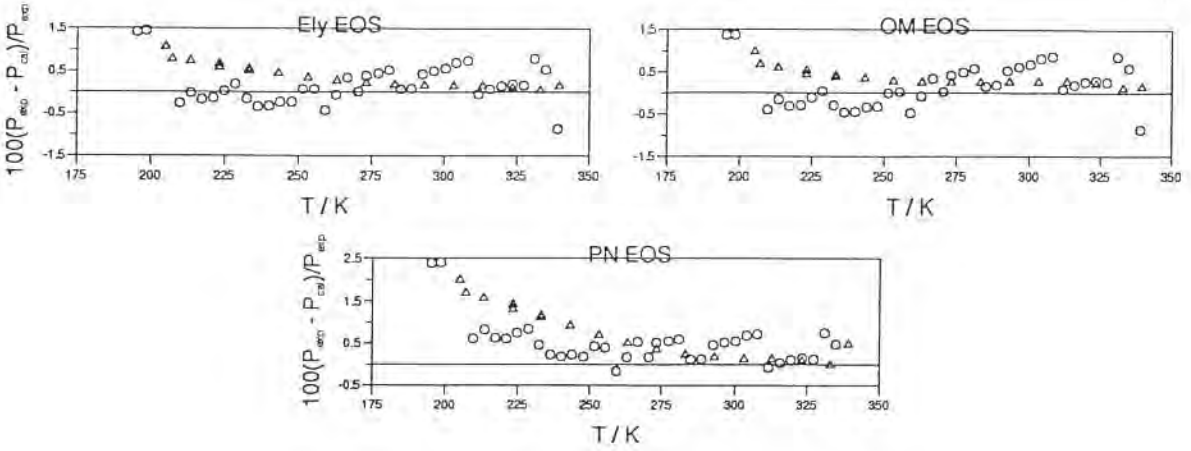

Figure 2.4 Comparison of group 3 experimental vapour pressures with values calculated from all three EOSs. (△) Nagel *et al.* (1993); (○) Wilson *et al.* (1992).

2.3.2 Saturated liquid density

The three sets of measurements and the ranges covered by each are listed in Table 2.D. The densities are represented in general by all three equations of state to within ±0.5%, except close to the critical temperature, as shown in figure 2.5. Between 339 K and the critical temperature none of the EOSs represent the data of Higashi (1994) particularly well. Maximum deviations in density are 9% for the PNEOS at 339.1K, and -13% and -14% at 339.2 K for the OM and Ely EOSs respectively.

Table 2.D Saturated density measurements for R125

Authors	Date	Temperature range/K	No. of points
Saturated liquid densities			
Defibaugh & Morrison	1992	275–338	9
Higashi	1994	324–340	9
Magee & Howley	1993	173–309	7
Saturated vapour densities			
Higashi	1994	326–340	8

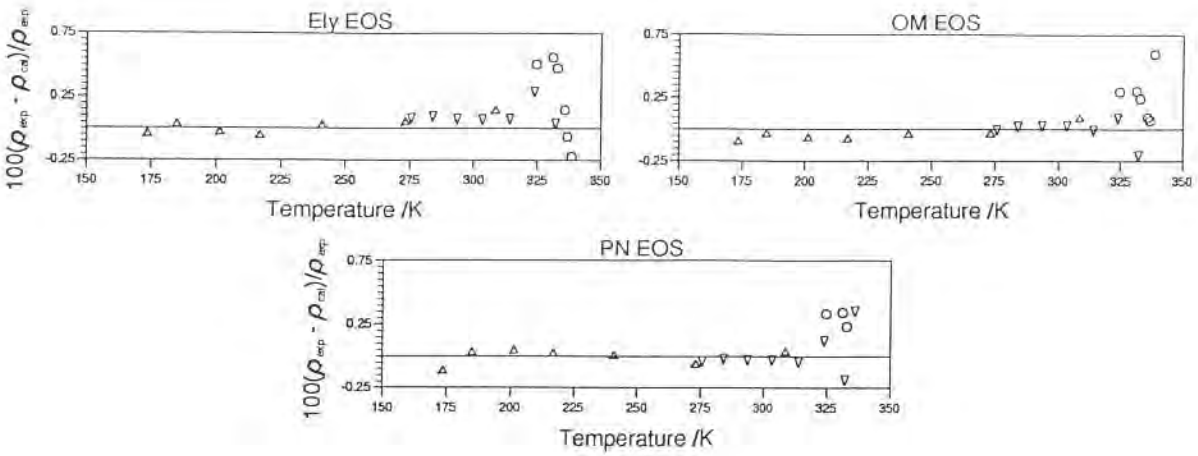

Figure 2.5 Comparison of experimental saturated liquid densities with values calculated from all three EOSs. (△) Magee & Howley (1993); (○) Higashi (1994); (▽) Defibaugh and Morrison (1992).

2.3.3 Saturated vapour density

The range covered by the one set of measurements of Higashi (1994) is given in Table 2.D and comparisons with each of the equations of state are shown in figure 2.6. Except for the OM EOS between 334 K and 339 K the data generally deviate from all the EOSs by between 1% and 2.5% except within 2 K of the critical temperature where, there are the following exceptions; one point of the OM EOS with 9% at 339.2 K, two points of the Ely EOS with a maximum of 11% at 339.2 K and three points of the PN EOS with a maximum of -40% at 339.1 K.

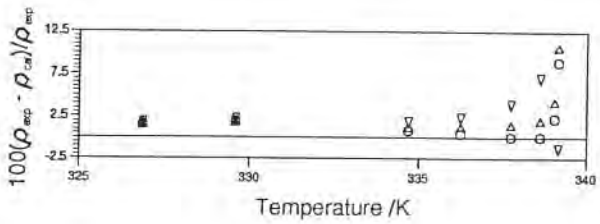

Figure 2.6 Comparison of experimental saturated vapour densities with values calculated from all three EOSs. (△) Ely EOS; (○) OM EOS; (▽) PN EOS.

2.3.4 Heat capacity of the saturated liquid

The property C_σ has only been measured by Luddecke and Magee (1993) (see Table 2. E). The deviations of the data from all three EOSs are shown in figure 2.7, which illustrates the good agreement with the Ely EOS, where the deviations are within ±0.5% with only three points lying outside this range. For T > 185 K the deviations from the

OM EOS lie generally between -0.75% and 0.25%. There are two points, which deviate more than this in this temperature range. For T < 185 K there are a further ten points where deviations exceed 0.25% and reach a maximum of 1.2% at 176 K. The data show systematic deviations from the PN EOS. For 175 < T/K < 210 the deviations rise from -1.4% to 1% and then for T > 210 K they fall steadily to -0.75%.

Table 2.E Heat capacity measurements of the saturated liquid for R125

Author	Date	Temperature range/K	No. of points
Luddecke and Magee	1993	175–278	85

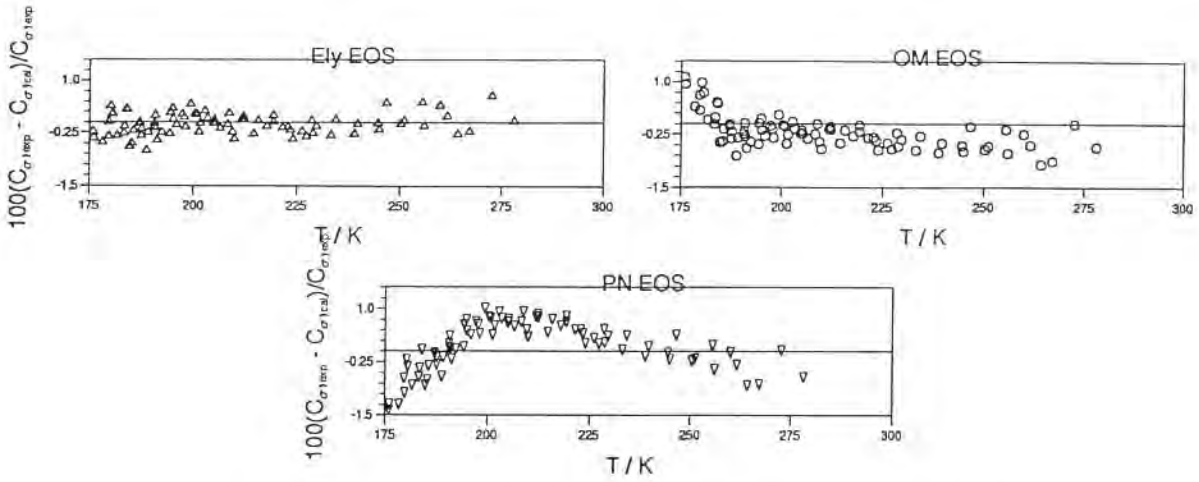

Figure 2.7 Comparison of experimental heat capacities of the saturated liquid by Luddecke and Magee (1993) with values calculated from all three EOSs. (△) Ely EOS; (◯) OM EOS; (▽) PN EOS.

2.4 Comparisons of single-phase properties

The single-phase properties available for comparison include experimental values for PVT , second virial coefficients, isochoric, C_V, and isobaric, C_P, heat capacities and speed of sound. All of these are compared with the three equations of state.

2.4.1 PVT data

There are seven sets of PVT measurements, with a total of 967 points, which are listed in Table 2.F together with the range covered by each set.

Table 2.F *PVT* and second virial coefficient data for R125

Authors	Date	No. of points	Temperature range/K	Pressure range/MPa	Density range/mol m^{-3}
PVT data					
Defibaugh and Morrison	1992	162	275–370	1.5–6.4	2153–11235
Magee and Howley	1993	79	178–399	3.5–35.4	9286–14029
Holste	1993	170	180–350	1.2–68.0	1418–14159
Wilson *et al.*	1992	83	198–449	1.7–10.5	892–13558
de Vries	1994	287	263–344	0.018–9.82	6.50–9913
Boyes and Weber	1995	92	273–364	0.33–4.6	117–2831
Ye *et al.*	1995	94	290–390	0.116–3.6	40–1911
Second virial coefficient					
Bignell and Dunlop	1993	3	290–310		
Gillis and Moldover	1993	9	240–400		
Ye *et al.*	1995	11	290–390		

The liquid phase data of Defibaugh *et al.* (1994) are well represented (figure 2.8a and figure 2.8b) by all three EOSs. The deviations in density from the OM EOS for $T \leq 334$ K are better than ±0.04%, whereas for $T \geq 343$ K the deviations have increased and are generally between ±0.75%. However, six points on the 353 K isotherm, four on the 348 K isotherm and three points on the 343 K isotherm exceed these limits with a maximum value of 12.1% at 3.95 MPa and 343.3 K. For the two near critical isotherms at 339 K and 340.5 K the deviations are generally within 0.75%, with four points outside this range. The deviations increase as the critical pressure is approached with a maximum of 30.4% at 3.69 MPa and 340.5 K. The deviations from the Ely EOS for $T \leq 334$ K lie between 0.02% and 0.23%. Along the 324 K and 334 K isotherms the deviations are larger than at lower temperatures and increase as the pressure falls towards the saturation value. The two near critical isotherms at 339 K and 340.5 K follow the same systematic trend with the deviations rising as the critical pressure is approached. The maximum value is 31.3% at 3.69 MPa and 340.5 K. For $T \geq 343$ K the deviations are generally between ±0.9% with eleven points outside this range with a maximum of 11.8% at 343 K and 3.95 MPa. For the PN EOS the deviations for $T < 334$ K range from -0.06% to 0.16%. Along the 324 K and 334 K isotherms the deviations are positive and increase as the saturation pressure is approached. The density deviations on the near critical isotherms at 339 K and 340.5 K are all positive with the largest deviations occurring near the critical pressure. The maximum value is 33.8% at 340.5 K and 3.69 MPa, although values around 0.1% to 0.4% are more typical. For temperatures greater than 343 K the majority of densities are predicted to within ±0.9% with four points each on the 343 K and 348 K isotherms and seven points on the 353 K isotherm outside this range.

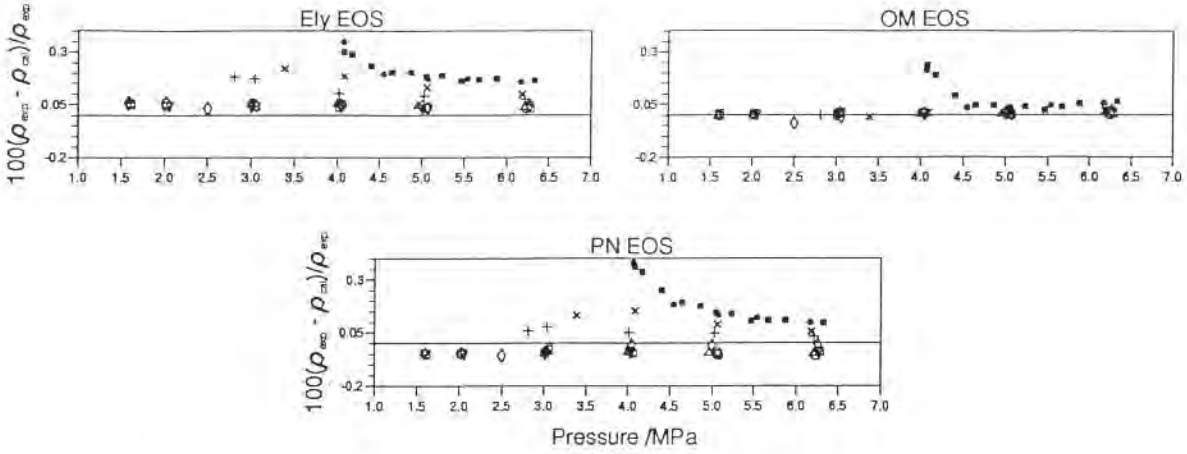

Figure 2.8a Comparison of experimental densities of Defibaugh and Morrison (1992) with values calculated from all three EOSs. Isotherms: (△) 275 K; (○) 284 K; (▽) 293 K; (□) 303 K; (◇) 314 K; (+) 324 K; (×) 334 K; (•) 339 K; (▪) 341 K.

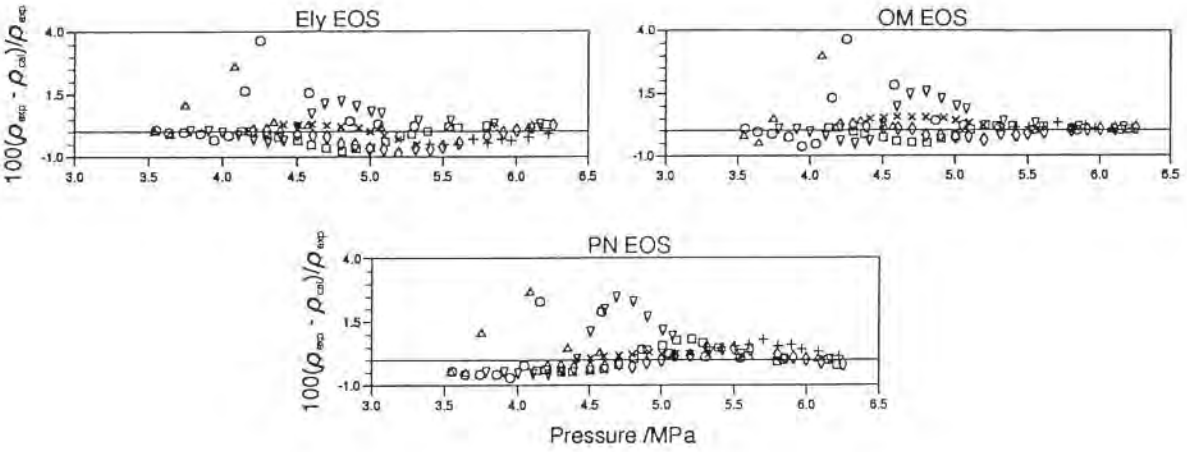

Figure 2.8b Comparison of experimental densities of Defibaugh and Morrison (1992) with values calculated from all three EOSs. Isotherms: (△) 343 K; (○) 348 K; (▽) 354 K; (□) 359 K; (◇) 364 K; (+) 368 K; (×) 369 K.

The isochoric liquid phase density measurements of Magee and Howley (1993) comprise seven isochores in the range 9.3 mol dm^{-3} - 14.0 mol dm^{-3}. The deviations in density (figure 2.9) from the OM EOS lie between -0.02% and 0.16%. The density deviations of each isochore increase smoothly with rising temperature with the exception of the 9.3 mol dm^{-3} isochore which follows the trend to 375 K and there after the deviations decrease. The densities deviate from the PN EOS by between -0.05% and 0.16%. The deviations increase with temperature for the 9.3 mol dm^{-3}, 11.0 mol dm^{-3}, 13.7 mol dm^{-3}, and 14.0 mol dm^{-3} isochores whereas for the three isochores between 12.1 mol dm^{-3} and

13.2 mol dm^{-3} inclusive, the deviation slopes are negative. The densities are represented by the Ely EOS to within ±0.12%. The 9.3 mol dm^{-3} and 12.1 mol dm^{-3} isochores have smooth negative gradients with rising temperature whereas those ≥ 12.8 mol dm^{-3} have positive gradients. The deviations along the 11.0 mol dm^{-3} isochore, however pass through a minimum. For all three EOSs, the density deviations display a significant positive bias.

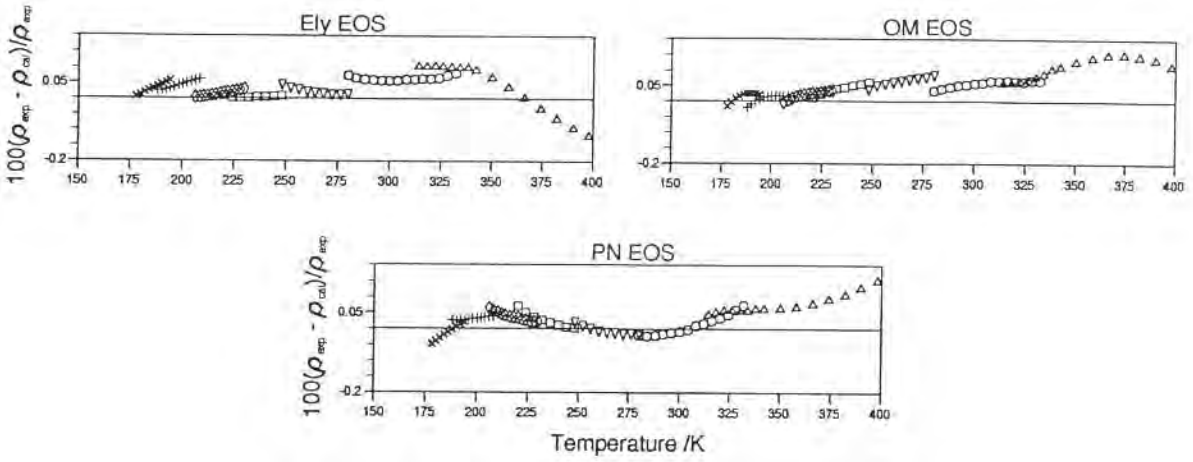

Figure 2.9 Comparison of experimental densities of Magee and Howley (1993) with values calculated from all three EOSs. Isochores in mol dm^{-3}: (△) 9.3; (○) 11.0; (▽) 12.1; (□) 12.8; (◇) 13.2; (+) 13.7;(×) 14.0.

With the exception of the 350 K isotherm the Holste (1993) densities are well represented by all three EOSs as shown in figure 2.10.

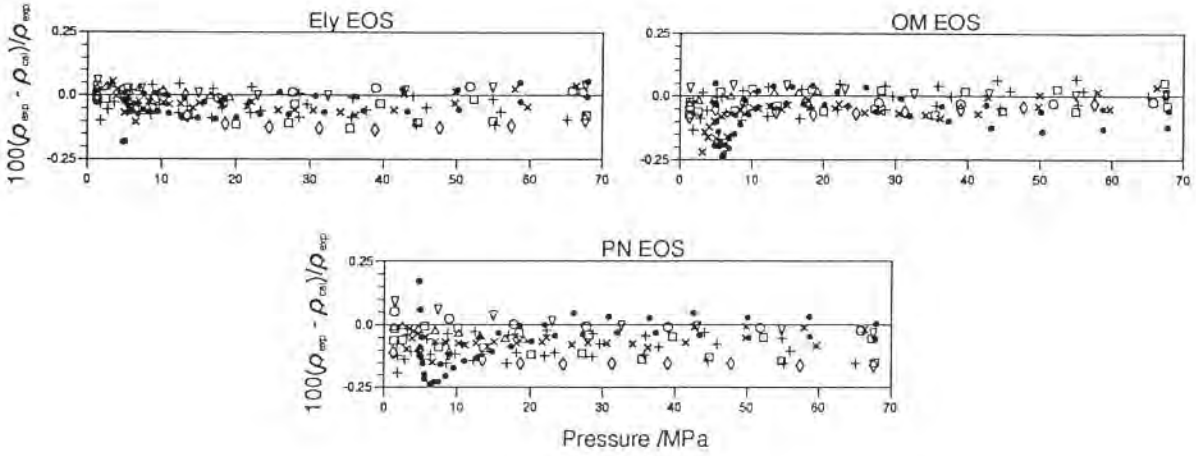

Figure 2.10 Comparison of experimental densities of Holste (1993) with values calculated from all three EOSs. Isotherms: (△) 180 K; (○) 205 K; (▽) 230 K; (□) 250 K; (◇) 270 K; (+) 300 K; (×) 330 K; (•) 350 K.

Of all the seven data sets, the data of Holste (1993) cover the greatest pressure range, from the low temperature compressed liquid to the supercritical dense fluid region, with a small overlap with the data of Defibaugh *et al.* (1992). In this region there appear to be small systematic differences of about 0.1% between the two sets of data. The 350 K isotherm usually deviates from all three EOSs by more than -0.15% at pressures below 5 MPa. The remaining data, however, deviate in density from all three EOSs by a similar amount. For the Ely EOS these deviations range from -0.12% to 0.06%; for the PN EOS from -0.19% to 0.09%, and for the OM EOS the range is -0.22% to 0.08%. For all three EOSs the density deviations display a negative bias.

The data of Wilson *et al.* (1992) cover the widest temperature range of all the data sets. The data for T < 324 K are well represented (figure 2.11a) by all three EOS.

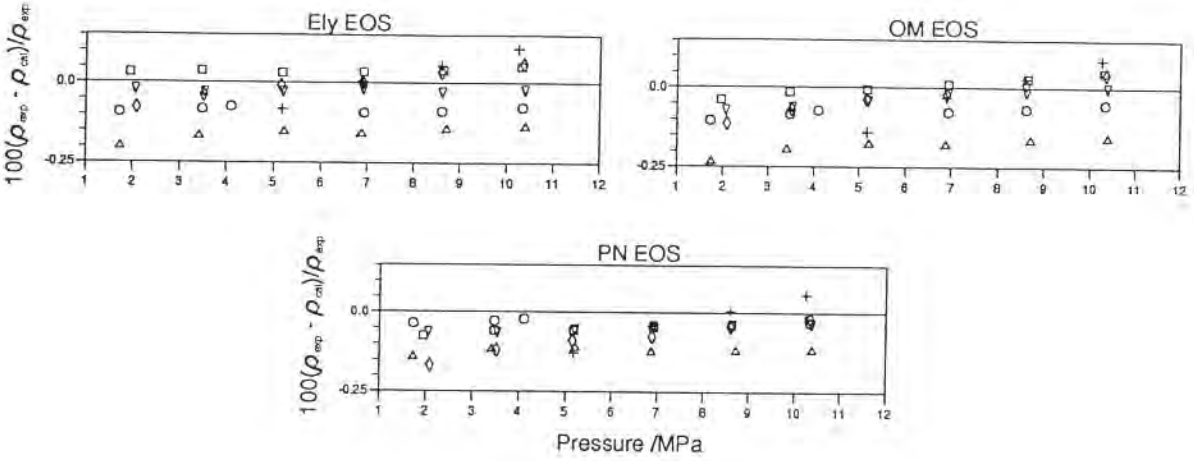

Figure 2.11a Comparison of experimental densities of Wilson *et al.* (1992) with values calculated from all three EOSs. Isotherms: (△) 198 K; (○) 223 K; (▽) 248 K; (□) 273 K; (◇) 298 K; (+) 323 K.

For those six isotherms the data deviate from the PN EOS by -0.17% to 0.06%. The densities on the isotherms where T < 274 K show systematic deviations of near zero slope from the EOS, whereas those for the 298 K and 323 K isotherms show a positive gradient. The deviations from the Ely EOS have a slightly wider range; from -0.2% to 0.1%. These systematic deviations from the Ely EOS have a pattern similar to that of the PN EOS. The deviations from the OM EOS show a slightly more negative bias than the others with a range of -0.23% to 0.1%. All the isotherms show small positive gradients with increasing temperature. The data for temperatures of 340 K and above show wider scatter (figure 2.11b) for all three EOSs. The density deviations display a negative bias with all three EOSs between -3.0% and 0.5% in general, although near the critical point much larger deviations of the order of 25% occur.

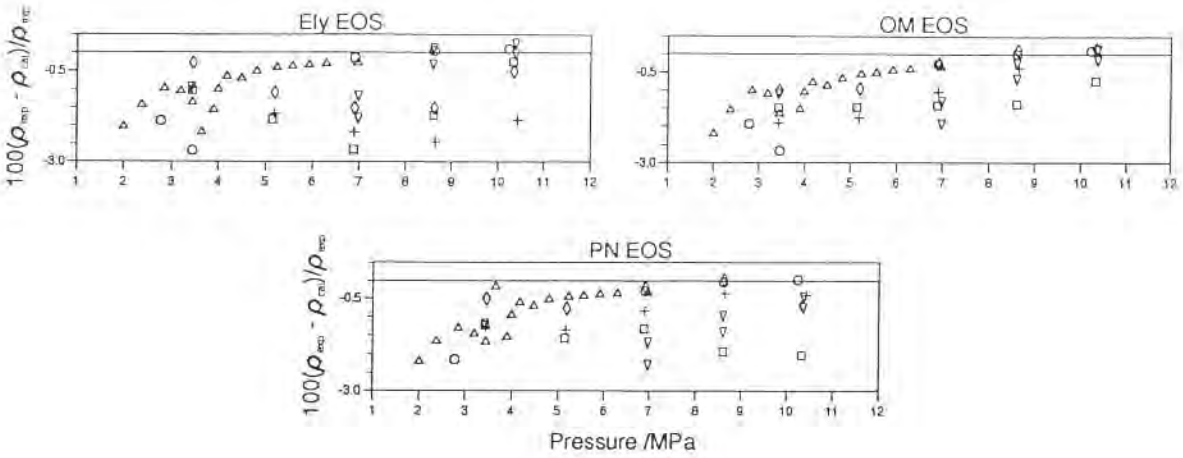

Figure 2.11b Comparison of experimental densities of Wilson *et al.* (1992) with values calculated from all three EOSs. Isotherms: (△) 340 K; (○) 348 K; (▽) 373 K; (□) 398 K; (◇) 423 K; (+) 448 K.

The gas phase data of de Vries (1994) are extensive and the deviation plots for all the EOSs are shown in figures 2.12a and 2.12b. The data are well represented by the Ely EOS where the deviations lie between -0.04% and 0.23% for the T < 324 K isotherms. The deviations tend towards zero at low pressures but increase with increasing pressure. For T > 325 K the deviation plots are more scattered. For pressures up to 3.0 MPa all the densities are represented to between -0.1% and 0.2%. Above this pressure, particularly on the three near critical isotherms (T ≥ 339 K) the data deviate much more widely with 13 points lying outside this range with 12 points lying between -2% and 1.65% and an outlier at 10% on the 340 K isotherm at 9.8 MPa. For the PN EOS the deviations for the T < 324 K isotherms show more scatter with values lying between -0.09% and 0.28%. As with the Ely EOS, the deviations tend towards zero at low pressures and increase with increasing pressure. The density deviations for the T > 325 K isotherms are close to zero at low pressure and in general show a near linear increase in the negative deviations as the pressure increases, reaching a maximum of -0.42% at 3.42 MPa along the 343 K isotherm. Up to 3.0 MPa the deviations lie between -0.35% and 0.03%. At the higher pressures along each isotherm the deviations first approach zero and then become positive with 16 points lying outside the -0.35% to 0.03% range. These in general lie between -2.6% and 2.4% with two outliers of 9.7% and 7.8% on the 340 K isotherm. The deviations from the OM EOS, for the T < 324 K isotherms, show a similar pattern to the PN EOS but with a different span from -0.14% to 0.26%. The deviation pattern for the T > 325 K isotherms is very similar to that of the Ely EOS but has a more negative bias with deviations ranging from -0.31% to 0.17% for pressures up to 3.0 MPa. Above this pressure the deviations are more widespread with 14 points outside the -0.31% to 0.17% range. In general these lie between -2.4% and 2.2% with the outlier at 9.8% at 340 K and 9.8 MPa.

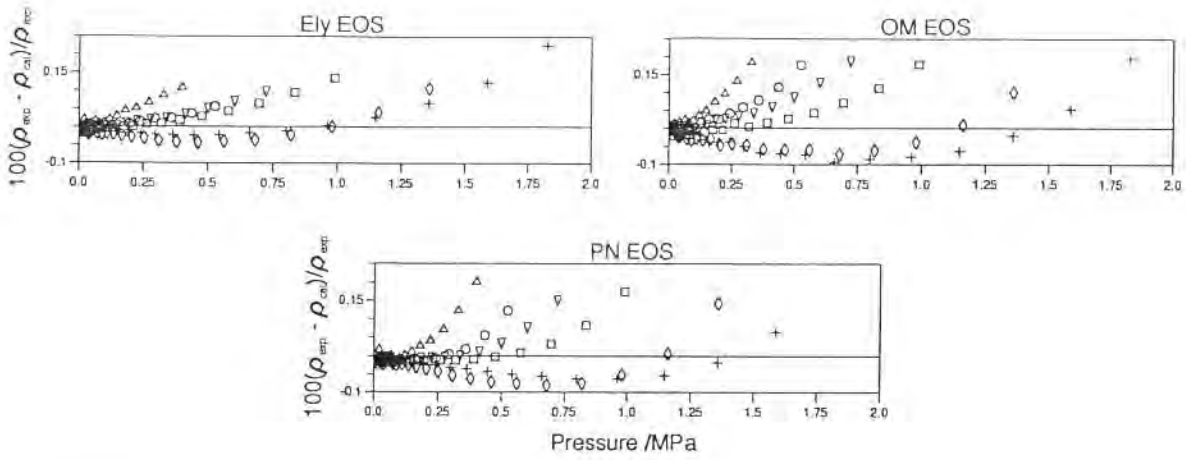

Figure 2.12a Comparison of experimental densities of de Vries (1994) with values calculated from all three EOSs. Isotherms: (△) 263 K; (○) 273 K: (▽) 283 K; (□) 293 K; (◇) 303 K; (+) 313 K.

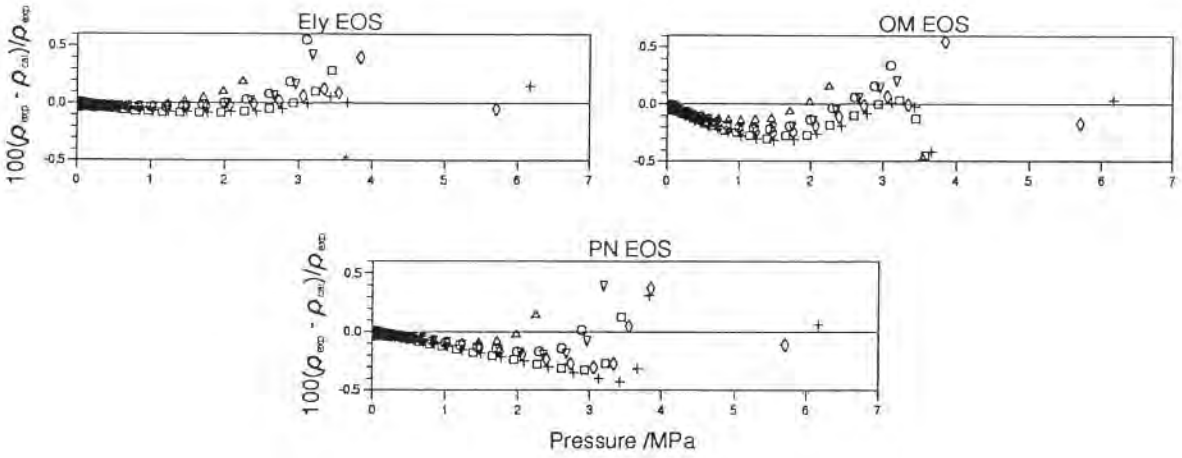

Figure 2.12b Comparison of experimental densities of de Vries (1994) with values calculated from all three EOSs. Isotherms: (△) 323 K; (○) 333 K; (▽) 335 K; (□) 339 K; (◇) 340 K; (+) 343 K.

The gas phase data of Boyes and Weber (1995) consist of one Burnett isotherm at 363 K and six isochores ranging from 0.157 mol dm^{-3} to 2.83 mol dm^{-3}. The density deviations from all the EOSs are shown in figures 2.13a and 2.13b. The density deviations of the 363 K isotherm from the Ely EOS lie between -0.11% and 0.19% with the exception of the highest pressure datum point whose deviation is -1.1%. With the exception of the 0.89 mol dm^{-3} isochore the density deviations for the isochoric data are ±0.12%. Below 325 K the deviations are generally positive while above they are generally negative. Deviations for the 0.89 mol dm^{-3} isochore follow the general trend, but below 318 K two points deviate by up to 0.24%. The data deviate in density from the PN EOS between -0.37% and 0.14% along the 363 K isotherm with the exception

of the highest pressure datum point whose deviation is -1.3%. Along the isochores the density deviations all lie between -0.45% and 0.32%. The trend in the deviations along the isochores is to go from positive at the lowest temperatures to negative at the highest ones. The density deviations from the OM EOS are similar to those of the PN EOS, but with a slightly more negative bias. Along the 363 K isotherm the deviations lie between -0.48% and 0.17% with the exception of the highest pressure datum point whose deviation is -0.9%. Along the isochores the density deviations all lie between -0.62% and 0.29%. The trends in the deviations along the isochores are in general similar to the PN EOS.

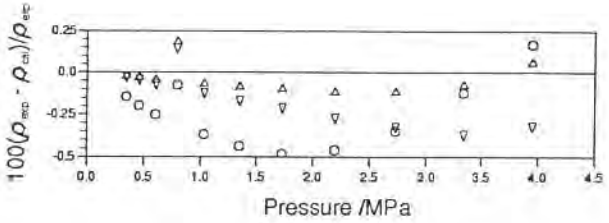

Figure 2.13a Comparison of experimental densities of Boyes and Weber (1995) with values calculated along the 363 K isotherm from all three EOSs. (△) Ely EOS; (○) OM EOS; (▽) PN EOS.

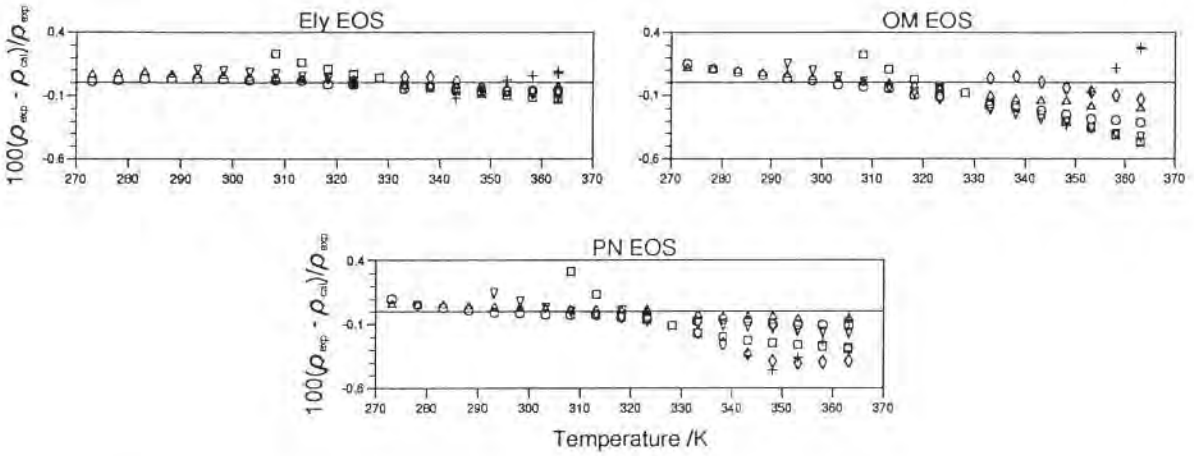

Figure 2.13b Comparison of experimental densities of Boyes and Weber (1995) with values calculated from all three EOSs. Isochores in mol dm^{-3}: (△) 0.16; (○) 0.28; (▽) 0.50; (□) 0.89; (◇) 1.59;(+) 2.83.

The Ye *et al.* (1995) data overlap those of de Vries (1994). Although in the range of overlap the former data set shows more scatter than the latter, the direct comparisons,

as shown in figure 2.14, along the 340 K isotherm suggest that the two sets of data are consistent.

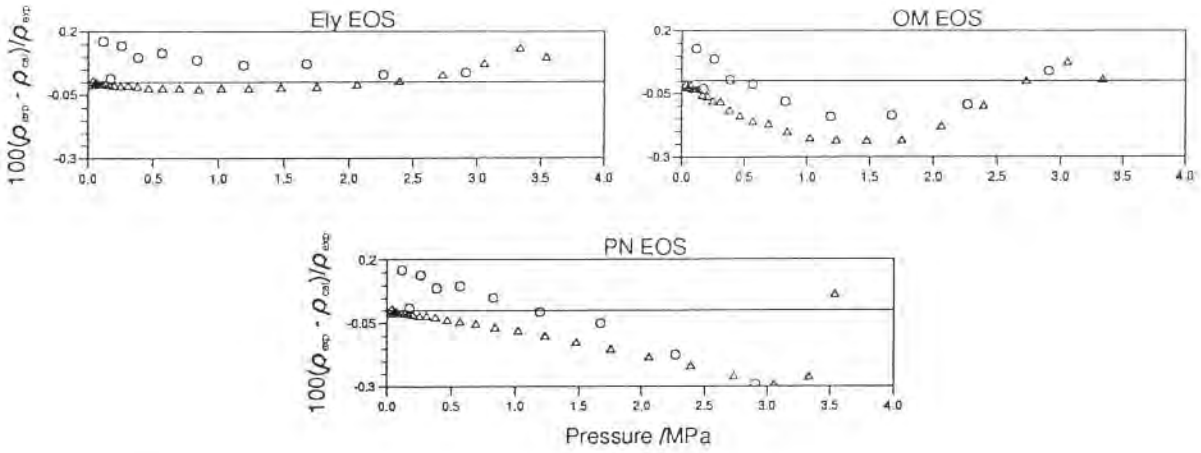

Figure 2.14 Comparison of experimental densities along the 340 K isotherm of de Vries (1994) and Ye *et al.* (1995) with values calculated from all three EOSs. (△) de Vries (1994); (○) Ye *et al.* (1995).

The density deviations from all the EOSs for the Ye *et al.* (1995) data are shown in figures 2.15a and 2.15b. The density deviations from the Ely EOS are ±0.5% for T < 341 K with a positive bias. However, for T > 341 K the deviations lie between -0.2% and 0.05% with a negative bias especially above 1.2 MPa. The data deviate in density from the PN EOS by between -0.55% and 0.62% for the T < 341 K isotherms.

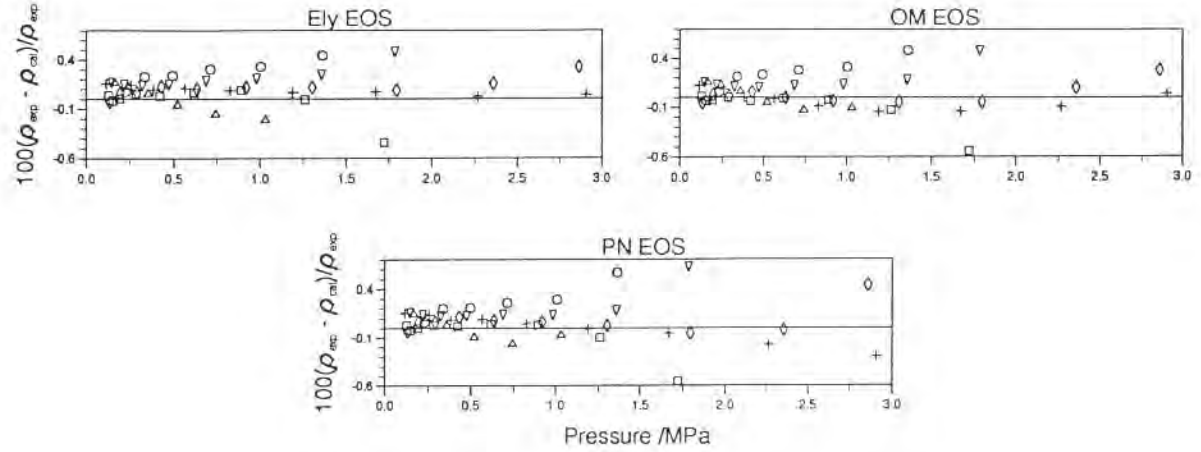

Figure 2.15a Comparison of experimental densities of Ye *et al.* (1995) with values calculated from all three EOSs. Isotherms: (△) 290 K; (○) 300 K; (▽) 310 K; (□) 320 K; (◇) 330 K; (+) 340 K.

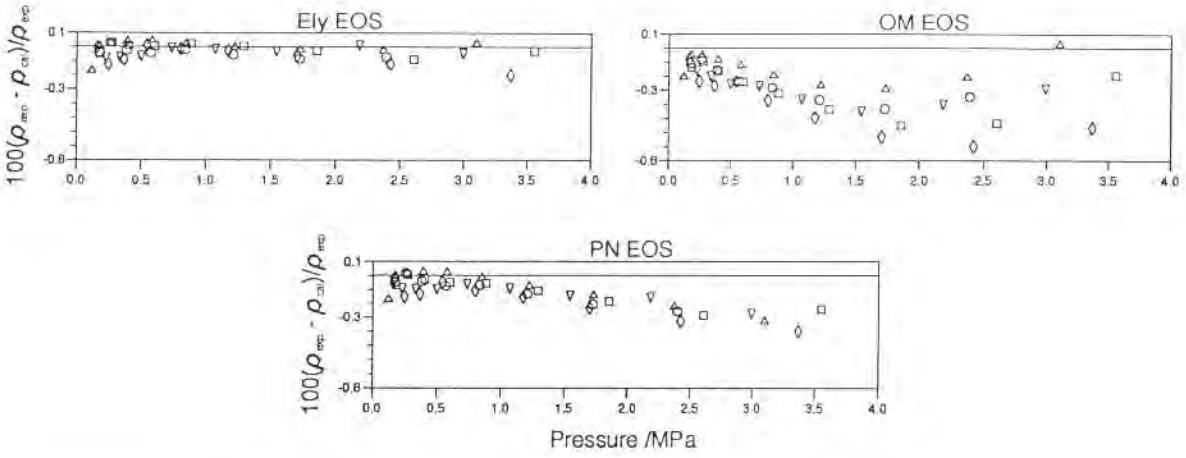

Figure 2.15b Comparison of experimental densities of Ye *et al.* (1995) with values calculated from all three EOSs. Isotherms: (△) 350 K; (○) 360 K; (▽) 370 K; (□) 380 K; (◇) 390 K.

Above this temperature the deviations lie between -0.39% and 0.04%. These deviations become more negative as the pressure increases. The density deviations from the OM EOS show a similar trend to the PN EOS ranging from -0.53% to 0.49% for the T < 341 K isotherms. For the high temperature isotherms the deviation range lies between -0.69% and 0.03%.

2.4.2 Second virial coefficient

There are three sets of second virial coefficient data whose ranges are shown in Table 2.F. The representations of these values by the Ely and OM EOSs are shown in figure 2.16.

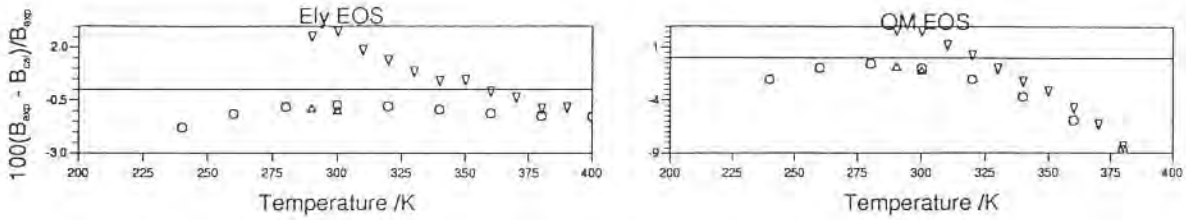

Figure 2.16 Comparison of experimental second virial coefficient values with values calculated from the Ely and OM EOSs. (△) Bignell and Dunlop (1993); (○) Gillis and Moldover (1993); (▽) Ye *et al.* (1995)

The PN EOS did not provide the functional capability to calculate these values. The data of Gillis and Moldover (1993) cover the greatest temperature span and were derived from their speed of sound measurements, whereas those of Ye *et al.* (1995) and Bignell and Dunlop (1993) were derived from volumetric measurements. The last data set is consistent with that of the first. The Gillis and Moldover (1993) data are

at most 13 cm^3 mol^{-1} less negative than those of Ye *et al.* (1995) in the range of overlap. The discrepancy is least at 375 K where the data sets effectively agree. The deviations of the Gillis and Moldover (1993) second virial coefficients from the Ely EOS range from 2.1 cm^3 mol^{-1} (-1.2%) at 400 K to 11 cm^3 mol^{-1} (-1.75%) at 240 K. The data of Ye *et al.* (1995) deviate from the Ely EOS by -10.3 cm^3 mol^{-1} (2.7%) at 300 K and 1.9 cm^3 mol^{-1} (-0.95%) at 380 K. The deviations from the OM EOS range from -10.55 cm^3 mol^{-1} (2.6%) (Ye *et al.* (1995)) to 21.0 cm^3 mol^{-1} (-12%) (Gillis and Moldover (1993)).

2.4.3 Isochoric heat capacity

The only C_V measurements are those for the liquid phase by Luddecke and Magee (1993) which cover the range shown in Table 2.G. Comparisons of all three equations of state with them are shown in figure 2.17. The deviations of the isochoric heat capacities from the PN EOS lie between ±1.7%, whereas those from the the OM EOS have a more positive bias lying between -0.91% and 1.64%. The data deviate from the Ely EOS from between -1.0% and 1.9% with a positive bias greater than for the other two EOSs.

Table 2.G Derived single-phase data for R125

Authors	Date	No. of points	Temperature range/K	Pressure range/MPa	Density range/mol m^{-3}
Isochoric Heat capacities					
Luddecke and Magee	1993	97	200–342		10533-13532
Isobaric heat capacities					
Wilson *et al.*	1992	5	233–334	0.13	
Speed of sound data					
Grebenkov *et al.*	1994	30	287–333	1.1–16.5	
Gillis	1993	149	240–400	0.038–1.03	

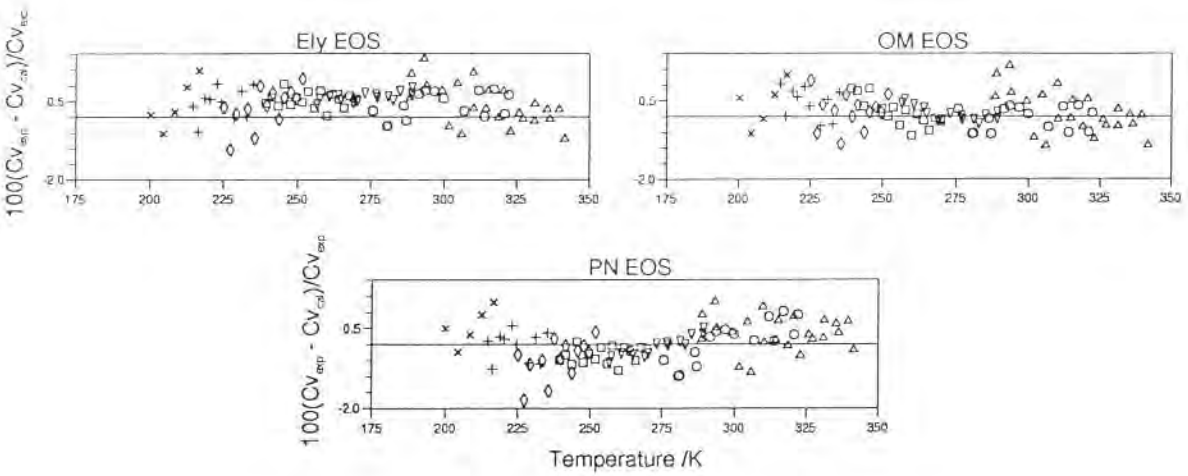

Figure 2.17 Comparison of experimental isochoric heat capacities of Luddecke and Magee (1993) with values calculated from all three EOSs. Isochores in mol dm^{-3} : ($\triangle$) 10.6; ($\bigcirc$) 11.1; ($\triangledown$) 11.8; ($\square$) 12.3; ($\diamond$) 12.7; (+) 13.0; ($\times$) 13.5.

2.4.4 Isobaric heat capacity

The only set of C_P data available is a single isobar at 0.13 MPa from Wilson *et al.* (1992) which covers the temperature range shown in Table 2.G. The data deviate from all three equations in a similar manner as shown in figure 2.18. The data points between 250 K and 300 K agree with all three EOSs to within $\pm 0.5\%$. The points at 233 K and 333 K show strong negative and strong positive deviations respectively for all three EOSs. For the PN EOS these extrema are -3.5% and 1.9% respectively, whereas for the OM EOS they are -3.9% and 1.1%, and for the Ely EOS they are -4.9% and 1.1%.

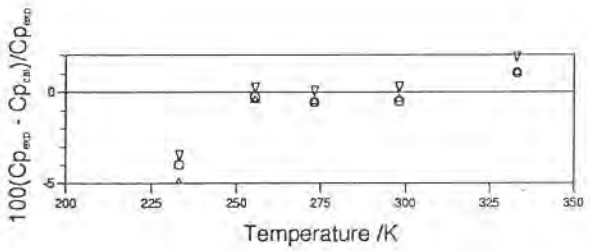

Figure 2.18 Comparison of experimental isobaric heat capacities of Wilson *et al.* (1992) with values calculated from all three EOSs. ($\triangle$) Ely EOS; ($\bigcirc$) OM EOS; ($\triangledown$) PN EOS.

2.4.5 Speed of Sound

The ranges covered by the two sets of speed of sound data are given in Table 2.G; the Grebenkov *et al.* (1994) values are in the liquid phase and those for Gillis (1993) in the

gas phase. Comparisons of the liquid phase values of Grebenkov *et al.* (1994) with the equations of state are shown in figure 2.19. The deviations for the Ely EOS lie betwen -0.22% and 0.36% while those for the OM EOS are within -0.8% and 0.05% and those for the PN EOS are are within -0.73% and 0.18%. The deviations from the OM and PN EOSs display a large negative bias; all the deviations from the OM EOS are negative.

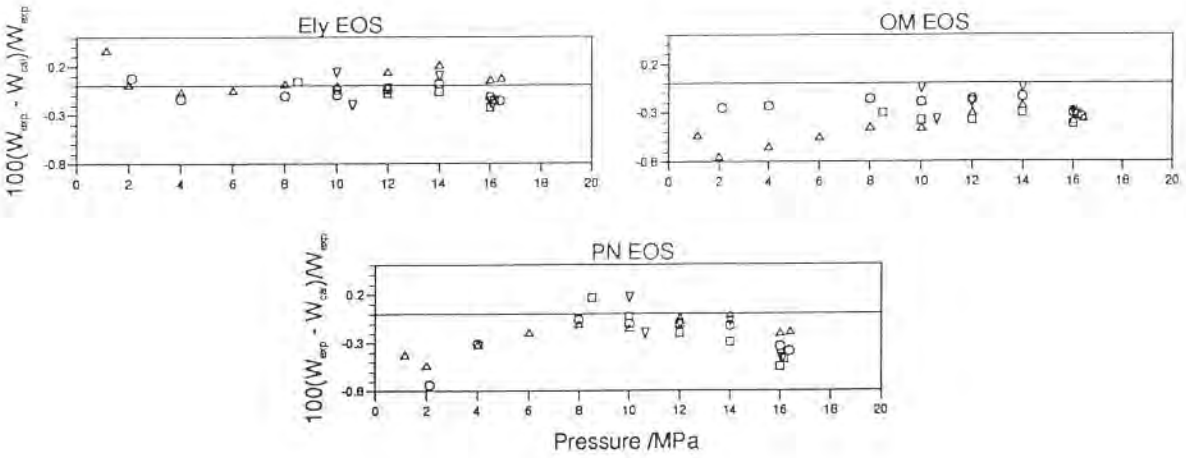

Figure 2.19 Comparison of experimental speed of sound values of Grebenkov *et al.* (1994) with values calculated from all three EOSs. Isotherms: (△) 288 K; (○) 303 K; (▽) 327 K; (□) 333 K.

As shown in figure 2.20 the predictions of the equations of state from the Gillis (1993) data in the gas phase are less than for the data in the liquid phase.

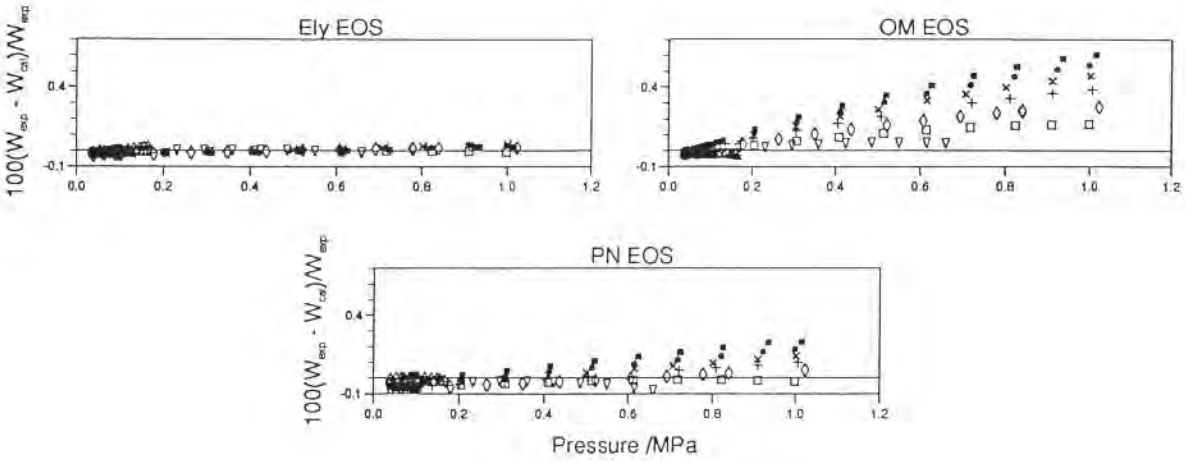

Figure 2.20 Comparison of experimental speed of sound values of Gillis (1993) with values calculated from all three EOSs. Isotherms: (△) 240 K; (○) 260 K; (▽) 280 K; (□) 300 K; (◇) 320 K; (+) 340 K; (×) 360 K; (•) 380 K; (▪) 400 K.

The deviations from the Ely EOS are lie between -0.028% and 0.048% whereas those from the PN EOS lie between -0.08% and 0.24%. Above 0.5MPa, the deviations increase

positively with increasing temperature along an isobar, and, above 320 K increase with increasing pressure along an isotherm, so that the largest deviation of 0.24% is at 400 K and 1.02 MPa. The deviations from the OM EOS range from -0.03% at 240 K and 0.165 MPa to 0.61% at the highest temperature and pressure. At the highest pressure of 1 MPa the deviations systematically increase with temperature and apart from the low temperature isotherms at 240 K and 260 K the deviations increase positively with increasing pressure along an isotherm.

2.5 Summary for R125

Systematic differences of about 2% exist between the ideal gas heat capacity data sets calculated from speed of sound data and from spectroscopic data. Below 500 K the data are well represented by both the Ely and OM EOSs. Above 500 K the ideal gas heat capacity data becomes poorly presented by the OM EOS showing that caution is always required if an EOS is extrapolated beyond its range of validity.

The saturated liquid densities are represented by all three EOSs to within ±0.5%. The saturated vapour densities are more scattered with the deviations from all three EOSs agreeing to within 2.5% except within 2 K of the critical temperature.

The saturated liquid phase heat capacity is best represented by the Ely EOS.

The liquid phase densities of Defibaugh and Morrison (1992) are best represented by the OM EOS. The isochoric liquid phase densities of Magee and Howley (1993) are well represented by the PN and Ely EOSs, with the former having slightly better overall statistics. The Holste (1993) data cover a wide pressure range and is well represented by all three EOSs. The gas phase data of de Vries (1994), Boyes and Weber (1995) and Ye *et al.* (1995) are best represented by the Ely EOS.

The second virial coefficients values from the volumetric data and speed of sound data show small discrepancies at the lower temperatures where they overlap. The second virial coefficients are represented in a similar way by both the Ely and OM EOSs with the former having slightly better overall statistics.

The isochoric heat capacity is well represented by all three EOSs.

Both the liquid phase and gas phase speed of sound measurements are best represented by the Ely EOS.

Acknowledgement

The work of the IUPAC Thermodynamic Tables Project Centre is supported by the Department of Trade and Industry of the United Kingdom.

References for R32

1. Bignell, C.M. and Dunlop, P.J. (1993), Second virial coefficients for fluoromethanes and their binary mixtures with helium and argon. *J. Chem. Eng. Data*, **38**, 139-140.
2. Bouchot, C. and Richon, D. (1994), Simultaneous measurements of phase equilibrium and volumetric properties by vibrating tube densimetry: Apparatus and results involving HFC. *Proceedings, CFC's, The Day After, Joint Meeting of IIR Commissions, Padova, Italy, September 21-23* 517-524.
3. Chase Jr, M.W., Davies, C.A., Downey Jr, J.R., Frurip, D.J., McDonald, R.A. and Syverund A.N. (1985), JANAF Thermochemical Tables, 3rd edition. *J. Phys. Chem. Ref. Data*, **14**, Supplement 1.
4. Defibaugh, D.R., Morrison, G. and Weber, L.A. (1994), Thermodynamic properties of difluoromethane. *J. Chem. Eng. Data*, **39**, 333-340.
5. Ely, J.F. (1995), Private communication to the IUPAC Thermodynamic Tables Project Centre.
6. Grebenkov, A.J., Kotelevsky, Yu. G., Saplitza, V.V., Beljaeva, O.V., Zajatz, T.A. and Timofeev, B.D. (1994), Experimental study of thermal conductivity of some ozone safe refrigerants and speed of sound in their liquid phase. *Proceedings, CFC's, The Day After, Joint Meeting of IIR Commissions, Padova, Italy, September 21-23* 419-429.
7. Higashi, Y. (1994), Critical parameters for HFC134a, HFC32 and HFC125. *Int. J. Refrig.*, **17(8)**, 524-531.
8. Higashi, Y., Imaizumi, H. and Usaba, S. (1992), *Proc. Thirteenth Jpn. Symp. Thermophys. Props.*. 65.
9. Holcomb, C.D., Niesen, V.G., van Poolen, L.J. and Outcalt, S.L. (1993), Coexisting densities, vapor pressures and critical densities of refrigerants R32 and R152a at 300-385 K. *Fluid Phase Equilibria*, **91**, 145-157.
10. Holste, J.C. (1993), ASME Winter Meeting, New Orleans, Nov. 28 - Dec. 3.
11. Hozumi, T., Sato, H. and Watanabe, K. (1994), Speed of sound in gaseous difluoromethane. *J. Chem. Eng. Data*, **39(3)**, 493-495.
12. Jacobsen, R.T. and Stewart, R.B. (1973), Thermodynamic properties of nitrogen including liquid and vapor phases from 63 K to 2000 K with pressures to 10 000 bar. *J. Phys. Chem. Ref. Data*, **2**, 757–922.
13. Kanungo, A., Oi, T., Popowicz, A. and Ishida, T. (1987), Vapor pressure isotope effects in liquid methylene difluoride. *J. Phys. Chem.*, **91(15)**, 4198 - 4203.
14. Kunimoto, Y., Kubota, H., Tanaka, Y., Matsuo, S. and Sotani, T. (1994), *Isobaric specific heat capacity of HFC32 under high pressure.* Proc. Fifteenth Jpn. Symp. Thermophys. Props..
15. Kuwabara, S., Aoyama, H., Sato, H. and Watanabe K. (1995), Vapor-Liquid coexistence curves in the critical region and the critical temperatures and densities of difluoromethane and pentafluoroethane. *J. Chem. Eng. Data*, **40(1)**, 112-116.
16. Magee, J.W. and Howley, J.B. (1993), Int. J. Thermophys. (to be submitted).
17. Magee, J.W. and Luddecke, T.O.D. (1993), Int. J. Thermophys. (to be submitted).
18. Malbrunot, P.F., Meunier, P.A., Scatena, G.M., Mears, W.H., Murphy, K.P. and Sinka, V. (1968), Pressure - volume - temperature behaviour of difluoromethane. *J. Chem. Eng. Data*, **13(1)**, 16-21.
19. Nagel, M., *et al.* (1993), DKV-Tagungsberichte 20, Band II.. *1* 39-59.
20. Outcalt, S.M. and McLinden, M.O. (1995), Equations of state for the thermodynamic properties of R32 (difluoromethane) and R125 (pentafluoroethane). *Int. J. Thermophys.*, **16(1)**, 79-89.
21. Piao, C.-C. and Noguchi, M. (1995), Private communication to the IUPAC Thermodynamic Tables Project Centre.

22. Piao, C.-C., Noguchi, M., Sato, H. and Watanabe K. (1995), Private communication to the IUPAC Thermodynamic Tables Project Centre.
23. Rodgers, A.S., Chao, J., Wilhoit, R.C. and Zwolinski, B.J. (1974), Ideal gas thermodynamic properties of eight chloro- and fluoromethanes. *J. Phys. Chem. Ref. Data*, **3(1)**, 131-140.
24. Schmidt, J.W. and Moldover, M.R. (1994), Alternative refrigerants CH_2F_2 and C_2HF_5: Critical temperature, refractive index, surface tension, and estimates of liquid, vapor, and critical densities. *J. Chem. Eng. Data*, **39(1)**, 39-44.
25. Shinsaka, K., Gee, N. and Freeman G.R. (1985), Densities against temperature of 17 organic liquids and of solid 2,2-dimethyl propane. *J. Chem. Thermodyn.*, **17**, 1111-1119.
26. Tillner-Roth, R. (1995), Private communication to the IUPAC Thermodynamic Tables Project Centre.
27. Weber, L.A. and Goodwin, A.R.H. (1993), Ebulliometric measurement of the vapor pressures of difluoromethane. *J. Chem. Eng. Data*, **38(2)**, 254-256.
28. Weber, L.A. and Silva, A.M. (1994), Measurements of the vapor pressures of difluoromethane, 1-Chloro-1,2,2,2-tetrafluoroethane and pentafluoroethane. *J. Chem. Eng. Data*, **39(4)**, 808-812.
29. Yomo, M., Sato, H. and Watanabe, K. (1994). *An experimental study of isobaric heat capacity of liquid HFC-32.* M.S. Thesis, Keio University.
30. de Vries, B. (1994), Private communication to the IUPAC Thermodynamic Tables Project Centre.

References for R125

31. Bignell, C.M. and Dunlop, P.J. (1993), Second virial coefficients of seven fluoroethanes and interaction second virial coefficients for their binary mixtures with helium and argon. *J. Chem. Phys.*, **98(6)**, 4889-4892.
32. Boyes, S.J. and Weber, L.A (1995), Vapour pressures and gas-phase (p,ρ,T) values for CF_3CHF_2 (R125). *J. Chem. Thermodyn.*, **27(2)**, 163-174.
33. Chen, S.S., Rodgers, A.S., Chao, J., Wilhoit R.C. and Zwolinski B.J. (1975), Ideal gas thermodynamic properties of six fluoroethanes. *J. Phys. Chem. Ref. Data*, **4**, 441-456.
34. Defibaugh, D.R. and Morrison, G. (1992), Compressed liquid densities and saturation densities of pentafluoroethane (R125). *Fluid Phase Equilibria*, **80**, 157-166.
35. Ely, J.F. (1995), Private communication to the IUPAC Thermodynamic Tables Project Centre.
36. Gillis, K.A. (1993), Private communication.
37. Gillis, K.A. and Moldover, M.R. (1993), NIST private communication.
38. Grebenkov, A.J., Kotelevsky, Yu. G., Saplitza, V.V., Beljaeva, O.V., Zajatz, T.A. and Timofeev, B.D. (1994), Experimental study of thermal conductivity of some ozone safe refrigerants and speed of sound in their liquid phase. *Proceedings, CFC's, The Day After, Joint Meeting of IIR Commissions, Padova, Italy, September 21-23*, 419-429.
39. Higashi, Y. (1994), Critical parameters for HFC134a, HFC32 and HFC125. *Int. J. Refrig.*, **17(8)**, 524-531.
40. Holste, J.C. (1993), *Thermodynamic properties of refrigerants R-125 and R-141b*. Final Report to ASHRAE on Project RP-654.
41. Jacobsen, R.T. and Stewart, R.B. (1973), Thermodynamic properties of nitrogen including liquid and vapor phases from 63 K to 2000 K with pressures to 10 000 bar. *J. Phys. Chem. Ref. Data*, **2**, 757-922.
42. Kuwabara S., Aoyama, H., Sato. H. and Watanabe K. (1995), Vapor-Liquid coexistence curves in the critical region and the critical temperatures and densities of difluoromethane and pentafluoroethane. *J. Chem. Eng. Data*, **40(1)**, 112-116.
43. Luddecke, T.O.D. and Magee, J.W. (1993), Int. J. Thermophys. (to be submitted).
44. Magee, J.W. and Howley, J.B. (1993), Int. J. Thermophys. (to be submitted).
45. Monluc *et al.* (1991), Proc. Twelfth Jpn. Symp. Thermophys. Props..
46. Nagel, M., *et al.* (1993), *DKV-Tagungsberichte 20, Band II.1*. 39-59.
47. Outcalt, S.M. and McLinden, M.O. (1995), Equations of state for the thermodynamic properties of R32 (difluoromethane) and R125 (pentafluoroethane). *Int. J. Thermophys.*, **16(1)**, 79-89.
48. Piao, C.-C. and Noguchi, M. (1995), Private communication to the IUPAC Thermodynamic Tables Project Centre.
49. Piao, C.-C., Noguchi, M., Sato, H. and Watanabe K. (1992), Private communication to the IUPAC Thermodynamic Tables Project Centre.
50. Schmidt, J.W. and Moldover, M.R. (1994), Alternative Refrigerants CH_2F_2 and C_2HF_5: Critical temperature, refractive index, surface tension, and estimates of liquid, vapor, and critical densities. *J. Chem. Eng. Data*, **39(1)**, 39-44.
51. Weber, L.A. and Silva, A.M. (1994), Measurements of the vapor pressures of difluoromethane, 1-Chloro-1,2,2,2-tetrafluoroethane and pentafluoroethane. *J. Chem. Eng. Data*, **39(4)**, 808-812.
52. Wilson, L.C., Wilding, W.V., Wilson, G.M., Rowley, R.L. Felix, V.M. and Chilsom-Carter, T. (1992), Thermophysical properties of HFC-125. *Fluid Phase Equilibria*, **80**, 167-177.
53. de Vries, B. (1994), Private communication to the IUPAC Thermodynamic Tables Project Centre.
54. Ye, F., Sato, H. and Watanabe, K. (1995), Gas-phase *PVT* properties and vapor pressure of pentafluoroethane (HFC-125) determined according to the Burnett method. *J. Chem. Eng. Data*, **40(1)**, 148-152.

Appendix 1 – Data Maps

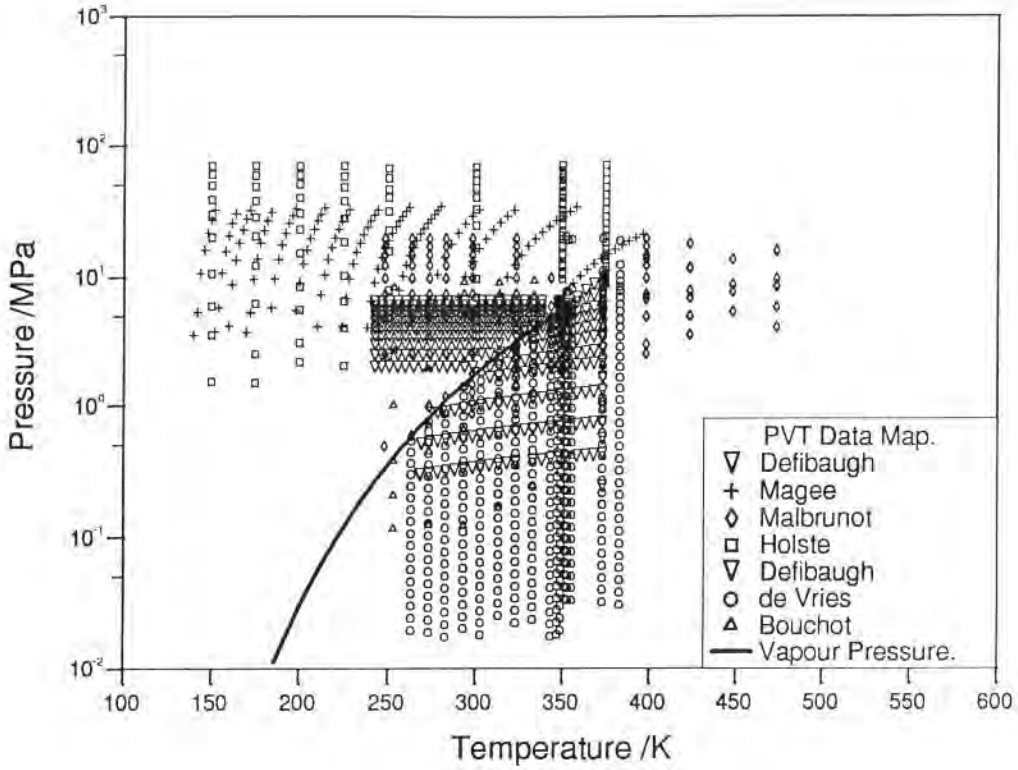

Figure A1.1 Data map for $P\rho T$ data for R32.

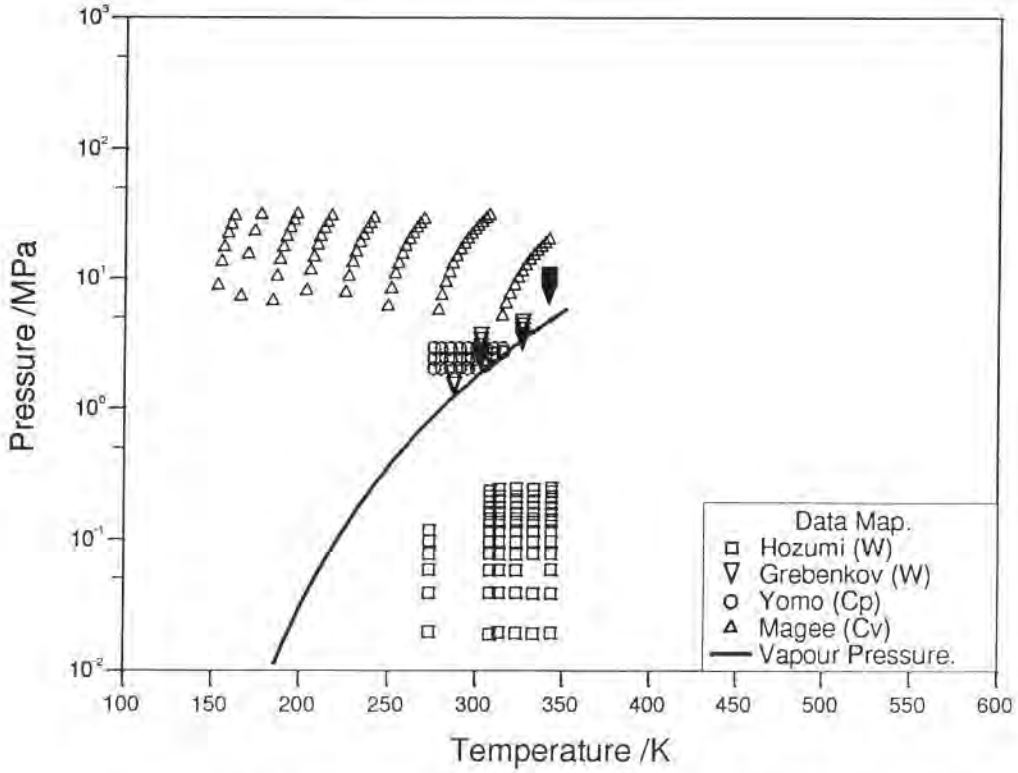

Figure A1.2 Data map for isochoric heat capacity, isobaric heat capacity and speed of sound data for R32

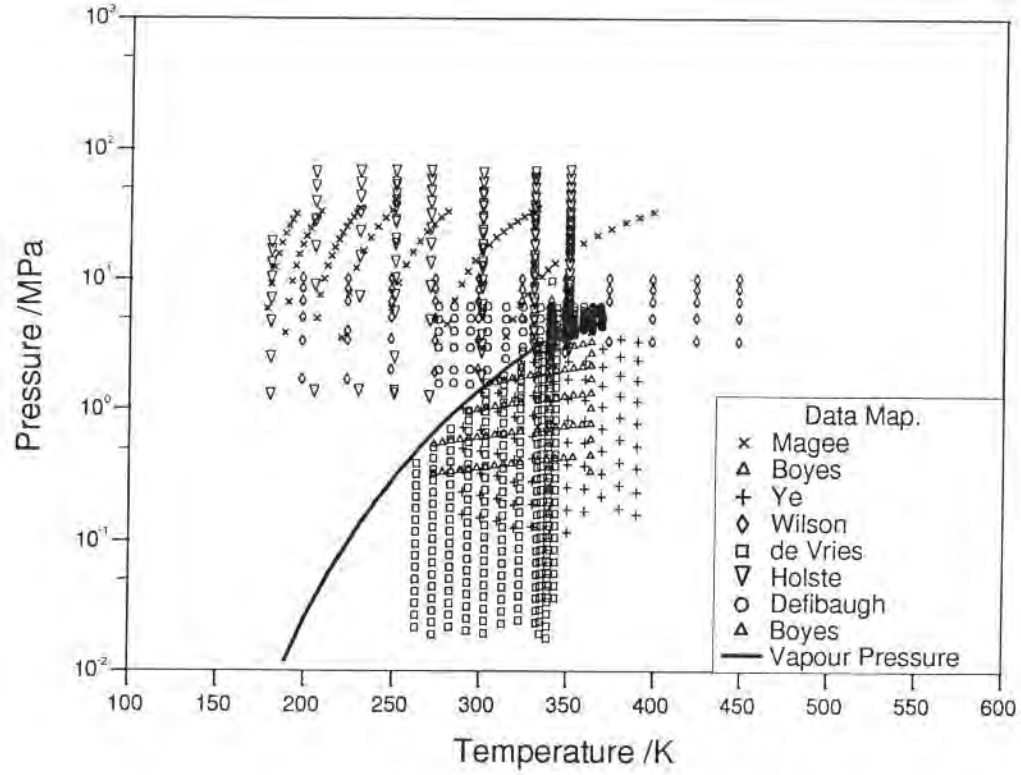

Figure A1.3 Data map for $P\rho T$ data for R125.

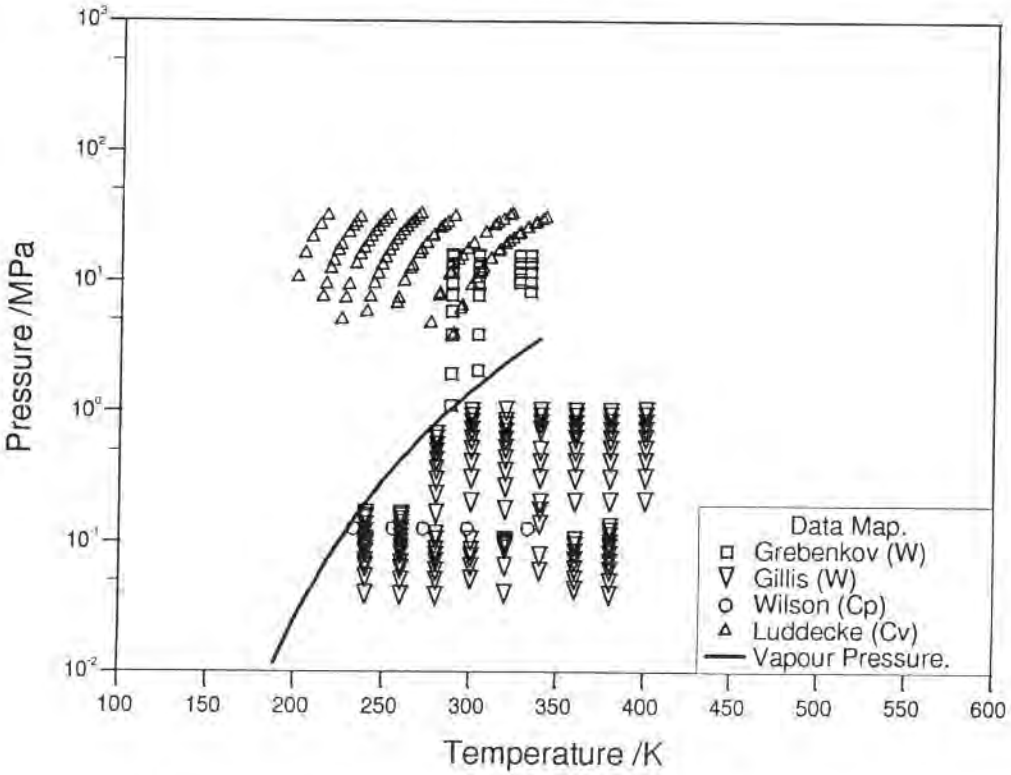

Figure A1.4 Data map for isochoric heat capacity, isobaric heat capacity and speed of sound data for R125.

Appendix 2 – Property Plots

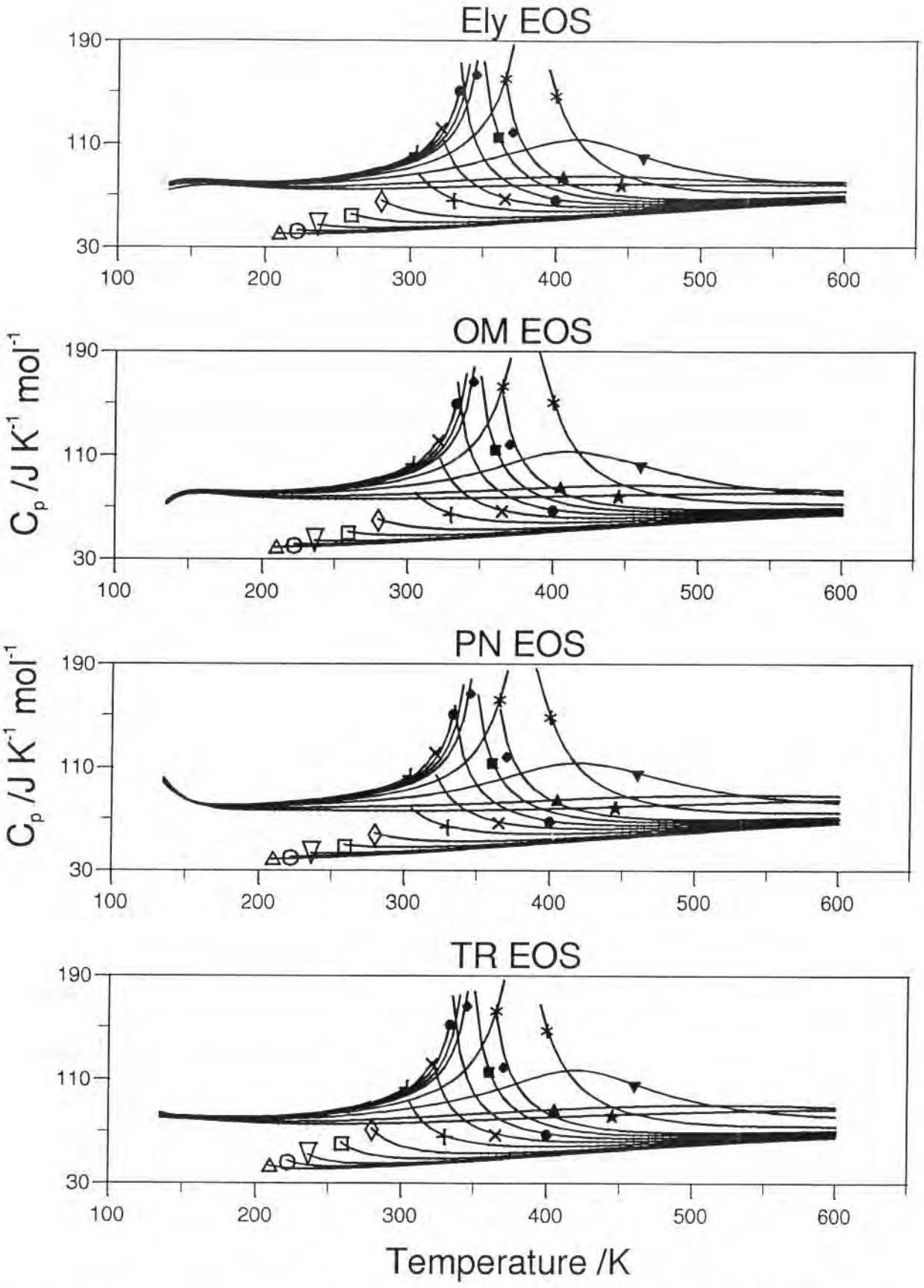

Figure A2.1 Isobaric heat capacity (C_P) property plot calculated from all four EOSs for R32. Isobars: (△) 0.05 MPa; (○) 0.1 MPa; (▽) 0.2 MPa; (□) 0.5 MPa; (◇) 1.0 MPa; (+) 2.0 MPa; (×) 3.0 MPa; (•) 4.0 MPa; (▪) 5.0 MPa; (♦) 6.0 MPa; (∗) 10.0 MPa; (▼) 20.0 MPa; (▲) 50.0 MPa; (⋆) 100.0 MPa.

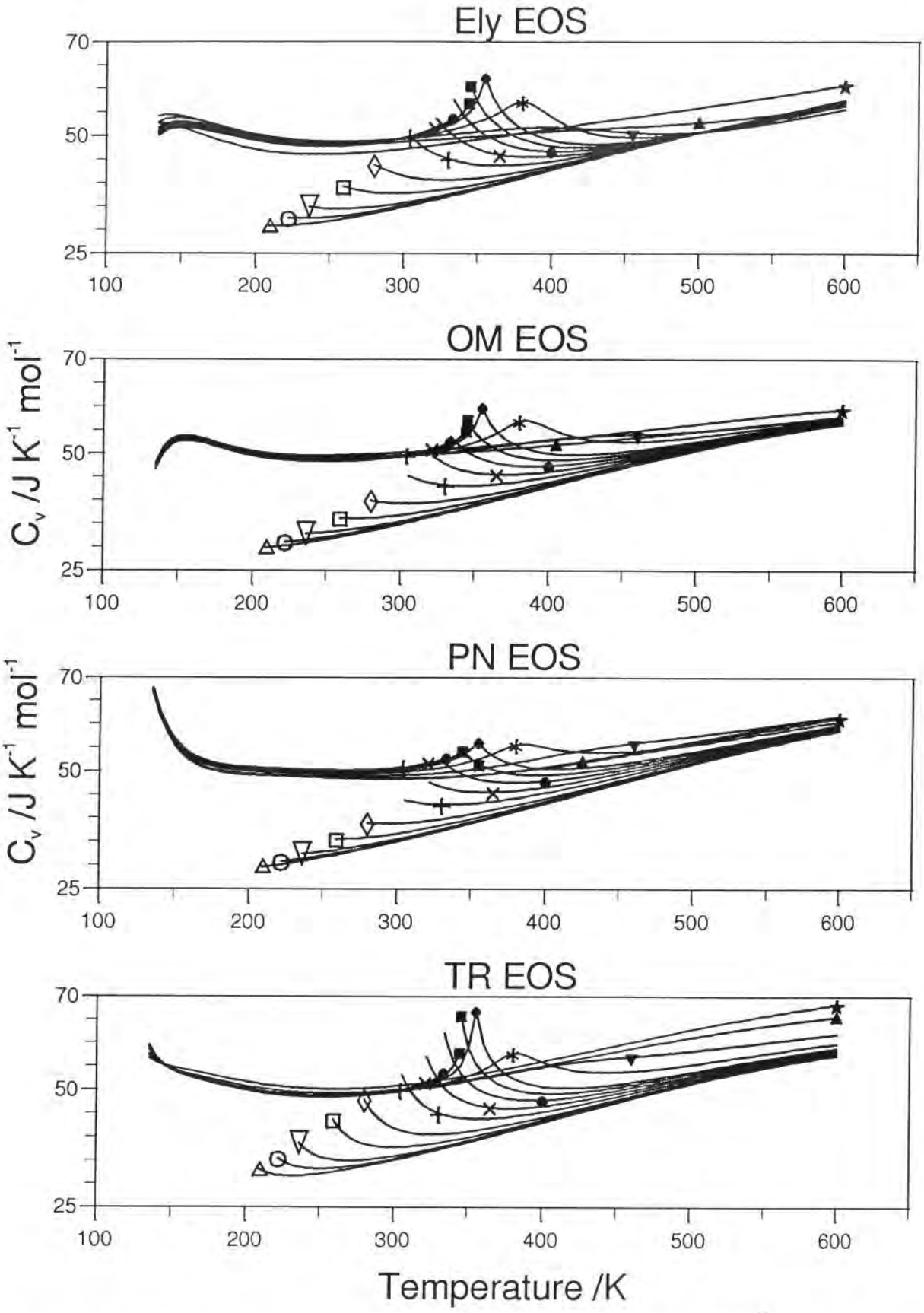

Figure A2.2 Isochoric heat capacity (C_V) property plot calculated from all four EOSs for R32. Isobars: (△) 0.05 MPa; (○) 0.1 MPa; (▽) 0.2 MPa; (□) 0.5 MPa; (◇) 1.0 MPa; (+) 2.0 MPa; (×) 3.0 MPa; (•) 4.0 MPa; (▪) 5.0 MPa; (◆) 6.0 MPa; (⋆) 10.0 MPa; (▼) 20.0 MPa; (▲) 50.0 MPa; (⋆) 100.0 MPa.

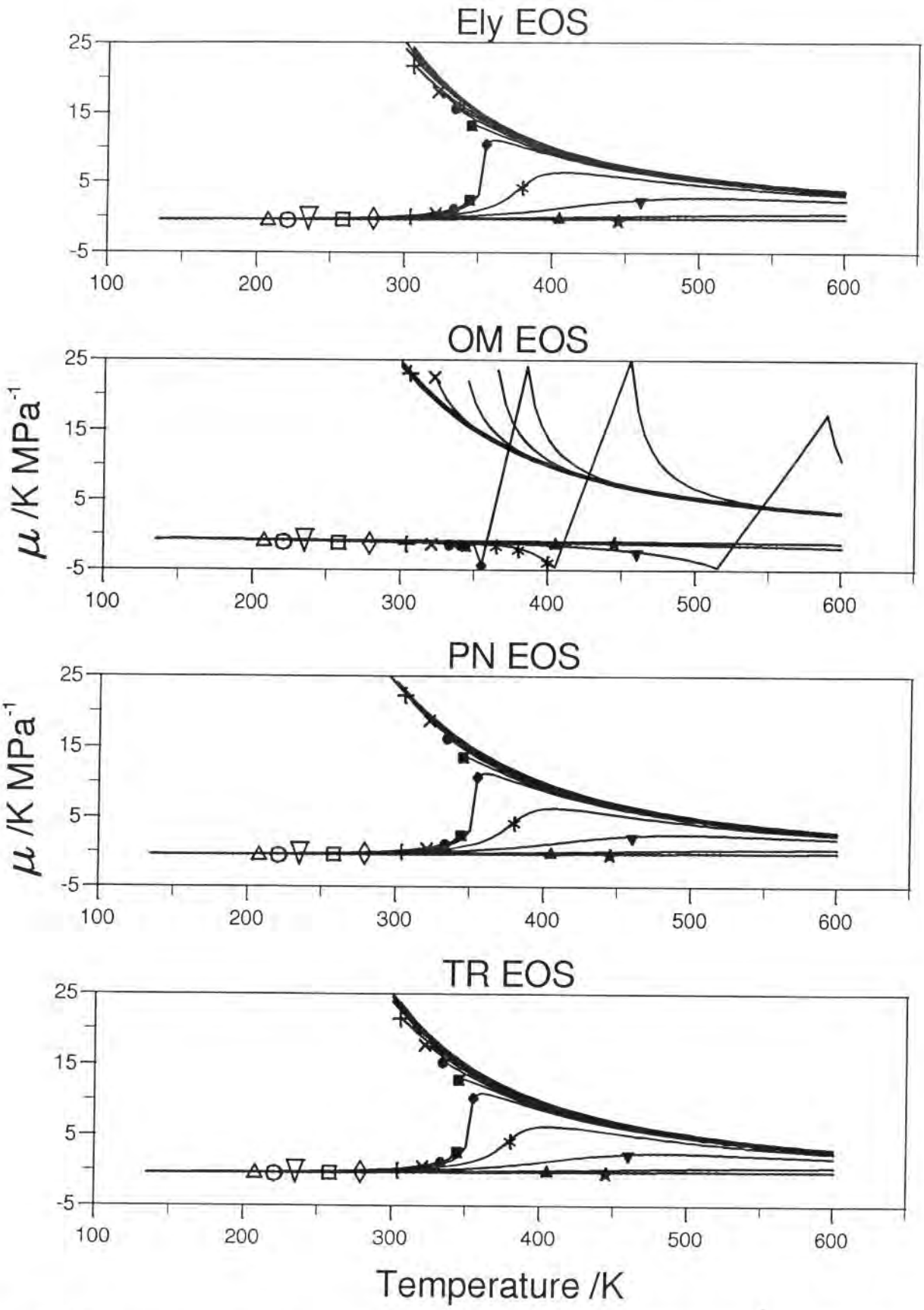

Figure A2.3 Isenthalpic Joule-Thomson $((\partial T/\partial P)_H)$ property plot calculated from all four EOSs for R32. Isobars: (△) 0.05 MPa; (○) 0.1 MPa; (▽) 0.2 MPa; (□) 0.5 MPa; (◇) 1.0 MPa; (+) 2.0 MPa; (×) 3.0 MPa; (•) 4.0 MPa; (▪) 5.0 MPa; (◆) 6.0 MPa; (∗) 10.0 MPa; (▼) 20.0 MPa; (▲) 50.0 MPa; (⋆) 100.0 MPa.

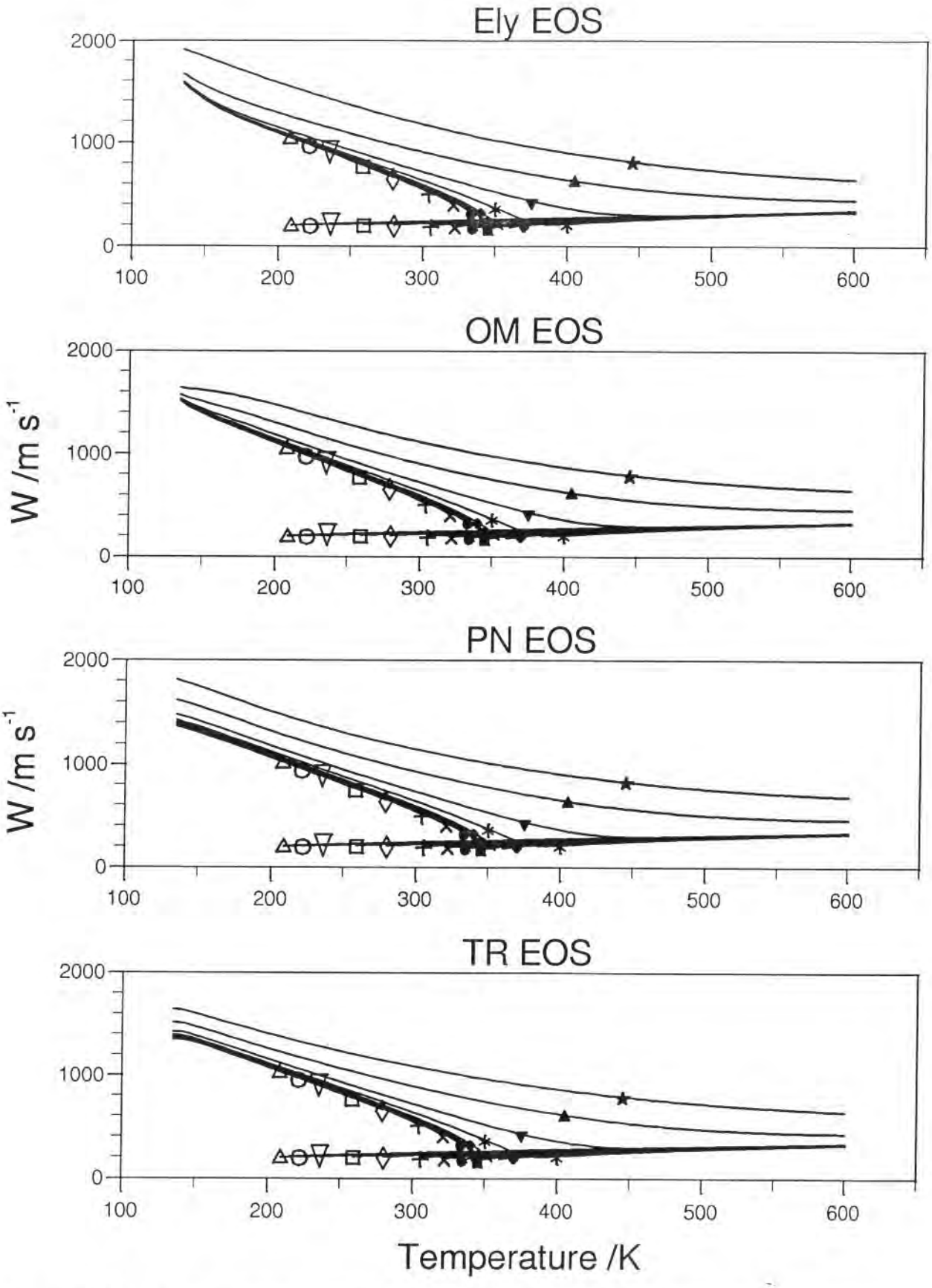

Figure A2.4 Speed of sound property plot calculated from all four EOSs for R32. Isobars: (△) 0.05 MPa; (○) 0.1 MPa; (▽) 0.2 MPa; (□) 0.5 MPa; (◇) 1.0 MPa; (+) 2.0 MPa; (×) 3.0 MPa; (•) 4.0 MPa; (▪) 5.0 MPa; (◆) 6.0 MPa; (∗) 10.0 MPa; (▼) 20.0 MPa; (▲) 50.0 MPa; (⋆) 100.0 MPa.

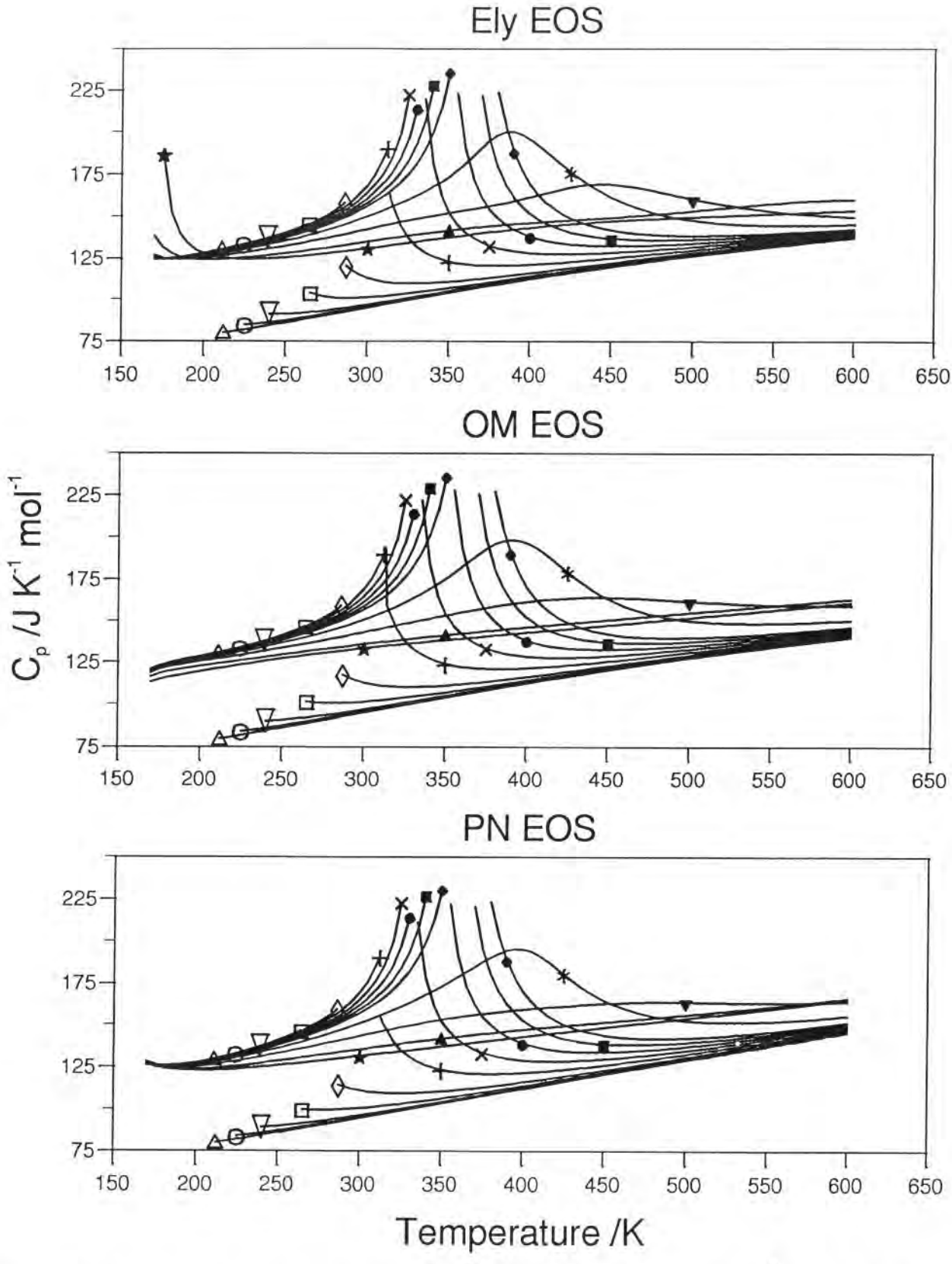

Figure A2.5 Isobaric heat capacity (C_P) property plot calculated from the all three EOSs for R125. Isobars: (△) 0.05 MPa; (○) 0.1 MPa; (▽) 0.2 MPa; (□) 0.5 MPa; (◇) 1.0 MPa; (+) 2.0 MPa; (×) 3.0 MPa; (•) 4.0 MPa; (▪) 5.0 MPa; (◆) 6.0 MPa; (∗) 10.0 MPa; (▼) 20.0 MPa; (▲) 50.0 MPa; (⋆) 100.0 MPa.

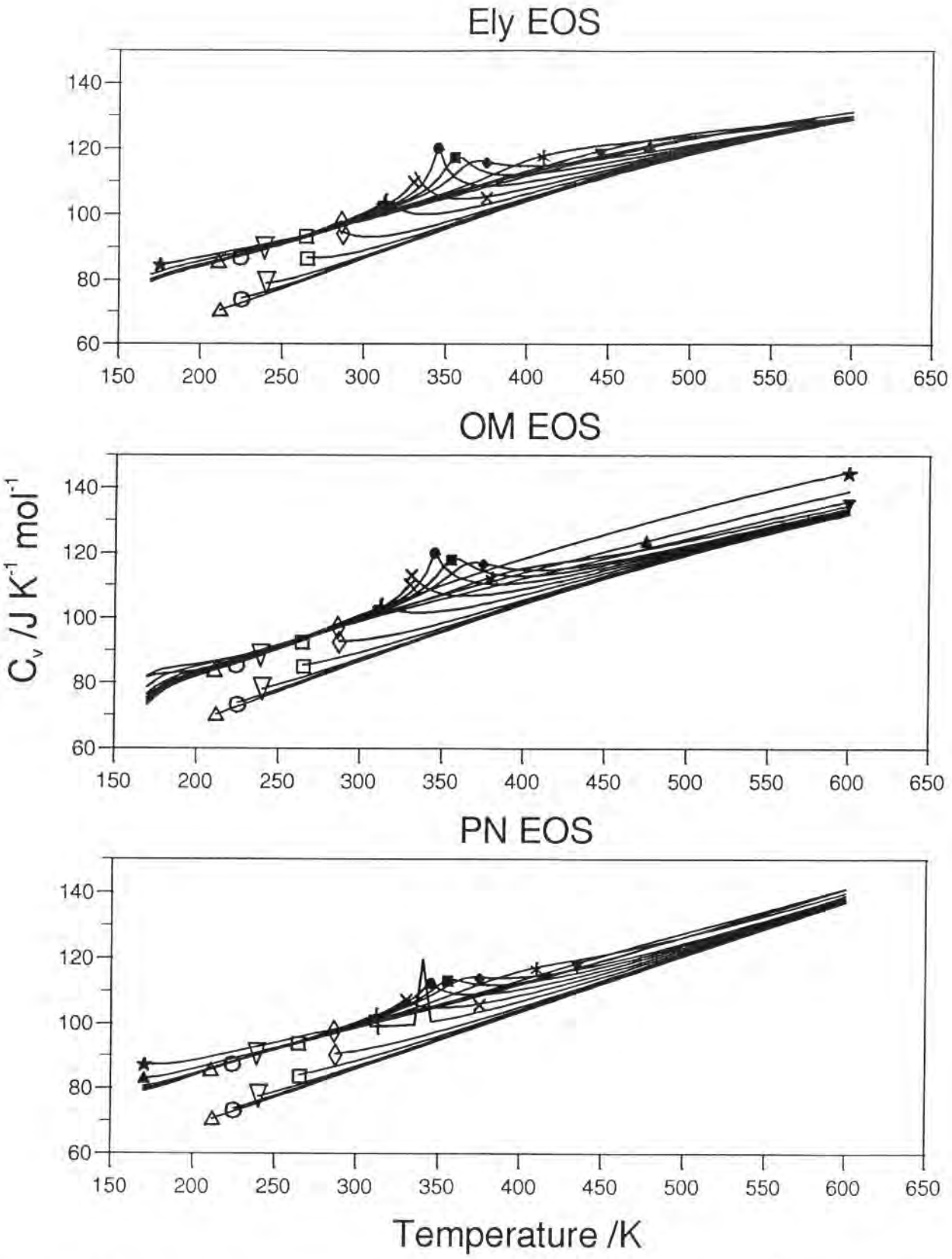

Figure A2.6 Isochoric heat capacity (C_V) property plot calculated from all three EOSs for R125. Isobars: (△) 0.05 MPa; (○) 0.1 MPa; (▽) 0.2 MPa; (□) 0.5 MPa; (◇) 1.0 MPa; (+) 2.0 MPa; (×) 3.0 MPa; (•) 4.0 MPa; (▪) 5.0 MPa; (◆) 6.0 MPa; (⋆) 10.0 MPa; (▼) 20.0 MPa; (▲) 50.0 MPa; (⋆) 100.0 MPa.

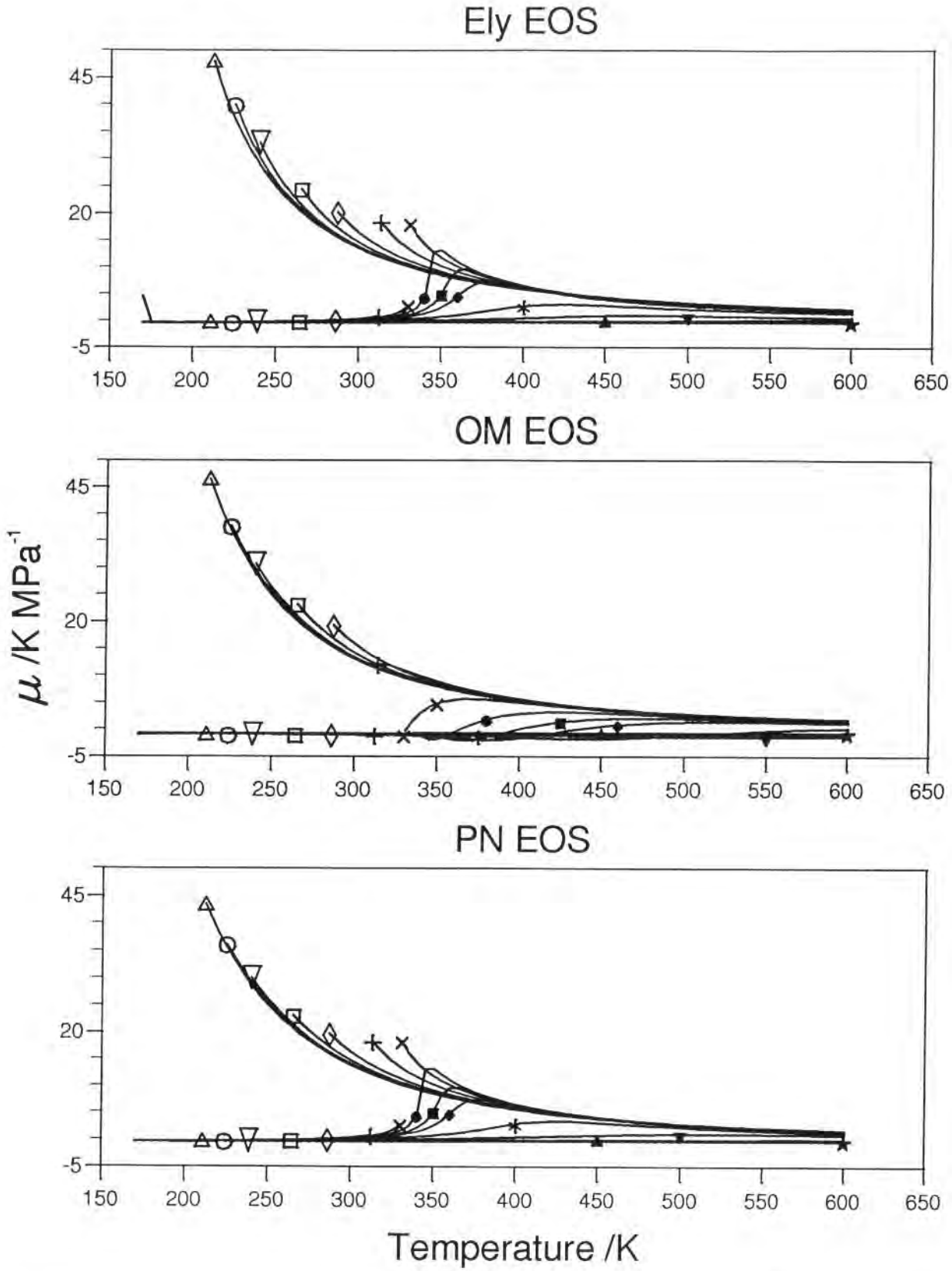

Figure A2.7 Isenthalpic Joule-Thomson $((\partial T/\partial P)_H)$ property plot calculated from all three EOSs for R125. Isobars: (△) 0.05 MPa; (○) 0.1 MPa; (▽) 0.2 MPa; (□) 0.5 MPa; (◇) 1.0 MPa; (+) 2.0 MPa; (×) 3.0 MPa; (•) 4.0 MPa; (▪) 5.0 MPa; (◆) 6.0 MPa; (⋆) 10.0 MPa; (▼) 20.0 MPa; (▲) 50.0 MPa; (⋆) 100.0 MPa.

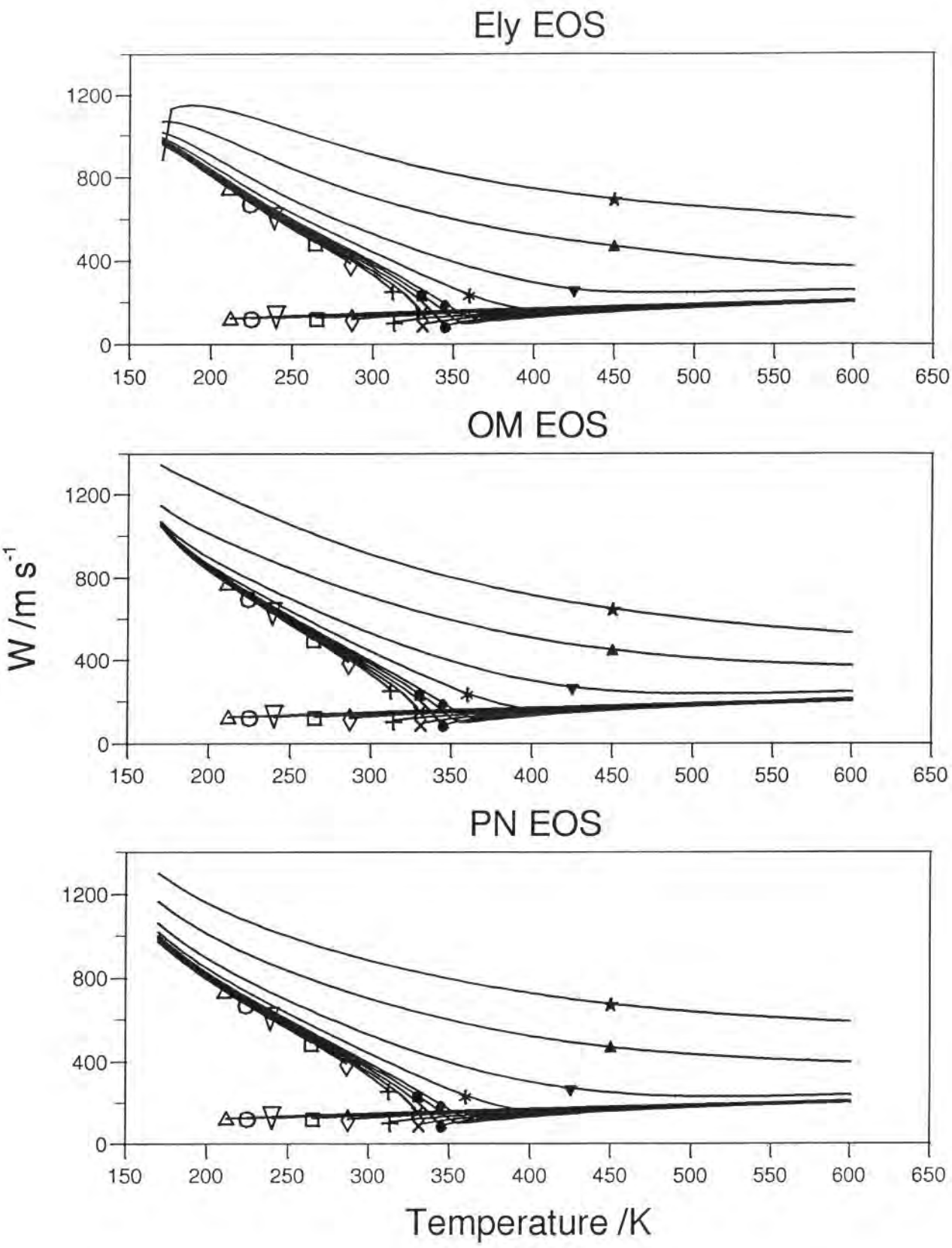

Figure A2.8 Speed of sound property plot calculated from all three EOSs for R125. Isobars: (△) 0.05 MPa; (○) 0.1 MPa; (▽) 0.2 MPa; (□) 0.5 MPa; (◇) 1.0 MPa; (+) 2.0 MPa; (×) 3.0 MPa; (•) 4.0 MPa; (▪) 5.0 MPa; (◆) 6.0 MPa; (∗) 10.0 MPa; (▼) 20.0 MPa; (▲) 50.0 MPa; (⋆) 100.0 MPa.

Appendix 3 – Statistical information

R32 Ideal Gas Heat Capacity Statistics

EOS	Author	Date	Points	AAD	Bias	Std Dev	RMS	Max Dev	Bad
Ely	Chase Jr M.W. *et al*	(1985)	64	0.7184E-01	0.6800E-01	0.5267E-01	0.8576E-01	0.1300E+00	0
	Rodgers A.S. *et al.*	(1974)	18	0.1911E-01	0.1522E-01	0.2242E-01	0.2658E-01	0.6700E-01	1
	Overall		82	0.6027E-01	0.5641E-01	0.5240E-01	0.7678E-01	0.1300E+00	1
OM	Chase Jr M.W. *et al*	(1985)	64	0.1620E+00	0.1159E+00	0.9277E+00	0.9277E+00	0.7126E+01	53
	Rodgers A.S. *et al*	(1974)	18	0.5743E+00	0.4155E+00	0.1749E+01	0.1750E+01	0.7129E+01	8
	Overall		82	0.2525E+00	0.1817E+00	0.1152E+01	0.1159E+01	0.7129E+01	61
TR	Chase Jr M.W. *et al*	(1985)	64	0.1319E+00	0.2976E-01	0.6320E+00	0.6277E+00	0.4798E+01	53
	Rodgers A.S. *et al*	(1974)	18	0.4316E+00	0.1670E+00	0.1195E+01	0.1173E+01	0.4801E+01	8
	Overall		82	0.1977E+00	0.5987E-01	0.7832E+00	0.7807E+00	0.4801E+01	61

R32 Saturated Vapour Pressure Statistics

EOS	Author	Date	Points	AAD	Bias	Std Dev	RMS	Max Dev	Bad
Ely	Bouchot C. *et al*	(1994)	8	0.2040E+00	0.1638E+00	0.1927E+00	0.2435E+00	0.4270E+00	0
	Defibaugh D.R. *et al*	(1994)	14	0.2529E-01	0.6714E-02	0.2937E-01	0.2908E-01	-0.5700E-01	0
	deVries B.	(1994)	112	0.6044E-01	0.5262E-01	0.4481E-01	0.6898E-01	0.1150E+00	0
	Holcomb C.D. *et al*	(1993)	25	0.1892E+00	0.1859E+00	0.1293E+00	0.2250E+00	0.6040E+00	0
	Kanungo A. *et al*	(1987)	11	0.3559E+00	0.3219E+00	0.2540E+00	0.4028E+00	0.5420E+00	0
	Magee & Howley	(1993)	7	0.8413E-01	-0.8226E-01	0.5574E-01	0.9711E-01	-0.1529E+00	0
	Malbrunot P.F *et al*	(1968)	30	0.2820E+00	0.9557E-01	0.3146E+00	0.3237E+00	0.6310E+00	0
	Nagel M. *et al.*	(1993)	27	0.7781E-01	0.7181E-01	0.6906E-01	0.9874E-01	0.2080E+00	0
	Weber & Goodwin	(1993)	27	0.2800E-01	0.1519E-01	0.3531E-01	0.3783E-01	0.7900E-01	0
	Weber & Silva	(1994)	17	0.2748E-01	-0.8094E-02	0.4468E-01	0.4410E-01	0.1605E+00	0
	Overall		278	0.1071E+00	0.7189E-01	0.1493E+00	0.1655E+00	0.6311E+00	0
OM	Bouchot C. *et al*	(1994)	8	0.1831E+00	0.8237E-01	0.2442E+00	0.2428E+00	0.4730E+00	0
	Defibaugh D.R. *et al*	(1994)	14	0.1033E+00	-0.1033E+00	0.6657E-01	0.1216E+00	-0.1990E+00	0
	deVries B.	(1994)	112	0.1136E+00	-0.1136E+00	0.4050E-01	0.1206E+00	-0.1610E+00	0
	Holcomb C.D. *et al*	(1993)	25	0.1149E+00	-0.2076E-01	0.1584E+00	0.1566E+00	0.5180E+00	0
	Kanungo A. *et al*	(1987)	11	0.7176E+00	0.7176E+00	0.3465E+00	0.7900E+00	0.1517E+01	0
	Magee & Howley	(1993)	7	0.1927E+00	-0.1927E+00	0.6461E-01	0.2018E+00	-0.2427E+00	0
	Malbrunot P.F *et al*	(1968)	30	0.2615E+00	0.2860E-01	0.3169E+00	0.3129E+00	0.6980E+00	0
	Nagel M. *et al.*	(1993)	27	0.8741E-01	-0.7185E-02	0.1057E+00	0.1040E+00	0.2080E+00	0
	Weber & Goodwin	(1993)	27	0.3196E-01	0.2167E-01	0.3409E-01	0.3985E-01	0.8600E-01	0
	Weber & Silva	(1994)	17	0.2625E-01	0.2625E-01	0.4595E-01	0.5173E-01	0.2025E+00	0
	Overall		278	0.1412E+00	-0.2083E-01	0.2188E+00	0.2194E+00	0.1517E+01	0
PN	Bouchot C. *et al*	(1994)	8	0.1945E+00	0.1215E+00	0.2061E+00	0.2279E+00	0.3880E+00	0
	Defibaugh D.R. *et al*	(1994)	14	0.2314E-01	-0.5143E-02	0.3232E-01	0.3156E-01	-0.9300E-01	0
	deVries B.	(1994)	112	0.3422E-01	0.6188E-02	0.5534E-01	0.5544E-01	-0.1700E+00	0
	Holcomb C.D. *et al*	(1993)	25	0.1262E+00	0.1036E+00	0.1679E+00	0.1944E+00	0.6190E+00	0
	Kanungo A. *et al*	(1987)	11	0.1698E+00	0.1655E+00	0.1335E+00	0.2087E+00	0.3970E+00	0
	Magee & Howley	(1993)	7	0.9744E-01	-0.9744E-01	0.3217E-01	0.1019E+00	-0.1499E+00	0
	Malbrunot P.F *et al*	(1968)	30	0.2727E+00	-0.1980E-01	0.3514E+00	0.3461E+00	0.8630E+00	0
	Nagel M. *et al.*	(1993)	27	0.8504E-01	-0.3644E-01	0.1085E+00	0.1125E+00	-0.2960E+00	0
	Weber & Goodwin	(1993)	27	0.3111E+00	-0.3111E+00	0.4857E-01	0.3147E+00	-0.4300E+00	0
	Weber & Silva	(1994)	17	0.1799E+00	-0.1692E+00	0.9584E-01	0.1930E+00	-0.2643E+00	0
	Overall		278	0.1200E+00	-0.2709E-01	0.1833E+00	0.1850E+00	0.8627E+00	0
TR	Bouchot C. *et al*	(1994)	8	0.1980E+00	0.1517E+00	0.2085E+00	0.2471E+00	0.4410E+00	0
	Defibaugh D.R. *et al*	(1994)	14	0.1600E-01	-0.6000E-02	0.2107E-01	0.2117E-01	-0.4600E-01	0
	deVries B.	(1994)	112	0.6170E-02	-0.2705E-02	0.6819E-02	0.7308E-02	-0.1600E-01	0
	Holcomb C.D. *et al*	(1993)	25	0.1159E+00	0.9824E-01	0.1599E+00	0.1849E+00	0.6120E+00	0
	Kanungo A. *et al*	(1987)	11	0.6751E+00	0.6751E+00	0.2575E+00	0.7184E+00	0.1107E+01	0
	Magee & Howley	(1993)	7	0.9693E-01	-0.9693E-01	0.2227E-01	0.9910E-01	-0.1211E+00	0
	Malbrunot P.F *et al*	(1968)	29	0.2657E+00	0.6634E-01	0.3137E+00	0.3153E+00	0.7920E+00	0
	Nagel M. *et al.*	(1993)	27	0.5574E-01	0.5559E-01	0.7007E-01	0.8842E-01	0.2640E+00	0
	Weber & Goodwin	(1993)	27	0.3559E-01	0.2263E-01	0.4616E-01	0.5064E-01	0.1240E+00	0
	Weber & Silva	(1994)	17	0.2734E-01	-0.3026E-02	0.5076E-01	0.4934E-01	0.1865E+00	0
	Overall		277	0.8714E-01	0.5060E-01	0.1865E+00	0.1929E+00	0.1107E+01	0

R32 Saturated Liquid Density Statistics

EOS	Author	Date	Points	AAD	Bias	Std Dev	RMS	Max Dev	Bad
Ely	Bouchot C. *et al*	(1994)	5	0.3660E-01	-0.2180E-01	0.4216E-01	0.4355E-01	-0.8000E-01	0
	Defibaugh D.R. *et al*	(1994)	21	0.6038E-01	0.6038E-01	0.6409E-01	0.8694E-01	0.2650E+00	0
	Higashi Y.	(1994)	8	0.1244E+01	-0.1080E+01	0.1666E+01	0.1896E+01	-0.4358E+01	2
	Holcomb C.D. *et al*	(1993)	25	0.1442E+00	-0.5052E-01	0.2301E+00	0.2310E+00	-0.7460E+00	0
	Magee & Howley	(1993)	13	0.4238E-01	0.2423E-01	0.4225E-01	0.4727E-01	0.7400E-01	0
	Malbrunot P.F. *et al*	(1968)	15	0.3888E+00	-0.3384E+00	0.5579E+00	0.6364E+00	-0.2164E+01	0
	Shinsaka K. *et al*	(1985)	20	0.9738E+00	-0.9738E+00	0.1084E+00	0.9795E+00	-0.1149E+01	0
	Overall		107	0.3819E+00	-0.3082E+00	0.6545E+00	0.7206E+00	-0.4358E+01	2
OM	Bouchot C. *et al*	(1994)	5	0.1102E+00	-0.1054E+00	0.1350E+00	0.1603E+00	-0.3250E+00	0
	Defibaugh D.R. *et al*	(1994)	21	0.3119E-01	-0.1005E-01	0.5627E-01	0.5582E-01	-0.2290E+00	0
	Higashi Y.	(1994)	8	0.1139E+01	-0.9085E+00	0.1465E+01	0.1644E+01	-0.3763E+01	2
	Holcomb C.D. *et al*	(1993)	25	0.3145E+00	-0.3135E+00	0.2413E+00	0.3927E+00	-0.7760E+00	0
	Magee & Howley	(1993)	13	0.2900E-01	-0.8692E-02	0.3435E-01	0.3413E-01	0.5900E-01	0
	Malbrunot P.F. *et al*	(1968)	15	0.4982E+00	-0.4982E+00	0.4683E+00	0.6730E+00	-0.1912E+01	0
	Shinsaka K. *et al*	(1985)	20	0.1025E+01	-0.1025E+01	0.9764E-01	0.1030E+01	-0.1146E+01	0
	Overall		107	0.4349E+00	-0.4106E+00	0.5800E+00	0.7084E+00	-0.3763E+01	2
PN	Bouchot C. *et al*	(1994)	5	0.5860E-01	-0.4200E-02	0.7528E-01	0.6746E-01	-0.1120E+00	0
	Defibaugh D.R. *et al*	(1994)	21	0.8338E-01	0.8338E-01	0.2645E-01	0.8728E-01	0.1820E+00	0
	Higashi Y.	(1994)	8	0.3200E+01	-0.2966E+00	0.4678E+01	0.4386E+01	0.9029E+01	0
	Holcomb C.D. *et al*	(1993)	25	0.1405E+00	-0.9160E-01	0.2544E+00	0.2655E+00	-0.1035E+01	0
	Magee & Howley	(1993)	13	0.5023E-01	0.4762E-01	0.4592E-01	0.6491E-01	0.1180E+00	1
	Malbrunot P.F. *et al*	(1968)	15	0.4239E+00	-0.3945E+00	0.7232E+00	0.8024E+00	-0.2893E+01	0
	Shinsaka K. *et al*	(1985)	20	0.9669E+00	-0.9669E+00	0.8614E-01	0.9706E+00	-0.1087E+01	0
	Overall		107	0.5374E+00	-0.2577E+00	0.1293E+01	0.1313E+01	0.9029E+01	1
TR	Bouchot C. *et al*	(1994)	5	0.4900E-01	-0.3420E-01	0.5546E-01	0.6025E-01	-0.1090E+00	0
	Defibaugh D.R. *et al*	(1994)	21	0.5195E-01	0.5167E-01	0.6109E-01	0.7889E-01	0.2240E+00	0
	Higashi Y.	(1994)	8	0.2810E+01	-0.1845E+01	0.4148E+01	0.4296E+01	-0.9373E+01	0
	Holcomb C.D. *et al*	(1993)	25	0.1908E+00	0.1823E+00	0.1849E+00	0.2570E+00	0.7130E+00	0
	Magee & Howley	(1993)	13	0.3077E-01	0.1969E-01	0.3577E-01	0.3961E-01	0.8300E-01	0
	Malbrunot P.F. *et al*	(1968)	15	0.2375E+00	-0.6853E-01	0.2912E+00	0.2896E+00	0.5810E+00	0
	Shinsaka K. *et al*	(1985)	20	0.9892E+00	-0.9892E+00	0.9762E-01	0.9937E+00	-0.1121E+01	0
	Overall		107	0.4891E+00	-0.2789E+00	0.1237E+01	0.1262E+01	-0.9373E+01	0

R32 Saturated Vapour Density Statistics

EOS	Author	Date	Points	AAD	Bias	Std Dev	RMS	Max Dev	Bad
Ely	Bouchot C. *et al*	(1994)	5	0.1334E+01	0.1334E+01	0.1060E+01	0.1636E+01	0.2701E+01	0
	Defibaugh D.R. *et al*	(1994)	28	0.1084E+00	0.8793E-01	0.1680E+00	0.1869E+00	0.5320E+00	0
	Higashi Y.	(1994)	9	0.2952E+01	0.2952E+01	0.1755E+01	0.3384E+01	0.5840E+01	0
	Holcomb C.D. *et al*	(1993)	25	0.1171E+01	0.1171E+01	0.5345E+00	0.1282E+01	0.2938E+01	0
	Overall		67	0.9782E+00	0.9696E+00	0.1203E+01	0.1538E+01	0.5840E+01	0
OM	Bouchot C. *et al*	(1994)	5	0.1580E+01	0.1580E+01	0.1190E+01	0.1905E+01	0.3367E+01	0
	Defibaugh D.R. *et al*	(1994)	28	0.3773E+00	0.3262E+00	0.3066E+00	0.4439E+00	0.6740E+00	0
	Higashi Y.	(1994)	9	0.3042E+01	0.3042E+01	0.1372E+01	0.3306E+01	0.5339E+01	0
	Holcomb C.D. *et al*	(1993)	25	0.8859E+00	0.8795E+00	0.7378E+00	0.1138E+01	0.3263E+01	0
	Overall		67	0.1015E+01	0.9911E+00	0.1159E+01	0.1518E+01	0.5339E+01	0
PN	Bouchot C. *et al*	(1994)	5	0.1905E+01	0.1905E+01	0.1021E+01	0.2113E+01	0.3389E+01	0
	Defibaugh D.R. *et al*	(1994)	28	0.5818E+00	0.5818E+00	0.1677E+00	0.6047E+00	0.8010E+00	0
	Higashi Y.	(1994)	9	0.4139E+01	0.4139E+01	0.2803E+01	0.4910E+01	0.7390E+01	2
	Holcomb C.D. *et al*	(1993)	25	0.1526E+01	0.1526E+01	0.8794E+00	0.1752E+01	0.3739E+01	0
	Overall		67	0.1511E+01	0.1511E+01	0.1621E+01	0.2207E+01	0.7390E+01	2
TR	Bouchot C. *et al*	(1994)	5	0.1092E+01	0.9628E+00	0.1079E+01	0.1363E+01	0.2568E+01	0
	Defibaugh D.R. *et al*	(1994)	28	0.3254E+00	-0.3254E+00	0.2098E+00	0.3852E+00	-0.7510E+00	0
	Higashi Y.	(1994)	9	0.2400E+01	0.2400E+01	0.1332E+01	0.2708E+01	0.4681E+01	0
	Holcomb C.D. *et al*	(1993)	25	0.4663E+00	0.2363E+00	0.7256E+00	0.7491E+00	0.2685E+01	0
	Overall		67	0.7139E+00	0.3464E+00	0.1138E+01	0.1181E+01	0.4681E+01	0

R32 Liquid Heat Capacity at Saturation

EOS	Author	Date	Points	AAD	Bias	Std Dev	RMS	Max Dev	Bad
Ely	Magee & Luddecke	(1993)	95	0.7399E+00	-0.4211E-02	0.1346E+01	0.1339E+01	-0.7851E+01	0
OM	Magee & Luddecke	(1993)	95	0.1087E+01	-0.7581E+00	0.1472E+01	0.1649E+01	-0.9429E+01	0
PN	Magee & Luddecke	(1993)	95	0.1583E+01	-0.1427E+01	0.2016E+01	0.2461E+01	-0.9367E+01	2
TR	Magee & Luddecke	(1993)	95	0.4946E+00	-0.2939E+00	0.1094E+01	0.1127E+01	-0.7670E+01	1

R32 Liquid Phase *PVT* Statistics

EOS	Author	Date	Points	AAD	Bias	Std Dev	RMS	Max Dev	Bad
Ely	Bouchot C. *et al*	(1994)	21	0.5221E-01	-0.4327E-01	0.5654E-01	0.7012E-01	-0.1456E+00	0
	Defibaugh D.R. *et al*	(1994)	219	0.4443E-01	0.3800E-01	0.1021E+00	0.1088E+00	0.1124E+01	4
	Holste J.C.	(1993)	126	0.1260E+00	-0.1030E+00	0.1474E+00	0.1793E+00	-0.9135E+00	0
	Malbrunot P.F. *et al*	(1968)	57	0.2039E+00	-0.2014E+00	0.1684E+00	0.2616E+00	-0.1075E+01	0
	Magee & Howley	(1993)	137	0.3725E-01	-0.2067E-01	0.5098E-01	0.5484E-01	-0.1931E+00	0
	Overall		560	0.7755E-01	-0.3549E-01	0.1361E+00	0.1405E+00	0.1124E+01	4
OM	Bouchot C. *et al*	(1994)	21	0.6810E-01	-0.6075E-01	0.6676E-01	0.8908E-01	-0.2093E+00	0
	Defibaugh D.R. *et al*	(1994)	219	0.4340E-01	0.3068E-01	0.1337E+00	0.1369E+00	0.1405E+01	4
	Holste J.C.	(1993)	126	0.1158E+00	-0.1013E+00	0.2128E+00	0.2349E+00	-0.1536E+01	0
	Malbrunot P.F. *et al*	(1968)	57	0.1993E+00	-0.1960E+00	0.1937E+00	0.2744E+00	-0.1174E+01	0
	Magee & Howley	(1993)	137	0.2361E-01	0.1347E-01	0.2982E-01	0.3263E-01	-0.1865E+00	0
	Overall		560	0.7164E-01	-0.2973E-01	0.1647E+00	0.1672E+00	-0.1536E+01	4
PN	Bouchot C. *et al*	(1994)	21	0.5774E-01	-0.2980E-01	0.6498E-01	0.7007E-01	-0.1464E+00	0
	Defibaugh D.R. *et al*	(1994)	219	0.1313E+00	0.1308E+00	0.4141E+00	0.4333E+00	0.5097E+01	0
	Holste J.C.	(1993)	126	0.1157E+00	-0.2904E-01	0.1598E+00	0.1618E+00	-0.8619E+00	0
	Malbrunot P.F. *et al*	(1968)	57	0.1788E+00	-0.1749E+00	0.1589E+00	0.2354E+00	-0.1020E+01	0
	Magee & Howley	(1993)	137	0.4683E-01	0.1550E-01	0.6360E-01	0.6524E-01	-0.2557E+00	0
	Overall		560	0.1092E+00	0.2947E-01	0.2924E+00	0.2936E+00	0.5097E+01	0
TR	Bouchot C. *et al*	(1994)	21	0.4944E-01	-0.3701E-01	0.5564E-01	0.6571E-01	-0.1345E+00	0
	Defibaugh D.R. *et al*	(1994)	219	0.9691E-01	0.9423E-01	0.2578E+00	0.2739E+00	0.2389E+01	4
	Holste J.C.	(1993)	126	0.1336E+00	-0.1264E+00	0.1134E+00	0.1695E+00	-0.9266E+00	0
	Malbrunot P.F. *et al*	(1968)	57	0.1836E+00	-0.1776E+00	0.1523E+00	0.2331E+00	-0.1016E+01	0
	Magee & Howley	(1993)	137	0.1811E-01	-0.7651E-02	0.3243E-01	0.3321E-01	-0.1873E+00	0
	Overall		560	0.9293E-01	-0.1292E-01	0.2041E+00	0.2044E+00	0.2389E+01	4

R32 Gas phase *PVT* Statistics

EOS	Author	Date	Points	AAD	Bias	Std Dev	RMS	Max Dev	Bad
Ely	Bouchot C. *et al*	(1994)	15	0.1971E+01	0.1654E+01	0.2505E+01	0.2931E+01	0.6204E+01	0
	de Vries B.	(1994)	476	0.8751E-01	0.3406E-01	0.3240E+00	0.3254E+00	0.3656E+01	0
	Defibaugh D.R.	(1994)	168	0.1146E+00	-0.2173E-01	0.2678E+00	0.2678E+00	-0.1645E+01	0
	Malbrunot P.F *et al*	(1968)	86	0.1439E+01	-0.9832E+00	0.1714E+01	0.1967E+01	-0.6382E+01	2
	Overall		745	0.2876E+00	-0.6335E-01	0.8370E+00	0.8388E+00	-0.6382E+01	2
OM	Bouchot C. *et al*	(1994)	15	0.2089E+01	0.1831E+01	0.2553E+01	0.3072E+01	0.6342E+01	0
	de Vries B.	(1994)	476	0.1371E+00	0.2363E-01	0.4384E+00	0.4386E+00	0.4059E+01	0
	Defibaugh D.R.	(1994)	168	0.1925E+00	-0.7167E-02	0.4813E+00	0.4799E+00	-0.2521E+01	0
	Malbrunot P.F *et al*	(1968)	86	0.1571E+01	-0.1082E+01	0.1887E+01	0.2166E+01	-0.5985E+01	2
	Overall		745	0.3544E+00	-0.7457E-01	0.9497E+00	0.9520E+00	0.6342E+01	2
PN	Bouchot C. *et al*	(1994)	15	0.2142E+01	0.1903E+01	0.2566E+01	0.3125E+01	0.6384E+01	0
	de Vries B.	(1994)	476	0.2442E+00	-0.3979E-02	0.3954E+00	0.3943E+00	0.2257E+01	0
	Defibaugh D.R.	(1994)	168	0.1309E+00	0.4453E-01	0.4845E+00	0.4861E+00	0.5790E+01	2
	Malbrunot P.F *et al*	(1968)	86	0.1483E+01	-0.9989E+00	0.1621E+01	0.1896E+01	-0.4956E+01	0
	Overall		745	0.3530E+00	-0.4943E-01	0.8923E+00	0.8930E+00	0.6384E+01	2
TR	Bouchot C. *et al*	(1994)	15	0.2001E+01	0.1586E+01	0.2551E+01	0.2931E+01	0.6219E+01	0
	de Vries B.	(1994)	476	0.3694E-01	0.1272E-02	0.1909E+00	0.1907E+00	0.3018E+01	0
	Defibaugh D.R.	(1994)	168	0.1213E+00	-0.5001E-01	0.2080E+00	0.2134E+00	-0.1674E+01	0
	Malbrunot P.F *et al*	(1968)	86	0.1468E+01	-0.1054E+01	0.1658E+01	0.1956E+01	-0.6185E+01	2
	Overall		745	0.2607E+00	-0.1002E+00	0.7994E+00	0.8051E+00	0.6219E+01	2

R32 Second Virial Coeficient Statistics

EOS	Author	Date	Points	AAD	Bias	Std Dev	RMS	Max Dev	Bad
Ely	Bignell & Dunlop	(1993)	3	0.2071E+01	-0.2071E+01	0.9480E+00	0.2211E+01	-0.2981E+01	0
OM	Bignell & Dunlop	(1993)	3	0.1777E+01	-0.1777E+01	0.8119E+00	0.1897E+01	-0.2393E+01	0
TR	Bignell & Dunlop	(1993)	3	0.2400E+01	-0.2400E+01	0.8563E+00	0.2499E+01	-0.2986E+01	0

R32 Liquid Phase Isochoric Heat Capacity Statistics

EOS	Author	Date	Points	AAD	Bias	Std Dev	RMS	Max Dev	Bad
Ely	Magee & Luddeckke	(1993)	74	0.4361E+00	0.2061E+00	0.5130E+00	0.5496E+00	0.1476E+01	0
OM	Magee & Luddeckke	(1993)	74	0.4557E+00	0.2704E+00	0.5490E+00	0.6086E+00	0.1359E+01	0
PN	Magee & Luddeckke	(1993)	74	0.1158E+01	0.1225E+00	0.1418E+01	0.1414E+01	0.3193E+01	0
TR	Magee & Luddeckke	(1993)	74	0.3427E+00	0.1720E+00	0.3952E+00	0.4285E+00	0.1168E+01	0

R32 Liquid Phase Isobaric Heat Capacity Statistics

EOS	Author	Date	Points	AAD	Bias	Std Dev	RMS	Max Dev	Bad
Ely	Yomo *et al*	(1994)	13	0.6172E+00	-0.6172E+00	0.2573E+00	0.6648E+00	-0.1032E+01	0
OM	Yomo *et al*	(1994)	13	0.9478E+00	-0.9478E+00	0.4362E+00	0.1036E+01	-0.1644E+01	0
PN	Yomo *et al*	(1994)	13	0.1016E+01	-0.1016E+01	0.6396E+00	0.1187E+01	-0.2056E+01	0
TR	Yomo *et al*	(1994)	13	0.9490E+00	-0.9490E+00	0.3015E+00	0.9922E+00	-0.1416E+01	0

R32 Liquid Phase Speed Of Sound Statistics

EOS	Author	Date	Points	AAD	Bias	Std Dev	RMS	Max Dev	Bad
Ely	Grebenkov A.J. *et al*	(1994)	30	0.2337E+00	0.2093E+00	0.1558E+00	0.2594E+00	0.6914E+00	0
OM	Grebenkov A.J. *et al*	(1994)	30	0.1013E+01	-0.1013E+01	0.5315E+00	0.1140E+01	-0.2585E+01	0
PN	Grebenkov A.J. *et al*	(1994)	30	0.5708E+00	0.4596E+00	0.8695E+00	0.9706E+00	0.2403E+01	0
TR	Grebenkov A.J. *et al*	(1994)	30	0.3462E+00	-0.3462E+00	0.1699E+00	0.3844E+00	-0.6964E+00	0

R32 Gas Phase Speed Of Sound Statistics

EOS	Author	Date	Points	AAD	Bias	Std Dev	RMS	Max Dev	Bad
Ely	Hozumi T. *et al*	(1994)	66	0.3481E-01	-0.3481E-01	0.4480E-02	0.3509E-01	-0.4669E-01	0
OM	Hozumi T. *et al*	(1994)	66	0.5513E-01	-0.5513E-01	0.1470E-01	0.5703E-01	-0.8149E-01	0
PN	Hozumi T. *et al*	(1994)	66	0.2364E-01	-0.2364E-01	0.1348E-01	0.2716E-01	-0.6676E-01	0
TR	Hozumi T. *et al*	(1994)	66	0.5020E-02	0.3243E-03	0.6820E-02	0.6776E-02	0.2104E-01	0

R125 Ideal Gas Heat Capacity Statistics

EOS	Author	Date	Points	AAD	Bias	Std Dev	RMS	Max Dev	Bad
Ely	Chen S.S. et al	(1975)	19	0.4361E+00	0.3357E+00	0.5933E+00	0.6680E+00	0.1432E+01	1
	Gillis & Moldover	(1993)	8	0.4074E+00	-0.4074E+00	0.5754E-01	0.4109E+00	-0.4950E+00	0
	Overall		27	0.4276E+00	0.1156E+00	0.6035E+00	0.6034E+00	0.1432E+01	1
OM	Chen S.S. et al	(1975)	19	0.2211E+01	-0.2677E+00	0.3196E+01	0.3122E+01	0.8630E+01	2
	Gillis & Moldover	(1993)	8	0.3675E+00	-0.3675E+00	0.5084E-01	0.3706E+00	-0.4220E+00	0
	Overall		27	0.1665E+01	-0.2973E+00	0.2660E+01	0.2627E+01	0.8630E+01	2

R125 Saturated Vapour Pressure Statistics

EOS	Author	Date	Points	AAD	Bias	Std Dev	RMS	Max Dev	Bad
Ely	Boyes & Weber	(1995)	29	0.5134E-01	-0.3276E-02	0.5804E-01	0.5713E-01	-0.9900E-01	0
	de Vries B.	(1994)	81	0.5096E-01	0.7506E-02	0.1481E+00	0.1474E+00	-0.1283E+01	0
	Holste J.C.	(1993)	18	0.1536E+00	0.1323E+00	0.1918E+00	0.2286E+00	0.7670E+00	0
	Magee & Howley	(1993)	33	0.1442E+00	-0.1405E+00	0.7398E-01	0.1583E+00	-0.2630E+00	0
	Monluc et al	(1991)	23	0.6061E-01	0.5391E-02	0.8149E-01	0.7988E-01	-0.2110E+00	0
	Nagel et al	(1993)	18	0.4208E+00	0.4208E+00	0.2915E+00	0.5073E+00	0.1102E+01	0
	Weber & Silva	(1994)	40	0.4113E-01	-0.2732E-01	0.6401E-01	0.6886E-01	-0.3580E+00	0
	Wilson et al	(1992)	39	0.4383E+00	0.2857E+00	0.5784E+00	0.6384E+00	0.1859E+01	0
	Ye. F et al	(1995)	12	0.8467E-01	0.8433E-01	0.3577E-01	0.9102E-01	0.1140E+00	0
	Overall		293	0.1429E+00	0.5808E-01	0.2843E+00	0.2879E+00	0.1859E+01	0
OM	Boyes & Weber	(1995)	29	0.1020E+00	0.9293E-01	0.7023E-01	0.1158E+00	0.1690E+00	0
	de Vries B.	(1994)	81	0.1087E+00	0.7706E-01	0.1562E+00	0.1733E+00	-0.1281E+01	0
	Holste J.C.	(1993)	18	0.1814E+00	0.1534E+00	0.1697E+00	0.2252E+00	0.6210E+00	0
	Magee & Howley	(1993)	33	0.1743E+00	-0.1685E+00	0.1076E+00	0.1990E+00	-0.3300E+00	0
	Monluc et al	(1991)	23	0.9987E-01	0.8587E-01	0.7782E-01	0.1147E+00	0.1830E+00	0
	Nagel et al	(1993)	18	0.3954E+00	0.3954E+00	0.2117E+00	0.4457E+00	0.9980E+00	0
	Weber & Silva	(1994)	40	0.1631E+00	-0.1631E-01	0.5935E-01	0.1733E+00	-0.5050E+00	0
	Wilson et al	(1992)	39	0.4966E+00	0.2797E+00	0.6037E+00	0.6583E+00	0.1751E+01	0
	Ye. F et al	(1995)	12	0.1638E+00	0.1638E+00	0.3138E-01	0.1666E+00	0.2070E+00	0
	Overall		293	0.1981E+00	0.7366E-01	0.2971E+00	0.3056E+00	0.1751E+01	0
PN	Boyes & Weber	(1995)	29	0.2548E-01	0.5345E-02	0.3022E-01	0.3017E-01	0.7100E-01	0
	de Vries B.	(1994)	81	0.4877E-01	-0.1659E-01	0.1592E+00	0.1591E+00	-0.1333E+01	0
	Holste J.C.	(1993)	18	0.2937E+00	0.2937E+00	0.3952E+00	0.4835E+00	0.1538E+01	0
	Magee & Howley	(1993)	33	0.3297E+00	0.2074E+00	0.3587E+00	0.4096E+00	0.8370E+00	0
	Monluc et al	(1991)	23	0.5743E-01	-0.3065E-01	0.7558E-01	0.8002E-01	-0.2290E+00	0
	Nagel et al	(1993)	18	0.8039E+00	0.8039E+00	0.6342E+00	0.1013E+01	0.2019E+01	0
	Weber & Silva	(1994)	40	0.6280E+00	0.6280E+00	0.1526E+00	0.6459E+00	0.8150E+00	0
	Wilson et al	(1992)	39	0.6702E+00	0.6156E+00	0.7448E+00	0.9589E+00	0.2762E+01	0
	Ye. F et al	(1995)	12	0.5442E-01	0.5358E-01	0.3493E-01	0.6316E-01	0.1410E+00	0
	Overall		293	0.3022E+00	0.2542E+00	0.4685E+00	0.5323E+00	0.2762E+01	0

R125 Saturated Liquid Density Statistics

EOS	Author	Date	Points	AAD	Bias	Std Dev	RMS	Max Dev	Bad
Ely	Magee & Howley	(1993)	7	0.5371E-01	0.2086E-01	0.6790E-01	0.6623E-01	0.1450E+00	0
	Higashi Y.	(1994)	9	0.7401E+00	-0.3581E+00	0.1642E+0	0.1589E+01	-0.4671E+01	2
	Defibaugh D.R. et al	(1992)	9	0.4876E+00	0.4876E+00	0.9296E+0	0.1003E+01	0.2880E+01	0
	Overall		25	0.4570E+00	0.5244E-01	0.1150E+0	0.1128E+01	-0.4671E+01	2
OM	Magee & Howley	(1993)	7	0.6057E-01	-0.3400E-01	0.6064E-01	0.6564E-01	-0.9400E-01	0
	Higashi Y.	(1994)	9	0.5727E+00	-0.2047E+00	0.1250E+0	0.1196E+01	-0.3498E+01	2
	Defibaugh D.R. et al	(1992)	9	0.4926E+00	0.4417E+00	0.1093E+0	0.1121E+01	0.3265E+01	0
	Overall		25	0.4004E+00	0.7580E-01	0.1001E+0	0.9842E+00	-0.3498E+01	2
PN	Magee & Howley	(1993)	7	0.4686E-01	-0.2857E-02	0.6078E-01	0.5634E-01	-0.1130E+00	0
	Higashi Y.	(1994)	9	0.1880E+01	0.7270E+00	0.3456E+0	0.3338E+01	0.9204E+01	0
	Defibaugh D.R. et al	(1992)	9	0.2679E+00	0.1868E+00	0.5417E+0	0.5438E+00	0.1575E+01	0
	Overall		25	0.7865E+00	0.3282E+00	0.2044E+0	0.2030E+01	0.9204E+01	0

R125 Saturated Vapour Density Statistics

EOS	Author	Date	Points	AAD	Bias	Std Dev	RMS	Max Dev	Bad
Ely	Higashi Y.	(1994)	8	0.1647E+01	0.1647E+01	0.1194E+01	0.1990E+01	0.4222E+01	1
OM	Higashi Y.	(1994)	8	0.2122E+01	0.2122E+01	0.2913E+01	0.3454E+01	0.9043E+01	0
PN	Higashi Y.	(1994)	8	0.2515E+01	0.2169E+01	0.2484E+01	0.3179E+01	0.6942E+01	1

R125 Liquid Heat Capacity at Saturation

EOS	Author	Date	Points	AAD	Bias	Std Dev	RMS	Max Dev	Bad
Ely	Luddecke and Magee	(1993)	85	0.2023E+00	-0.2433E-01	0.2546E+00	0.2543E+00	0.6590E+00	0
OM	Luddecke and Magee	(1993)	85	0.3454E+00	-0.1573E+00	0.4077E+00	0.4348E+00	0.1147E+01	0
PN	Luddecke and Magee	(1993)	85	0.4765E+00	0.1160E+00	0.5633E+00	0.5718E+00	-0.1384E+01	0

R125 Liquid Phase *PVT* Statistics

EOS	Author	Date	Points	AAD	Bias	Std Dev	RMS	Max Dev	Bad
Ely	Defibaugh *et al*	(1992)	162	0.4076E+00	0.2110E+00	0.1020E+01	0.1038E+01	0.9979E+01	3
	Holste J.C	(1993)	170	0.9599E-01	-0.8132E-01	0.2574E+00	0.2692E+00	-0.1998E+01	0
	Magee & Howley	(1993)	79	0.4454E-01	0.3693E-01	0.4040E-01	0.5454E-01	-0.1172E+00	0
	Wilson L.C. *et al*	(1992)	83	0.5958E+00	-0.5692E+00	0.7765E+00	0.9590E+00	-0.2662E+01	5
	Overall		494	0.2739E+00	-0.4851E-01	0.7295E+00	0.7304E+00	0.9979E+01	8
OM	Defibaugh *et al*	(1992)	162	0.3573E+00	0.2654E+00	0.9652E+00	0.9981E+00	0.9288E+01	3
	Holste J.C	(1993)	170	0.1043E+00	-0.9006E-01	0.2495E+00	0.2646E+00	-0.1853E+01	0
	Magee & Howley	(1993)	79	0.5152E-01	0.5049E-01	0.3934E-01	0.6385E-01	0.1543E+00	0
	Wilson L.C. *et al*	(1992)	83	0.5579E+00	-0.5326E+00	0.7432E+00	0.9107E+00	-0.3437E+01	5
	Overall		494	0.2550E+00	-0.2538E-01	0.7008E+00	0.7006E+00	0.9288E+01	8
PN	Defibaugh *et al*	(1992)	162	0.4265E+00	0.2679E+00	0.8417E+00	0.8808E+00	0.5743E+01	4
	Holste J.C	(1993)	170	0.1146E+00	-0.1022E+00	0.1858E+00	0.2116E+00	-0.1149E+01	0
	Magee & Howley	(1993)	79	0.3865E-01	0.3078E-01	0.3721E-01	0.4811E-01	0.1546E+00	0
	Wilson L.C. *et al*	(1992)	83	0.6066E+00	-0.6020E+00	0.7793E+00	0.9810E+00	-0.3292E+01	4
	Overall		494	0.2874E+00	-0.4353E-01	0.6564E+00	0.6572E+00	0.5743E+01	8

R125 Gas Phase *PVT* Statistics

EOS	Author	Date	Points	AAD	Bias	Std Dev	RMS	Max Dev	Bad
Ely	Boyes & Weber	(1995)	92	0.7104E-01	-0.6987E-02	0.1390E+00	0.1384E+00	-0.1139E+01	0
	deVries B.	(1994)	287	0.9793E-01	0.4085E-01	0.6161E+00	0.6164E+00	0.9779E+01	0
	Ye F. *et al.*	(1995)	94	0.9618E-01	0.4457E-01	0.1319E+00	0.1386E+00	0.4761E+00	0
	Overall		473	0.9235E-01	0.3228E-01	0.4874E+00	0.4879E+00	0.9779E+01	0
OM	Boyes & Weber	(1995)	92	0.1803E+00	-0.1088E+00	0.2151E+00	0.2400E+00	-0.9379E+00	0
	deVries B.	(1994)	287	0.1547E+00	-0.1621E-01	0.6530E+00	0.6521E+00	0.9770E+01	0
	Ye F. *et al.*	(1995)	94	0.1915E+00	-0.1005E+00	0.2310E+00	0.2508E+00	-0.6889E+00	0
	Overall		473	0.1670E+00	-0.5098E-01	0.5288E+00	0.5307E+00	0.9770E+01	0
PN	Boyes & Weber	(1995)	92	0.1403E+00	-0.1062E+00	0.1906E+00	0.2173E+00	-0.1274E+01	0
	deVries B.	(1994)	287	0.1620E+00	0.5175E-01	0.7987E+00	0.7989E+00	0.9735E+01	0
	Ye F. *et al.*	(1995)	94	0.1295E+00	-0.1367E-01	0.1793E+00	0.1789E+00	0.6248E+00	0
	Overall		473	0.1513E+00	0.8023E-02	0.6353E+00	0.6347E+00	0.9735E+01	0

R125 Second Virial Coeficient Statistics

EOS	Author	Date	Points	AAD	Bias	Std Dev	RMS	Max Dev	Bad
Ely	Bignell C.M.	(1993)	3	0.6373E+00	-0.6373E+00	0.5537E+00	0.7814E+00	-0.1000E+01	1
	Gillis & Moldover	(1993)	9	0.1052E+01	-0.1052E+01	0.3256E+00	0.1096E+01	-0.1745E+01	0
	Ye F	(1995)	11	0.1132E+01	0.7039E+00	0.1283E+01	0.1411E+01	0.2728E+01	0
	Overall		23	0.1036E+01	-0.1580E+00	0.1242E+01	0.1225E+01	0.2728E+01	1
OM	Bignell C.M.	(1993)	3	0.6860E+00	-0.6860E+00	0.6259E+00	0.8554E+00	-0.1226E+01	1
	Gillis & Mold	(1993)	9	0.2695E+01	-0.2695E+01	0.2864E+01	0.3815E+01	-0.8629E+01	1
	Ye F	(1995)	11	0.3862E+01	-0.2679E+01	0.4287E+01	0.4887E+01	-0.9893E+01	0
	Overall		23	0.2991E+01	-0.2425E+01	0.3442E+01	0.4149E+01	-0.9893E+01	2

R125 Liquid Phase Isochoric Heat Capacity Statistics

EOS	Author	Date	Points	AAD	Bias	Std Dev	RMS	Max Dev	Bad
Ely	Luddecke & Magee	(1993)	97	0.5836E+00	0.4764E+00	0.4985E+00	0.6877E+00	0.1859E+01	0
OM	Luddecke & Magee	(1993)	97	0.4250E+00	0.1717E+00	0.5216E+00	0.5466E+00	0.1639E+01	0
PN	Luddecke & Magee	(1993)	97	0.4513E+00	0.2251E-01	0.5752E+00	0.5726E+00	-0.1689E+01	0

R125 Liquid Phase Isobaric Heat Capacity Statistics

EOS	Author	Date	Points	AAD	Bias	Std Dev	RMS	Max Dev	Bad
Ely	Wilson L.C	(1992)	5	0.1449E+01	-0.9926E+00	0.2292E+01	0.2278E+01	-0.4916E+01	0
OM	Wilson L.C	(1992)	5	0.1236E+01	-0.8003E+00	0.1870E+01	0.1854E+01	-0.3939E+01	0
PN	Wilson L.C	(1992)	5	0.1171E+01	-0.2194E+00	0.1967E+01	0.1773E+01	-0.3477E+01	0

R125 Liquid Phase Speed Of Sound Statistics

EOS	Author	Date	Points	AAD	Bias	Std Dev	RMS	Max Dev	Bad
Ely	Grebenkov A.J *et al*	(1994)	30	0.1042E+00	-0.1938E-01	0.1314E+00	0.1306E+00	0.3616E+00	0
OM	Grebenkov A.J *et al*	(1994)	30	0.3246E+00	-0.3246E+00	0.1607E+00	0.3610E+00	-0.7495E+00	0
PN	Grebenkov A.J *et al*	(1994)	30	0.2457E+00	-0.2228E+00	0.2089E+00	0.3030E+00	-0.7264E+00	0

R125 Gas Phase Speed Of Sound Statistics

EOS	Author	Date	Points	AAD	Bias	Std Dev	RMS	Max Dev	Bad
Ely	Gillis	(1993)	149	0.1420E-01	0.1333E-02	0.1745E-01	0.1744E-01	0.4825E-01	0
OM	Gillis	(1993)	149	0.1146E+00	0.1053E+00	0.1569E+00	0.1886E+00	0.6098E+00	0
PN	Gillis	(1993)	149	0.4361E-01	0.3594E-02	0.6110E-01	0.6100E-01	0.2349E+00	0